Department of Industrial Engineering
University of Stellenbosch

Improving and implementing advanced milling techniques for the manufacture of selected titanium aerospace parts

Ruan de Bruyn

Thesis presented in partial fulfilment of the requirements for the degree of
Master of Industrial Engineering in the Faculty of Engineering
at
Stellenbosch University

Supervisor: Mr NF Treurnicht

Co-supervisor: Mr T Dirkse van Schalkwyk

December 2014

Declaration

By submitting this thesis electronically, I declare that the entirety of the work contained therein is my own original work, that I am the sole author thereof (save to the extent explicitly otherwise stated), that reproduction and publication thereof by Stellenbosch University will not infringe any third party rights and that I have not previously, in its entirety or in part, submitted it for obtaining any qualification.

Date: August 2014

Abstract

There is a strong focus on the use of titanium and its alloys in the aerospace industry due to the high ultimate tensile strength and high strength-to-weight ratio of the material. The high performance nature of the material also makes it difficult and costly to machine. South Africa has the second most abundant titanium resources in the world in the form of rutile and ilmenite but no value chain to produce titanium parts from the ore. Currently, the ore is sold overseas at low prices. There exists an initiative to create a full titanium value chain in South Africa by the Department of Science and Technology. This project forms part of this initiative, where local industry is equipped with knowledge and skills to produce and machine titanium parts.

The focus of this study is to determine whether it is possible to machine titanium aerospace parts at a local industry partner and equip the industry partner with knowledge and skills in order to facilitate effective and economical machining of these parts. Daliff Precision Engineering was selected as the local industry partner and specific demonstrator parts were selected on which to base the study. The process the industry partner currently uses to machine aerospace parts from difficult-to-machine alloys was studied and evaluated. It was found that about 70% of the machining time was spent on a single roughing process, hence the decision to study the roughing process in an attempt to establish whether improvement was possible. Pilot tests were done at the facilities of the industry partner and time savings of 95% were realised on the roughing process.

A 2-level 3-factor Design of Experiments methodology was followed for experimentation and analysis of titanium machining at the industry partner. The roughing process of the demonstrator part was simulated on the CNC machining centre and the depth of cut, cutting speed and feed per tooth were selected as the factors, and the response was tool wear. A statistical analysis was done using Modde 9.1 design of experiments software and an optimisation model was created in order to determine a feasible set of cutting parameters, maximise material removal rate and have a target amount of tool wear.

The findings show that it is possible to economically machine titanium aerospace parts with a selected geometry at the industry partner without the need for significant capital investments. The industry partner can use the knowledge generated in this project to validate their titanium machining capabilities and form part of the titanium value chain that is being developed in South Africa.

Opsomming

Daar is ‘n groot fokus op die gebruik van titaan allooie in die lugvaart nywerheid, as gevolg van die material se hoë trek-sterkte en hoë sterkte-tot-gewig verhouding. Die eienskappe wat die material so aantreklik maak, is ook die rede wat dit moeilik en duur maak om te masjineer. Suid-Afrika het die tweede grootste titaan reserwes in die wêreld in die vorm van rutiel en ilmeniet erts, maar geen waarde ketting om titaan onderdele te vervaardig van die erts af nie. Die erts word tans oorsee verkoop teen lae pryse. Daar is tans ‘n inisiatief om ‘n titaan waardeketting in Suid-Afrika te skep deur die Departement van Wetenskap en Tegnologie. Hierdie projek vorm deel van hierdie inisiatief om die plaaslike nywerheid toe te rus met kennis en vaardighede om titaan produkte te vervaardig.

The fokus van hierdie studie is om te bepaal of dit moontlik is om titaan lugvaart onderdele te masjineer by ‘n plaaslike industrie-vennoot en om hierdie vennoot met kennis en vaardighede toe te rus om hierdie onderdele effektief en ekonomies te vervaardig. Daliff Precision Engineering is gekies as die plaaslike industrie-vennoot en spesifieke demonstrator onderdele is gekies om die studie op te baseer. Die proses wat die industrie-vennoot tans gebruik om moeilik-om-te-masjineer allooie te masjineer is bestudeer en ge-evalueer. Daar was bevind dat 70% van die masjineringstyd bestee word aan ‘n enkele uitrof-proses. Daar is besluit om vas te stel of die uitrof-proses verbeter kan word. Loods-eksperimente is gedoen by die industrie-vennoot se fasiliteite en ‘n tydsbesparing van 95% is gevind op die uitrof-proses.

‘n 2-Vlak 3-faktor eksperimentele ontwerp metodologie is gevolg om eksperimente by die industrie-vennoot op titaan uit te voer en te analiseer. Die uitrof-proses van die demonstrator onderdeel is gesimuleer op die CNC masjineringsentrum en die diepte van snit, snyspoed en voer per tand is gekies as die faktore en beitel-slytasie is gekies as die respons. ‘n Statistiese analise is gedoen deur Modde 9.1 eksperimentele ontwerp sagteware te gebruik om ‘n moontlike stel van sny-parameters te identifiseer om die materiaal-verwyderingstempo te maksimeer en die teiken waarde vir beitel-slytasie te bereik.

Daar is gevind dat dit moontlik is on titaan lugvaart onderdele met ‘n spesifieke geometrie ekonomies te masjineer by die industrie-vennoot, sonder om enige beduidende kapitaal uitgawes aan te gaan. Die industrie-vennoot kan die kennis gebruik wat geskep is deur die projek om hulle titaan masjineringsvaardighede te valideer en om deel te vorm van die titaan waardeketting wat besig is om in Suid-Afrika ontwikkel te word.

Acknowledgements

The Author expresses his gratitude to the following organizations and individuals for their contribution to this study:

The Department of Science and Technology for funding and providing this research initiative

Mr. N.F. Treurnicht for his guidance and advice

Mr. T Dirkse van Schalkwyk for his insight and advice

Prof. D.M. Dimitrov for leading the research group

Mr. C. Prins as partner for the industry project

Daliff Precision Engineering for the use of their facilities

Family, friends and colleagues for continued support and patience

Table of Contents

List of figures

List of tables

1. Introduction

1.1 Overview and background

There is an increased interest in research into improved titanium machining techniques and the growth of the titanium industry in South Africa. These techniques have been found to be favourable in the improvement of the manufacturing of titanium parts at the research institutes but there is a gap in the transfer and implementation of these technologies to the industry. Being the second largest producer of titanium bearing raw material in the world, South Africa has a growing titanium industry. However, the country has no means of refining it.

The potential for establishing a titanium industry has been identified in a number of government studies, with the Department of Science and Technology (DST) at the forefront of the initiative. The key studies and strategies include the following (van Vuuren, 2009):

- Foresight studies in the 1990's, conducted by the former Department of Arts, Culture, Science and Technology, which recommended that government and industry should jointly support research and development in the production of titanium and titanium dioxide from local raw material.
- Chemical sector development strategy of the DTI, including the Titanium Beneficiation Initiative (TBI), whose aim is to achieve sufficient beneficiation of titanium slag in order to prevent weakening of long-term revenue earnings in the broad-based mineral sector.
- The National Advanced Manufacturing Strategy (AMTS), released in 2003, with the aim of supporting the growth and competitiveness of the South African manufacturing sector through the advancement of technological innovation. This study forms part of the implementation of this strategy.

Starting in 2007, the DST has been leading a research-led industrialisation initiative called the South Africa Titanium Industry Strategy. The initiative is aimed at establishing a titanium metals industry in South Africa. This framework has been formulated in order to deliver key competencies across the entire titanium value chain ranging from developing new techniques of refining rutile and ilmenite that would produce titanium raw material to those to those that turn this raw material into usable products. This research would be used to establish the entire titanium value chain inside South Africa, in an attempt to make South Africa a global player in the titanium industry.

The development work is carried out under guidance from the Titanium Centre of Competence (TiCoC), led by the CSIR, to develop and commercialise the technology building blocks required for the establishment of a titanium industry. The TiCoC consists of various research institutions, industry

partners and universities, which collaborate in an attempt to establish a base of competencies for the titanium industry.

Stellenbosch University, in collaboration with the University of Johannesburg, the University of Cape Town and the Fraunhofer IWU in Germany, have been focussing on high performance machining of titanium funded by the AMTS. A large base of competencies regarding titanium machining have already been established in South Africa by these institutions, and have been successful in demonstrating substantial reductions in machining times.

With the current state of research, the focus has been mainly on improving machining times but no focus on the needs and capabilities of the South African manufacturing industry. South Africa has some large companies with world class capabilities and regular international customers such as Aerosud. However, smaller companies, which the titanium initiative also aims to support, do not have the capabilites like those of larger companies. The on-going research is aimed at supplying South Africa with proprietary and state of the art technologies and knowledge. While larger companies have the capital and business prospects to justify substantial investments and expenses incorporating and sustaining the new technologies, smaller companies are falling behind in the titanium race as the new research is out of their reach.

1.2 Problem Statement

Groundbreaking and novel research is being done at research institutions with little focus on implementing this research in the industry. The research institutions have a focus on the latest machinery and tool technology with access to state-of-the-art technologies that have the potential to revolutionise the industry. These latest machinery and tool technologies require extensive capital investment to procure and expertise to operate. Large companies in the industry have access to such machinery, tools, necessary expertise, and have the existing customer base and demand to fund procurement of these resources. Small to medium companies, however, do not have enough resources or drive to procure and sustain these technologies.

In this way, manufacturing technologies and techniques that can otherwise have an impact on the industry are falling into disuse. This results in the wastage of resources that could have been used more effectively, which ultimately lead to an increase in the cost to produce a part. Furthermore, problems with regard to quality and part compliance may also arise, which leads to the following research question:

Can the improved machining technologies be used to contribute to a significantly improved titanium aerospace parts manufacturing process in the South African industry?

1.3 Rationale

The use of titanium in the aerospace industry has seen extensive growth in the recent years due to its favourable strength to weight ratio. South Africa is the second largest producer of titanium bearing raw material, but has no means of converting the raw material to usable titanium parts on an industrial and profitable scale. Titanium is seen as a difficult to machine material due to its physical properties. However, this difficulty is what makes titanium an attractive material to use. The Department of Science and Technology has invested heavily in the South African titanium industry to exploit these reserves with extensive research being done to improve titanium machining and the refining of raw materials. The result is research that yields improved titanium machining techniques but with little focus on implementing these results.

1.4 Purpose of the project

The purpose of this project is to improve the machining process to create a specific aerospace part made from titanium at an industry partner using novel manufacturing techniques. The industry partner has been identified as Daliff Precision Engineering (PTY) LTD, which produces parts of the aerospace industry. The industry partner currently uses conventional well-established manufacturing techniques to produce this part but experience certain issues with the current manufacturing process. This being the case, the explicit aim of this project is to create a novel process that would incorporate the new and existing research and to implement this research at the industry partner.

1.5 Methodology

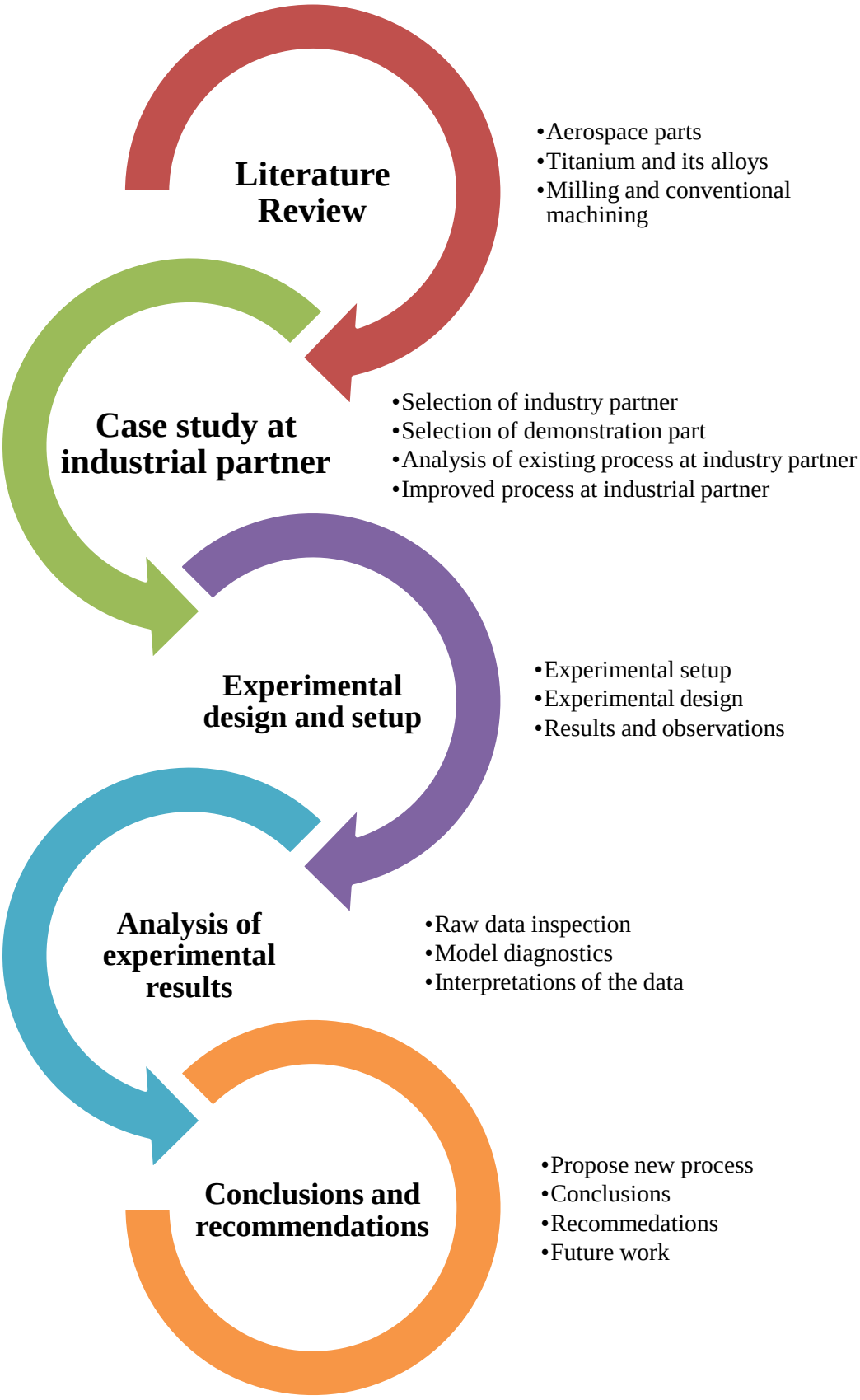

Figure 1: Research approach

2. Literature review

2.1 Introduction

Chapter one provided the background to the study as well as the problem statement, the rationale for the study, the purpose of the project and the methodology adopted in executing this study. Before the manufacturing process for titanium aerospace parts can be improved, all the aspects of the aerospace parts, titanium properties, milling and related tool design have to be considered. This chapter, therefore, presents a detailed review of current literature relating to the topic under investigation including an overview of aerospace parts, titanium and its alloys, and machining titanium alloys.

2.2 Aerospace parts

Aerospace parts are high performance parts with complex geometries and high strength alloys that are hard to manufacture. Commercial airliners, such as the Boeing 777, consist of over 3 million different parts from over 500 suppliers, with the overall weight of the airplane consisting of about 15% titanium and its alloys (Boeing, 2014). The following sections provide an overview of the properties as well as the geometries and features, and some of the implications of machining these parts.

2.2.1 Properties

Aerospace parts tend to have certain properties owing to their high performance nature. The focus in the aerospace industry is to: (i) create aircrafts that are extremely light, (ii) increase fuel efficiency, and (iii) increase passenger safety and comfort (Ezugwu, 2005) (Williams & Starke, 2003). The parts have a similar design philosophy. The high strength and low weight results in parts with complex geometries. Therefore, such parts have to be made from a material that has a high strength to weight ratio (Brewer, et al., 1998). Due to the lightweight nature and complex geometries of aerospace parts, a large proportion of the material has to be removed from the original billet. In order to achieve this, processes that have to be considered include those with a high material removal rate and near-net shape processing.

Quality is critical during the manufacturing process and operational life of the part (Boyer, 1995). Defective parts are unacceptable to ensure airline safety. In this regard, quality has to be built into the parts to ensure the part functions as designed. Considering airline passenger safety, traceability has to be designed into the manufacturing process. Every step and aspect of the manufacturing process has to be documented and filed to ensure that defects and failures can be traced to source.

2.2.2 Geometries and features

Aerospace parts tend to have complex geometries and features, which results from their high performance and lightweight nature. To understand the manufacturing process, these features have to be identified to ensure the manufacturing process is capable of producing them. Typically, an aerospace

part has a combination of these features, and sometimes the manufacturing techniques have to be adjusted to accommodate the features and their geometries.

Pockets

Pockets are amongst the most common operations in machining metal parts. It is defined as It is defined as removing all the material inside some arbitrary closed boundary on a flat surface of a workpiece to a fixed depth (Kramer, 1992), as illustrated in Figure 2. The boundary could be enclosed around all sides, or at least three sides, to be classified as a pocket. Material is removed to keep the part as low-weight as possible, while still having the required geometry.

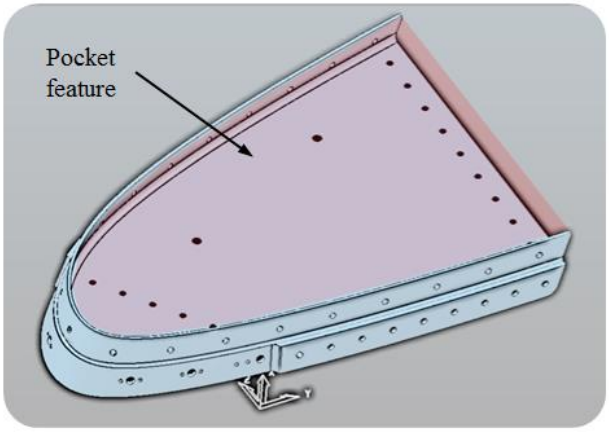

Figure 2: Pocket feature

Thin-walled

Thin-walled parts are characterised by having wall-thickness (t) that is significantly lower than its height (h), and a relatively small wall thickness (Huang, et al., 2014). An example of a thin-walled and thin-based part is shown in Figure 3. It is difficult to give an exact quantitative definition for thin-walled parts, as it may vary according to where it is applied. For the purpose of this project and the aerospace parts that have been studied, a broad definition was made that a thin-walled part has a height-to-thickness ratio of 6:1 and a wall thickness of less than 8mm. This definition depends heavily on scale and has to be re-evaluated for larger parts. In addition, care has to be taken when machining thin-walled parts, as the wall may deform due to the sideway cutting forces. Cutting strategies, such as the 8:1 rule, is used to minimise deformation of the wall during machining, as illustrated in Figure 36.

Thin-based

Thin-based parts are similar to thin-walled parts, with a thickness (b) that is significantly lower than its width (w), and a relatively small width. The definition of a thin-based part for this project is a feature with a width-to-thickness ratio of 10:1, and a thickness of less than 5mm. This definition is only valid for this project and is generally dependent on scale and application. During machining, care has to be taken that the vertical cutting forces in the tool do not deform the thin-base of the material. Appropriate cutting strategies and tools have to be used to avoid this deformation.

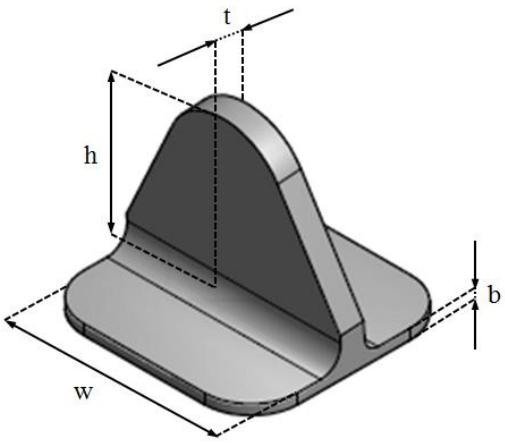

Figure 3: Thin-walled and thin-based part

Boss

A boss is a protruding feature on a part that is used to locate one part within a feature on another part, such as a hole or pocket (Ogot & Kremer, 2006). Figure 4 shows an example of a boss feature on the face of a part.

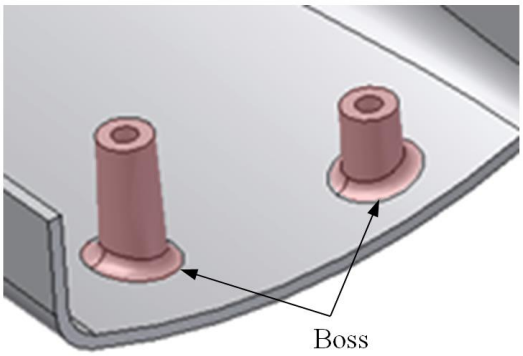

Figure 4: Boss feature

Holes

Holes are openings in material, usually round, that are used for positioning and fitment of one part to another (Ogot & Kremer, 2006). A bolt or rivet is generally inserted through the hole to affix a part to the other. A drill is used to create the hole and secondary processing, such as reaming and tapping, can be applied, according to application.

Ribs

Ribs are a special type of protrusion that helps strengthen the features on a part (Ogot & Kremer, 2006). A rib resembles a thin-wall intersecting two perpendicular surfaces, which are to be strengthened as illustrated in Figure 5.

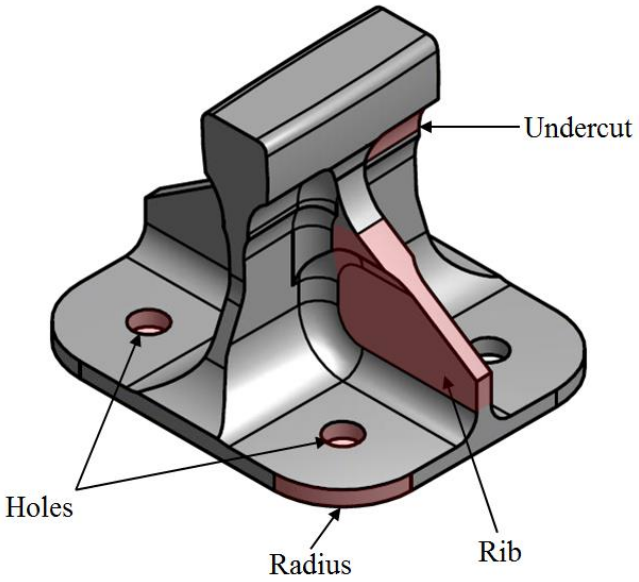

Figure 5: Illustration of various aerospace part features

Radii

A radius is a feature on a part where the corner is rounded to a certain degree. This allows the part to be handled without the risk of injury and help with fitting of the part.

Undercuts

An undercut is an overhanging feature on a part, illustrated in Figure 4. It is used in fitting or positioning one part to another. A special cutter has to be used to machine this feature.

2.3 Titanium and its alloys

2.3.1 Introducing titanium

Titanium is a chemical element with a low density and a dark grey to silver colour. It is the 9th most abundant element in the earth's crust where it is commonly found in two types of ore: rutile and ilmenite (Zhang, et al., 2011). Rutile ore consists mostly of TiO_2 while ilmenite ore is a combination of FeO and TiO_2. Rutile ore is preferred as it has a higher titanium concentration than ilmenite ore. The ore is put through a process called the Kroll process, which yields commercially pure titanium sponge (Chunxiang, et al., 2011) (Nagesh & Ramachandran, 2007).

Titanium has various properties that make it attractive to use in aerospace, automotive and biomedical applications. Its high strength-to-weight ratio is especially desirable for the aerospace industry, and so is its high corrosion resistance in harsh environments (Boyer, 1995). The same reasons that make it desirable to use, make it difficult and expensive to make a part. It is typically 20 times more expensive to produce a titanium part than a similar aluminium part (Boyer, 1996). As shown in Figure 6, it can be observed that the use of titanium alloys has increased on Boeing commercial airliners since the late 1950s. The latest Boeing 787 'Dreamliner" is approximately 15% titanium alloys by weight. This

indicates the importance of improving the production process of titanium aerospace parts in order to make it more cost effective. The following section focuses on the different properties of titanium and its alloys, especially the physical material properties, metallurgy, machinability as well as the challenges of machining this material.

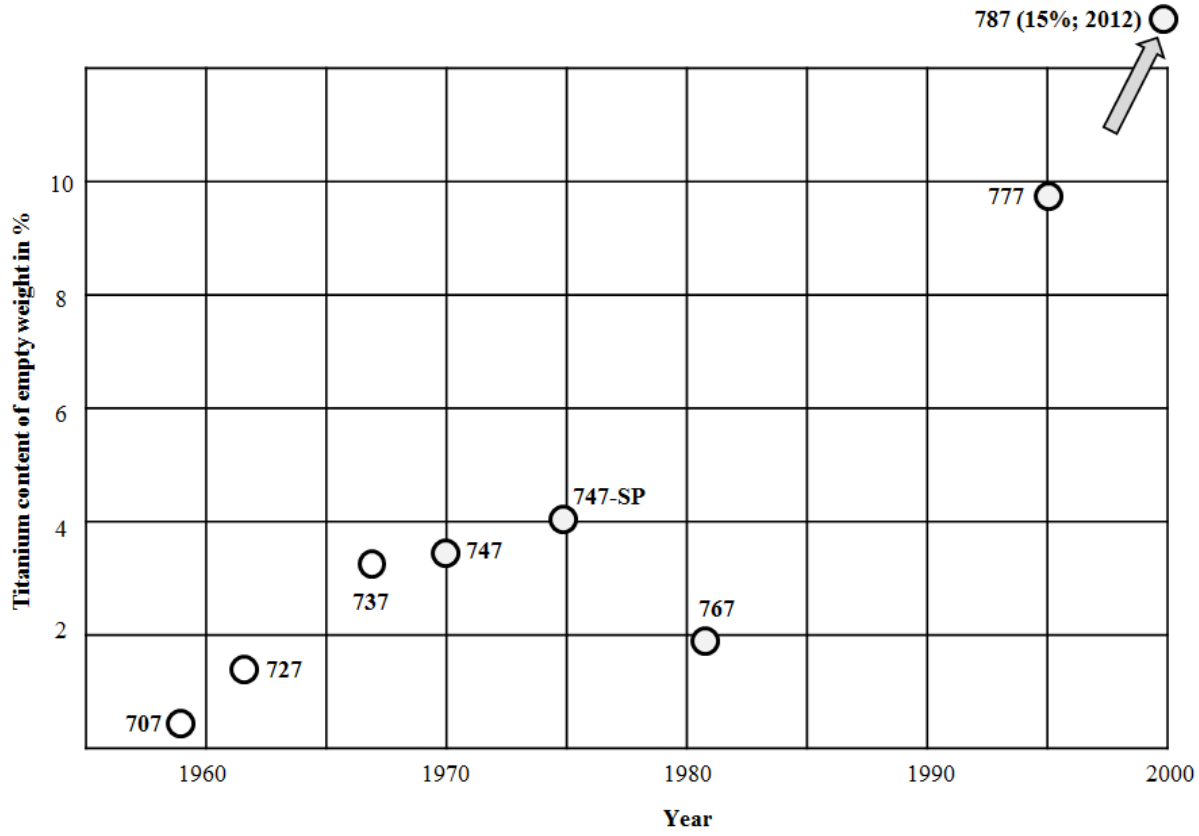

Figure 6: Increase in application of titanium alloys in Boeing aircraft (Leyens & Peters, 2003)

2.3.2 Physical material properties

Titanium has desirable physical properties as the material has a high ultimate tensile strength, strength at elevated temperature, corrosion resistance and a high strength-to weight ratio. For these reasons, titanium is a preferred material for use in aerospace applications. On the one hand, titanium is galvanically compatible with composite materials, which explains why it is used on new-generation commercial airliners. On the other hand, it has a low thermal conductivity, high chemical affinity and work hardening characteristics, which makes it difficult and costly to machine. A complete list of physical and mechanical properties of elemental titanium is provided in appendix A.

The commercial pure grade of titanium is rarely used in the aerospace industry and the metal is mostly used in some form of alloy. Ti-6Al-4V is the commonly used titanium alloy with about 70% of all uses in the aerospace industry (Boyer, 1996). The Ti-6Al-4V is significantly stronger than commercially pure titanium albeit with the same stiffness and thermal properties. Ti-6Al-4V is also heat treatable.

Table 1: Physical properties of selected aerospace alloys

Material	Density (g/cm^2)	UTS (MPa)	Hardness (Brinell)	Modulus of Elasticity (GPa)	Melting Point (°C)	Thermal Conductivity (W/m-K)
6061 Al T6	2.70	310	95	68.9	582	167
Ti-6Al-4V	4.43	950	334	113.8	1604	6.7
15-5 PH SS	7.80	1014	331	200	1405	17.8

(Boyer, et al., 1994)

Table 1 shows some of the physical properties of Ti-6Al-4V compared to selected aerospace alloys. It can be seen that Ti-6Al-4V has a similar ultimate tensile strength and hardness as 15-5 PH stainless steel, but with a 43% lower density. The result is that parts made from Ti-6Al-4V have a similar strength to those made from 15-5 PH stainless steel but having a 43% less weight. With more parts made from titanium on commercial airliners, this represents a significant reduction in overall weight.

2.3.3 Metallurgy of titanium alloys

Titanium consists of two crystalline states: α hexagonal close packed (HCP) and β body-centered cubic (BCC) (Patankar, et al., 2001). The two allotropic forms of titanium are illustrated in Figure 7. The α-phase occurs at temperatures below 882°C, which is the beta transus temperature (Ribeiro, et al., 2003) and the β-phase occurs above this temperature. The HCP structure of the α-phase has a limited number of slip or shear planes, whereas the BCC structure has more slip planes that allow more local deformation. This results in the material losing some of its hardness if the temperature is elevated. While titanium has a relatively high hot-hardness relative to other materials, some of its alloys can be used in operating temperatures of up to 540°C (Ezugwu, et al., 2003).

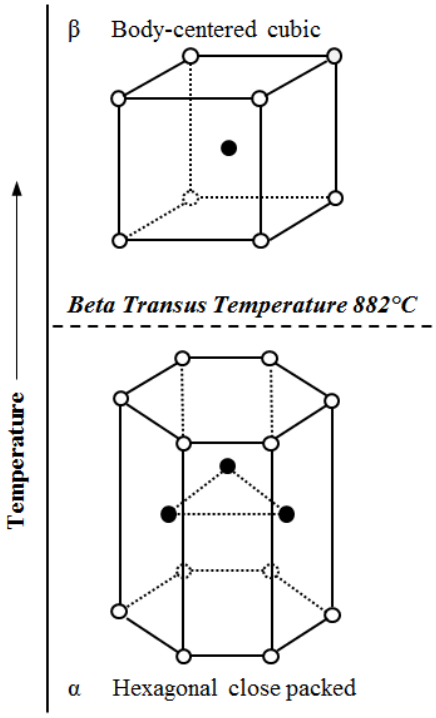

Figure 7: The two allotropic forms of titanium (Yang & Liu, 1999)

The beta transus temperature can be raised or lowered by adding certain elements. By adding α stabilising elements such as Al, O, N, Ga and C, the beta transus temperature can be increased, thus, raising hot-hardness strength. Adding β stabilising elements such as Mo, V and Ta, called isomorphous formers, or Cu, Cr, Fe, Mn, Ni, Co and H, called eutectoid formers, the beta transus temperature can be decreased. Elements such as Sn, Si and Zr are neutral and have little influence on the beta transus temperature. By adding different α and β stabilisers, the following titanium alloys can be created, each with distinct properties and different applications (Yang & Liu, 1999):

- Commercially pure titanium that has no added stabilisers and has excellent corrosion resistance and low-strength properties.
- α and near α alloys that have α stabilisers and excellent creep resistance.
- α-β alloys that have α and β stabilisers, which have excellent strength and can be heat treated.
- β alloys that have significant amounts of β stabilisers with a high hardenability and higher density.
- Titanium Aluminides, such as Ti_3Al (α_2) and TiAl (γ), that can be used in applications in the range of 760-816°C and has low ductility at room temperature (Loria, 2000).

Through adding different amounts of α and β stabilisers, the properties of titanium and its alloys can be adjusted to be used in various applications that other materials are not suited for.

2.3.4 Machinability of titanium and its alloys

Machinability is broadly defined as the relative ease with which a material can be machined using appropriate tooling and cutting conditions (Groover, 2007). Various criteria could be used to assess machinability, the most important being tool life, surface finish, cutting forces and power required.

Additionally, chip formation and part accuracy could also be used during assessment of machinability. It should be noted that one material could yield a better tool life, while another material yields a better surface finish. Each material has a different effect on each of the criteria that have an influence on machinability, which makes evaluation of machinability challenging. Different process parameters also have an influence on the machinability of material where, if process parameters are changed, machinability may improve for a certain material and deteriorate for another.

Machinability is measured relative to a base material according to a specified measure of performance such as tool life, tool wear, cutting force, machining power requirements, cutting temperature and material removal rate under specific testing conditions. It could also be a combination of several of these aforementioned factors. Shaw (Shaw, 2005) states that the best criterion for rating machinability is machining cost per part as all these factors can be translated to cost. When determining the machinability rating, the base material is given a rating of 1.00, where materials that can be machined easier than the base material have a rating of less than 1.00, and more difficult materials have a rating of more than 1.00. Progress in the machining of titanium alloys has not kept pace with advances in the machining of

other materials due to high temperature strength, low thermal conductivity, relatively low modulus of elasticity and high chemical reactivity (Ezugwu & Wang, 1997). Success in the machining of titanium alloys, therefore, depends largely on overcoming the principal challenges associated with the inherent properties of these materials.

It is problematic to assign a machinability rating to titanium and its alloys because a single measure of performance cannot be used to adequately describe all the factors that influence machinability. Cost can be used as a basis for calculating machinability since the total cost to manufacture a part can be determined. The cost would include raw material cost, tooling costs, machine and operator costs, cutting fluid costs, overheads, etc. Boyer states that titanium raw material may cost anywhere from 3 to 10 times as much as steel or aluminium, and the total machining costs are generally significantly higher than other materials, for instance at least 10 times the cost of machining aluminium (Boyer, 1996). The machinability factor for titanium would have to be determined for each specific case where it would be used, but based on a cost basis, it can be assumed that it is 20 times more expensive than making the same part from aluminium. The machinability factor for titanium would then be 20.0, if aluminium was taken as a basis of 1.00. However, as machining tools, milling machines and cutting strategies are improved, the machinability of titanium is continually improved (Rao, et al., 2011).

2.3.5 Challenges of machining titanium and its alloys

Titanium and its alloys are classified as difficult-to-machine materials partly due to their thermal properties. Table 2 shows the thermal properties of Ti-6Al-4V and selected aerospace materials. Ti-6Al-4V has a low thermal conductivity and consequently, low thermal diffusivity. The thermal diffusivity of a material measures the ability of a material to conduct thermal energy relative to its ability to store thermal energy. It is determined by using the thermal conductivity, density and specific heat coefficient of a material.

Table 2: Thermal properties of Ti-6Al-4V and comparative materials

Material	Thermal conductivity λ (W/m°C)	Density ρ (kg/m^3)	Specific heat c (J/kg°C)	Thermal diffusivity α (m^2/s)
Ti-6Al-4V	6.7	4430	586	0.026
Inconel 718	12.1	8190	435	0.034
AISI 4340 Steel	33.4	7830	460	0.093
AISI Steel	59	7850	460	0.165
Al 2024	164	2780	883	0.666
Al 6061-T6	177	2710	892	0.733

(Boyer, et al., 1994)

$$\alpha = \frac{\lambda}{\rho c}$$

where α = thermal diffusivity [m^2/s]
λ = thermal conductivity [W/m°C]
ρ = density [kg/m^3]
c = specific heat [J/kg°C]
(Netzsch Thermal Analysis, 2014)

A material with low thermal diffusivity stores heat locally to where it is applied and slowly releases the heat through the rest of the material. As a result, the heat generated when machining titanium cannot dissipate quickly and forms a large thermal gradient at the cutting edge-workpiece interface.

The increase in heat at the tool tip causes the tool to weld to the workpiece surface, resulting in adhesion wear as well as diffusion wear due to the chemical reactivity of titanium (Abdel-Aal, et al., 2009). The different wear mechanisms such as adhesion and diffusion wear are discussed in section 2.4.4.

The increase of temperature is not only a risk for tool failure, but also negatively influences the workpiece surface. At elevated temperatures, titanium reacts with oxygen in the atmosphere to form a layer on the workpiece surface known as α-case (Guilin, et al., 2007). Oxygen, which serves as an α-stabiliser, forms a hard and brittle layer on the machined surface. This layer serves as crack initiation sites for fatigue failure causing premature and catastrophic failure of parts that experience cyclic or dynamic loading (McEvily, 2004). It is therefore, of critical importance, to control and limit the temperature generated during the machining process through the use of appropriate coolant and cutting conditions.

2.4 Milling and conventional machining

2.4.1 Introducing milling

Milling is one of the most important manufacturing processes. There are four different types of manufacturing process for metals, each differing from the others in a fundamental way:

- Solidification processes such as casting and moulding.
- Particulate processing such as pressing and sintering.
- Deformation processes such as forging, extrusion and rolling.
- Material removal processes such as turning, drilling, milling and grinding.

The material removal processes can further be classified into 3 groups, namely conventional machining, abrasive processes and non-traditional machining. Titanium aerospace parts are commonly machined from a solid metal billet, which is manufactured using a combination of manufacturing processes for metals. Typically, the parts are machined from forged billets formed from the titanium sponge which results from the Kroll process after dome further processing (Nagesh & Ramachandran, 2007).

The focus of this project is the milling process that constitutes conventional machining together with drilling and turning. Milling is a machining operation in which a workpiece is fed past a rotating cylindrical tool with multiple cutting edges. The axis of rotation of the cutting tool is mostly perpendicular to the direction of feed. The starting material is a solid piece usually in the form of a forged block or billet. Excess material is removed from the workpiece using sharp cutting tools, that are harder and stronger than the work material, until a desired geometry is formed (Boothroyd, 1989).

The milling process has several benefits. A large variety of material and virtually any solid metal can be machined. It can create a variety of part shapes and geometrical features, which are mostly limited only by tool geometries and the number of axis a machine has. Excellent dimensional accuracy of machined parts is possible with generally good surface finish, depending on the tool geometry and processing parameters used.

As machining is a material removal process, there is a large waste because the original material is simply converted into chips to form the desired part. This conversion into chips constitutes a waste of time, energy and material.

In the following section, several aspects of the milling process are discussed, such as tool properties, cutting strategies and machine requirements. For each of these aspects, the effect of machining on titanium is also discussed.

2.4.2 Tool material

The ideal tool material has a combination of the following properties:

- Toughness – the ability of a material to absorb energy without failing. This is a combination of strength and ductility that is needed to avoid fracture failure of the tool during machining.
- Hot hardness – the ability of a material to retain its hardness at elevated temperature. The tool operates in a high temperature environment as a large amount of heat is generated at the tool tip during machining.
- Wear resistance – the ability of the tool to resist abrasive wear. There are several factors that could influence the wear resistance of a tool such as surface finish, tool-workpiece chemistry and the use of a cutting fluid.

There are numerous tool materials available on the market. It is important to select the right grade for the specific application for which it is to be used. Figure 8 shows the relationship between different tool materials in terms of hardness and toughness. The ideal tool material has a combination of high hardness and high toughness. Considering that titanium and its alloys are classified as difficult-to-machine materials, the most desirable tool material appears to be coated carbide or cemented carbide as shown in Figure 8. This is because the material has the best combination of both hardness and toughness.

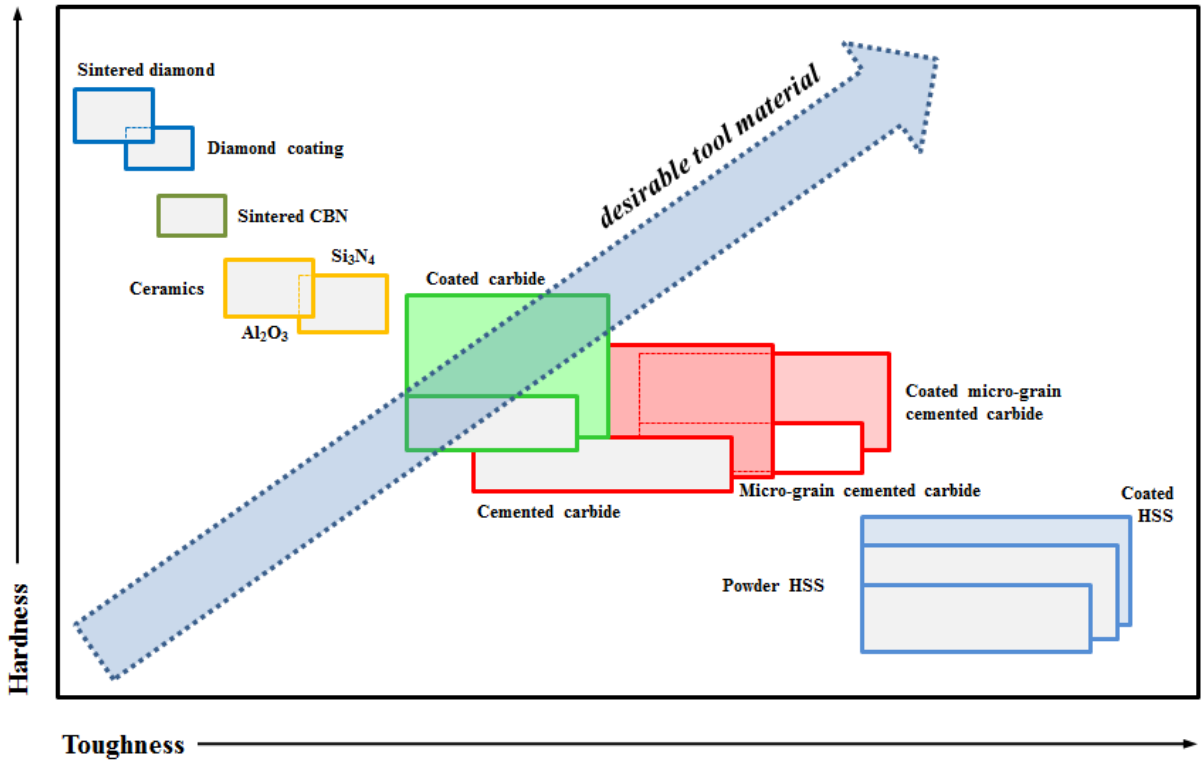

Figure 8: Relationship between various tool materials (Mitsubishi Materials Corporation, 2013)

Figure 9 shows that cemented carbide and sintered diamond can be used to machine non-ferrous metals such as titanium alloys and other high-temperature alloys. The processing parameters of the machining process determine which of the two tool materials should be used.

Sintered diamond is recommended for high-speed machining where the cutting speed is high but the feed per tooth is low. As such, it has an excellent balance between hardness at elevated temperature and fracture resistance. The hot-hardness characteristic of the sintered diamond is important with regards to the elevated temperature but, since the feed rate is low, the toughness of the material can also be low.

Cemented carbides are preferred for lower cutting speeds and higher feed rates. Cemented carbide provides a fair compromise between hot-hardness and toughness and has a high rigidity as well as wear resistance. As a result, it can handle the increased cutting forces that are present when using higher feed rates but cannot be used during high speed machining. Figure 10 shows the difference in microstructures between cemented carbides and sintered diamond substrate.

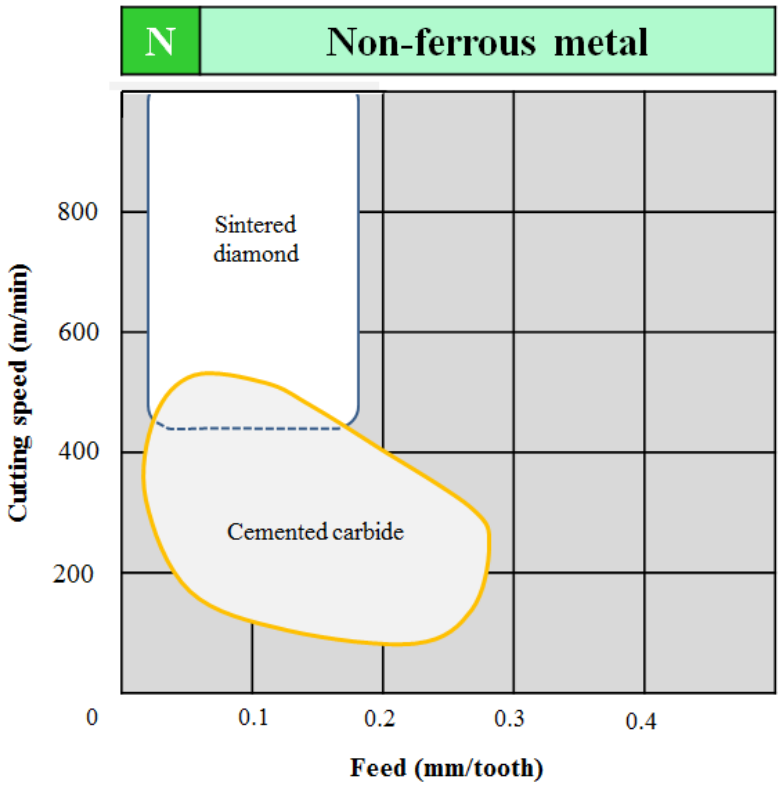

Figure 9: Tool material for machining non-ferrous metal (Leyens & Peters, 2003)

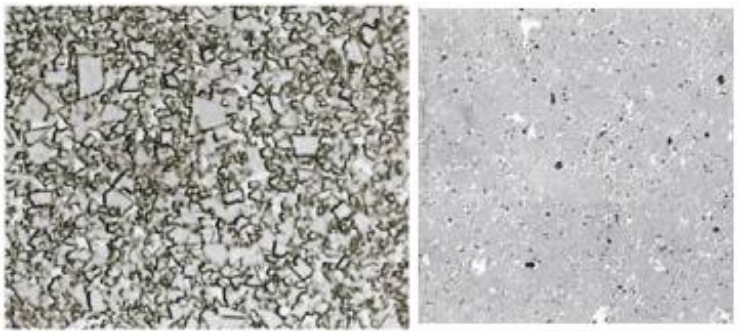

Figure 10: Microstructure of cemented carbide (left) and sintered diamond (right) substrate (100x magnification) (Mitsubishi Materials Corporation, 2013)

2.4.3 Tool coatings

Tool coatings are thin layers of chemical compounds that are applied to the surface of certain cutting tools such as cemented carbides, to improve cutting performance during machining. As shown in Figure 11, these layers can improve the toughness or hardness of a tool, reduce friction, prevent heat build-up between the tool-chip and tool-workpiece interface and, ultimately, improve tool life (Kopac, et al., 2001). The use of tool coatings on tools are dependent on the type of material being machined, the tool used during machining and the process parameters.

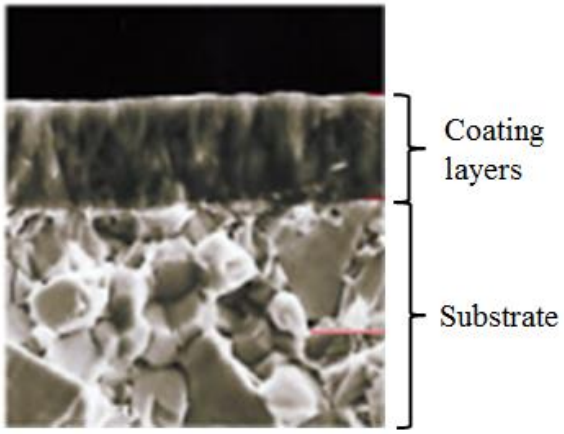

Figure 11: Coating layers on tool substrate (150x magnification) (Mitsubishi Materials Corporation, 2013)

Coated tools are used for ferrous materials such as iron, cast iron and stainless steel (Lin, 2002). Significant improvements of tool life have been realised when machining non-ferrous super alloys such as titanium alloys, especially when high-pressure coolant is not used. Uncoated tools are mostly used when machining non-ferrous or non-metal material such as aluminium, brass, composite materials and wood. However, productivity can be improved through the use of an appropriate diamond coating.

There are two types of tool coating application methods according to which different coatings are categorised, namely chemical vapour deposition (CVD) and physical vapour deposition (PVD) coatings. CVD is a thick coating (9 – 20 μm). The thick coating compromises the edge toughness and sharpness of the material, without which it is highly wear resistant. CVD has a tough fibrous structure that improves the wear and fracture resistance of the cutting surface, and it is highly suitable for the machining of steel and cast iron. CVD coated inserts work well in turning, milling and drilling. It also works better than PVD coatings for machining steel and cast iron.

The most common CVD coatings are TiN and TiC. TiN has excellent built-up-edge resistance. It works well with tough material and it is effective at low cutting speeds. Similarly, TiC has excellent wear resistance and works well in high heat conditions and abrasive materials. It offers excellent crater resistance, and it is suitable for medium to high cutting speeds.

In contrast, PVD is a thin coating (2 – 3 μm). It is tougher and smoother than a CVD coating. It is used to prolong tool life and makes tools with sharp edges possible without changing the quality of the insert substrate. It is used when machining super-alloys, titanium alloys and difficult-to-cut stainless steels.

Common grades of PVD include TiN, TiCN and TiAlN. TiN has excellent built-up edge resistance, and effective on high-temperature alloys and stainless steels. TiCN is harder than TiN coatings and is used on end mills when milling abrasive material. TiAlN is harder and more stable than other PVD coatings. It becomes harder and more stable over time. It can be effectively used on high-temperature alloys and stainless steels.

Currently, multi-layer tool coatings that are commonly used contain a combination of TiN, TiC, TiCN and Al_2O_3, deposited in different sequences (Nouari & Ginting, 2006). In machining titanium alloys, multi-layered PVD-coated carbide tools showed a good performance when face milling Ti-6Al-4V under wet conditions (Jawaid, et al., 2000) (Minevich, 1992). It is thus, recommended that a multi-layered PVD tool coating containing TiN and TiAlN be used during the machining of titanium alloys.

2.4.4 Tool life

Tool life is defined as the amount of time a tool can be used to cut effectively at specified process parameters and workpiece material. This amount of time is influenced by cutting forces, heat generated during machining and various other mechanisms, which cause the tool to fail prematurely. There are three types of modes that can cause a tool to fail, namely fracture failure, temperature failure and gradual wear (Groover, 2007). The first two factors can be prevented through the use of appropriate process parameters and cooling methods. Although gradual wear cannot be prevented, it can be managed to ensure the longest possible tool life against economic considerations. Gradual wear is due to various mechanisms as summarised in Table 3.

In experiments done by Jawaid (Jawaid, et al., 2000), the wear mechanisms that influence tool life when machining titanium alloys were coating delamination, adhesion of work material, attrition, diffusion, plastic deformation and thermal cracks. The coating delamination exposed the tool substrate to chemical and attrition wear processes and attrition was mostly attributed to diffusion. Most of the tool wear mechanisms were initiated once the coating delaminated. The delamination occurred approximately 10 seconds after the start of machining, which renders the effectiveness of the coating questionable. As observed by various researchers (Jawaid, et al., 2000) (Nabhani, 2001), delamination is attributable to either a chemical reaction or crack propagation at substrate level. Less delamination was seen at lower cutting speeds, which could indicate that the coating is sensitive to more aggressive cuts. Thus, the delamination of the coating on the insert has a significant influence on the initiation of tool wear. To maximise the tool life of coated carbide tools, the cutting parameters have to be selected accordingly.

Table 3: Tool wear mechanisms (Groover, 2007)

Wear type	Description
Abrasion	Mechanical wearing action due to hard particles in the work material gouging and removing small portions of the tool.
Adhesion	When two materials are forced into each other under high pressure and temperature, adhesion or welding occur between them. As the chip flows across the tool, small particles of the tool are broken away from the surface, resulting in attrition of the surface.
Diffusion	This is a process in which an exchange of atoms takes place across a close contact boundary between two materials. In the case of tool wear, diffusion occurs at the tool-chip boundary, causing the tool surface to become depleted of the atoms responsible for its hardness. As the process continues, the tool surface becomes more susceptible to abrasion and adhesion. Diffusion is believed to be a principle mechanism of crater wear and the rate of diffusion increases with an increase in temperature.
Chemical reactions	The high temperatures and clean surfaces at the tool-chip interface in machining at high speeds can result in chemical reactions, in particular, oxidation, on the rake face of the tool. The oxidised layer, being softer than the parent tool material, is sheared away, exposing new material to sustain the reaction process.
Plastic deformation	Another mechanism that contributes to tool wear is plastic deformation of the cutting edge. The cutting forces acting on the cutting edge at high temperature cause the edge to deform plastically, making it more vulnerable to abrasion of the tool surface. Plastic deformation contributes mainly to flank wear.

2.4.5 Insert geometry

This section provides an overview of the different geometric features on a cutting insert and the effects that changing the different features have on the machining process.

2.4.5.1 Rake angle

The rake face of the tool is oriented at an angle called the rake angle. The rake angle is measured to a plane perpendicular to the surface of the workpiece. The rake face determines the direction of chip flow and has a large influence on cutting resistance, chip formation and disposal, cutting temperature as well as the tool life. The rake angle is classified as positive, negative or neutral as depicted in Figure 12.

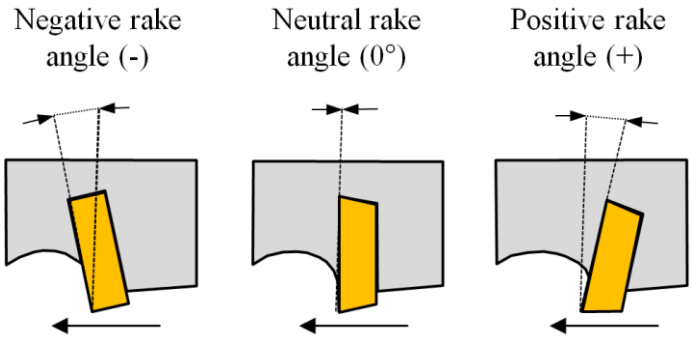

Figure 12: Positive and negative rake angles (Mitsubishi Materials Corporation, 2013)

A positive rake angle will be used on a soft workpiece that is easily machined and when the workpiece or machine has poor rigidity. An increase in the positive direction of the rake angle improves the sharpness of the cutting edge, which decreases the cutting power but lowers the cutting edge strength. However, when cutting edge strength is needed (such as interrupted cutting and hard workpieces), a reduction of the rake angle, even into negative values, is favourable.

When machining titanium, the general rule is to use a 5° to 20° positive rake angle. Increasing the rake angle by 1° cutting power decreases by 1% (Mitsubishi Materials Corporation, 2013). The increase in sharpness of the tool allows the insert to be used on a machine that is less powerful and has poor rigidity. The increase in rake angle also reduces the time the chip is in contact with the insert, thus, reducing tool wear on the rake face caused by diffusion wear.

2.4.5.2 Flank angle

The flank angle on a tool is the orientation of the flank face to a tool, measured relative to the surface of the workpiece. The flank angle, also known as the relief angle, provides a clearance between the tool and the new work surface, which prevents friction between the flank face and workpiece, and results in a reduction in the cutting forces, a smoother feed and reduced abrasive wear on the flank face of the insert.

An increase of the flank angle results in a decrease of the flank wear of an insert that also lowers the strength of the cutting edge. The relation of flank angle to flank wear is illustrated in Figure 13. The flank angle is to be increased when working on soft workpieces and those that tend to harden easily because an increase in flank angle results in less friction, and consequently, less heat is built up. The smaller flank angle is to be used on hard workpieces when a stronger cutting edge is required.

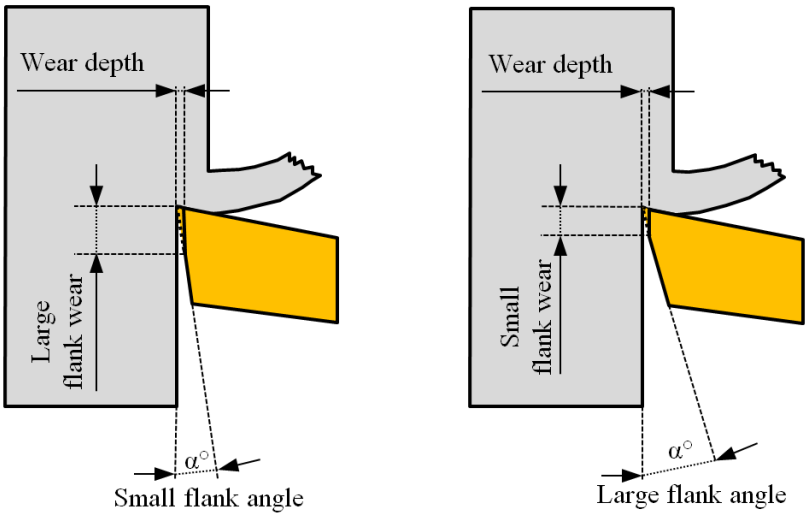

Figure 13: Flank angle relating to flank wear (Mitsubishi Materials Corporation, 2013)

When machining titanium, it is recommended that a flank angle of 6° to 12° be used (Defence Metals Information Center, 1965). Angles less than 5° encourage flank wear resulting from abrasion. Larger flank angles are better but they increase the likelihood for tool chipping.

2.4.5.3 Side cutting edge angle (lead angle)

The side cutting edge angle (also known as the lead angle) is the angle at which the cutting edge is orientated relative to a plane perpendicular to the surface of the workpiece. The side cutting edge has an influence on the cutting forces and chip thickness. An increase in the lead angle results in an increase in the contact area between the cutting edge and the workpiece, as well as a decrease in the chip thickness, as illustrated in Figure 14. This results in the cutting force being dispersed on a longer cutting edge, thus decreasing the cutting resistance and increasing the tool life.

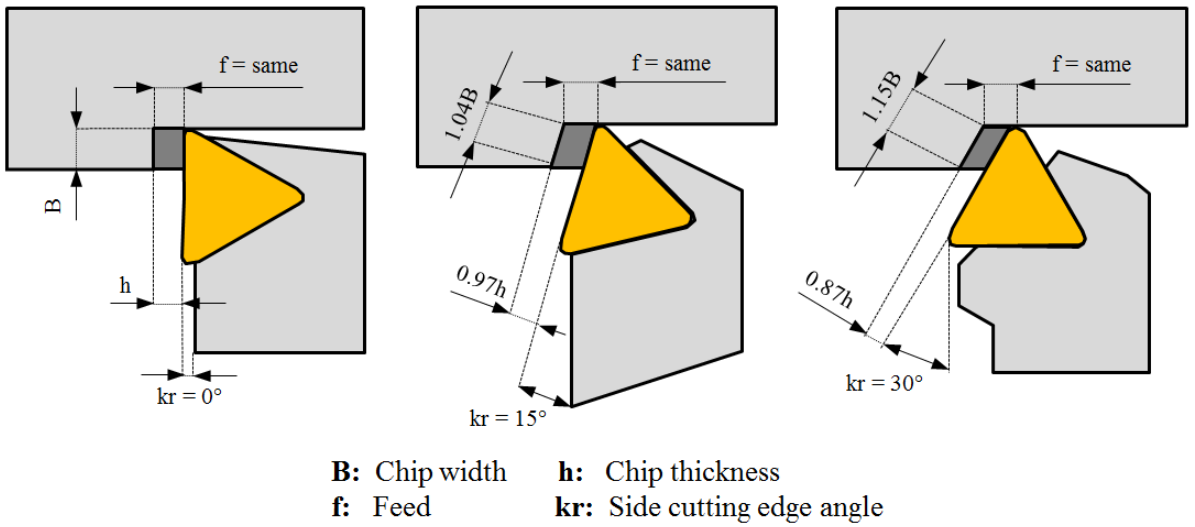

Figure 14: Side cutting edge angle and chip thickness (Mitsubishi Materials Corporation, 2013)

Figure 15 illustrates the influence that the lead angle has on the cutting forces occurring at the cutting tool-workpiece interface. A lead angle larger than 0° results in a change in vector of cutting force A, where the force gains an a and a' component. An increase in the lead angle increases the force a', causing long thin workpieces to experience deformation during machining.

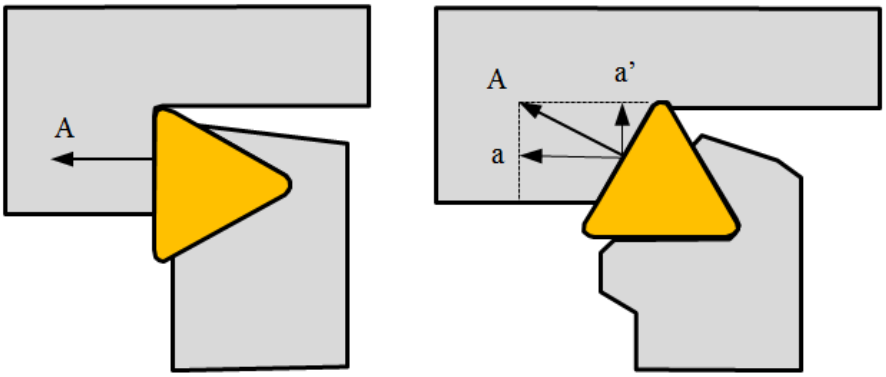

Figure 15: Distribution of cutting force A in lead angle = 0° (left) and lead angle > 0° (right) (Mitsubishi Materials Corporation, 2013)

When machining titanium, it is recommended that a large lead angle be used as this increases the contact area between the cutting edge and the workpiece surface, resulting in a decrease tool wear attributed to elevated temperature.

2.4.5.4 End cutting edge angle

The end cutting edge angle is the angle between the newly cut workpiece surface and the leading edge adjacent to the cutting edge. Figure 16 illustrates where this angle is located and how it is measured. The end cutting edge angle provides clearance between the insert and workpiece surface, and it is usually between 5° and 15°.

A smaller edge angle increases the cutting edge strength but it also reduces the clearance between the insert and the workpiece surface resulting in an increase in friction and cutting edge temperature. A smaller edge angle also increases the back force between the insert and the workpiece, which causes chattering and vibration during machining. It is thus recommended that a small end cutting edge angle be used in roughing and large angle be used in finishing operations.

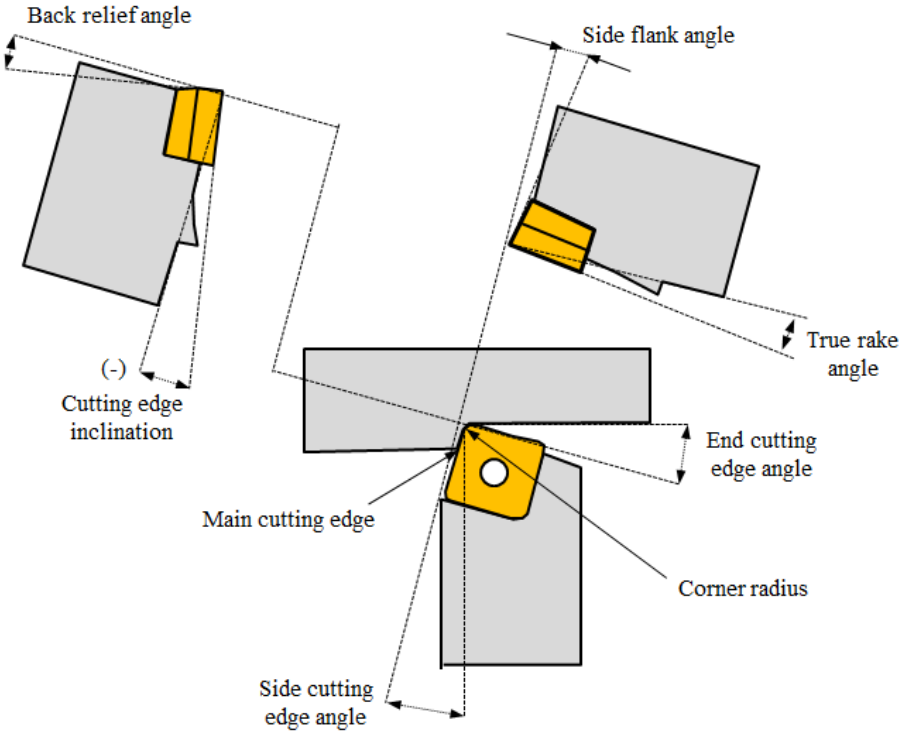

Figure 16: Classification of side and end cutting edge angles (Mitsubishi Materials Corporation, 2013)

2.4.5.5 Honing and land

Honing and land refers to the shape of the cutting edge that influences its strength. Honing can be either round or have a chamfer. A land is a flat area on the rake or flank face adjacent to the cutting edge. Figure 17 illustrates the different types of honing and land, and their use.

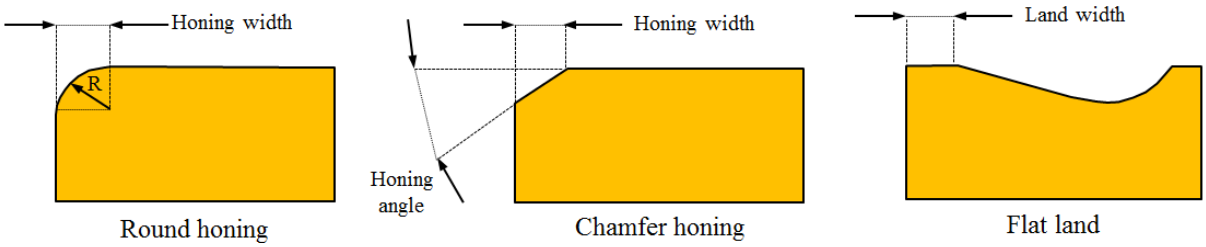

Figure 17: Illustration of honing and land (Mitsubishi Materials Corporation, 2013)

An increase in honing results in an increase in cutting edge strength and a reduction in cutting edge fracturing. As the cutting edge surface area is increased, the increase in honing also increases the occurrence of flank wear, cutting resistance and chattering. A land is used as a compromise between a sharp cutting edge with reduced power requirements and the strength of a dull tool. The most desirable honing and land width is approximately ½ of the feed per tooth.

When machining titanium, a sharp tool is recommended. Consequently, the use of honing is not recommended as the increase in contact area between the cutting edge and the workpiece results in an increase in the cutting forces and friction. The use of a land is recommended considering that a tool with

a sharp cutting edge can be sharp at the cutting edge, with the angle of the rake and/or flank face having a different angle according to requirements. The result is a sharp tool with an increase in cutting strength.

2.4.5.6 Corner radius

The corner radius refers to the radius of the corner between the side cutting edge and the end cutting edge, as illustrated in Figure 16 above. The corner radius affects the strength of the cutting edge and the surface finish of the machined workpiece. As such, an increase of the corner radius improves the cutting edge strength and surface finish of the workpiece. Figure 18 shows how an increase in the corner radius results in an improved theoretical surface roughness, if the feed and depth of cut is kept constant. A larger corner radius increases the insert cutting edge contact length, thus, increasing the cutting resistance and causing chattering. On the one hand, a large corner radius results in poor chip control as the width of the chip also increases with the corner radius. A decrease in corner radius, on the other hand, increases flank and rake wear, as the cutting forces is concentrated on a smaller surface (Endres & Kountanya, 2002).

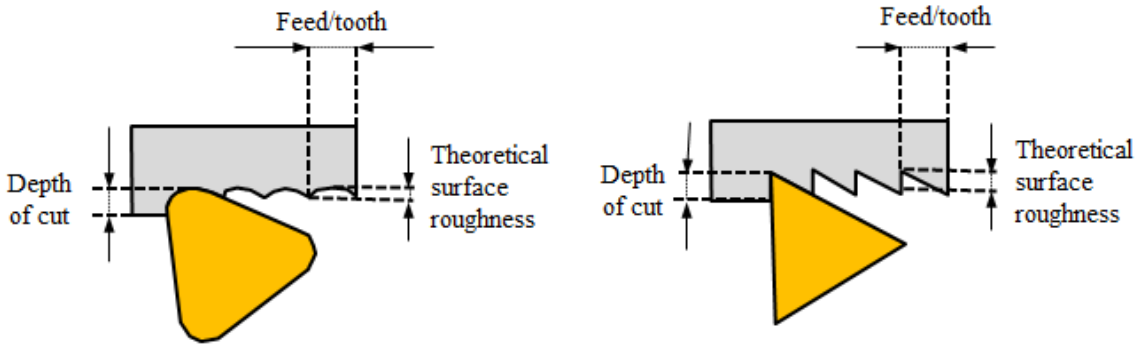

Figure 18: The effect of corner radius on surface finish (Groover, 2007)

When machining titanium, a larger corner radius is recommended to increase the strength of the cutting edge. Care should be taken not to make the corner radius too large to keep the cutting resistance to an acceptable level and to reduce chattering (Mitsubishi Materials Corporation, 2013).

2.4.5.7 Corner angle

The corner angle is the angle between the side cutting edge and the end cutting edge. The corner angle has an effect on the chip thickness. The larger the corner angle, the thinner the chip thickness, as illustrated in Figure 19. With a corner angle of 0°, the chip thickness is equal to the feed per tooth, where the chip thickness with a corner angle of 45° has a chip thickness of a factor of 0.75 the feed per tooth.

The corner angle has an additional effect on the crater wear on the rake face of a tool. With a smaller corner angle, the chip is thicker, increasing the cutting resistance and promoting crater wear. As the crater develops, the cutting edge strength is reduced until fracture of the cutting edge occurs. For titanium a relatively large corner is recommended to reduce chip thickness and the resulting cutting forces.

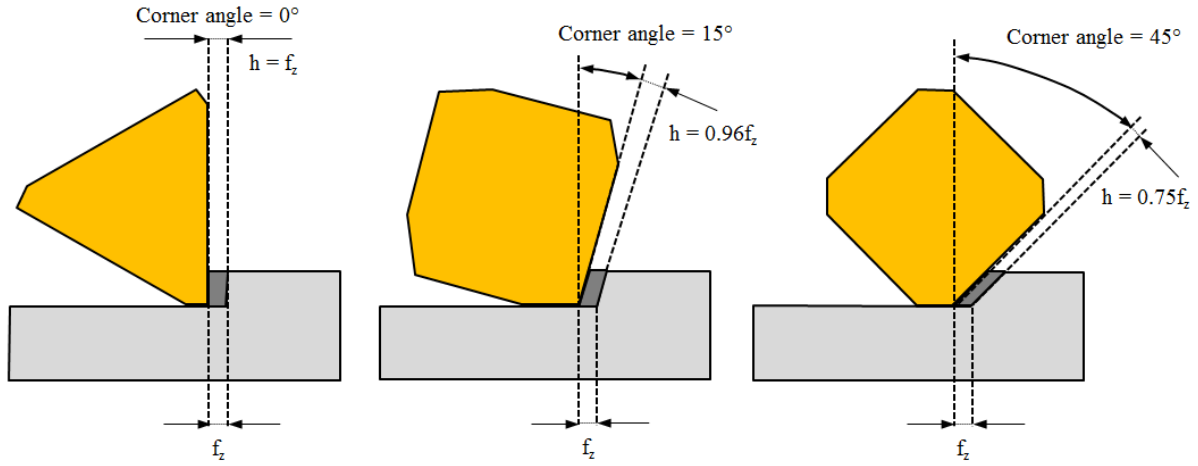

Figure 19: Effect on chip thickness with different corner angles (Mitsubishi Materials Corporation, 2013)

2.4.6 Other applicable angles

There are a few other minor angles that have an influence on the face milling process. These angles refer to the way in which the inserts are orientated on the tool holder relative to the workpiece and axle of tool rotation. Table 4 serves as a summary of these angles, which are illustrated in Figure 20.

Table 4: Function of each cutting edge angle in face milling

Type of angle	Function	Effect
Axial rake angle	Determines chip disposal direction	**Positive:** Excellent machinability
Radial rake angle	Determines sharpness	**Negative:** Excellent chip disposal
Corner angle	Determines chip thickness	**Large:** Thin chips and small cutting impact Large back force
True rake angle	Determines actual sharpness	**Positive(large):** Excellent machinability Minimal welding **Negative(large):** Poor machinability Strong cutting edge
Cutting edge inclination	Determines chip disposal direction	**Positive(large):** Excellent chip disposal Low cutting edge strength

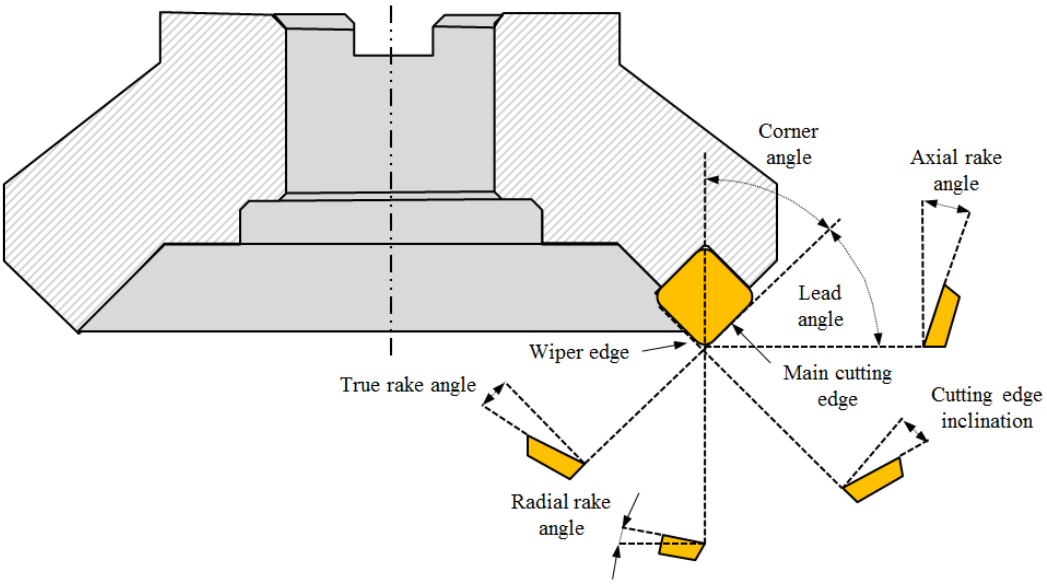

Figure 20: Cutting edge orientation in face milling (Mitsubishi Materials Corporation, 2013)

2.4.7 Cutting direction

The cutting direction refers to the direction of rotation of the tool cutter. The two directions can be distinguished into conventional milling and climb milling, as illustrated in Figure 21.

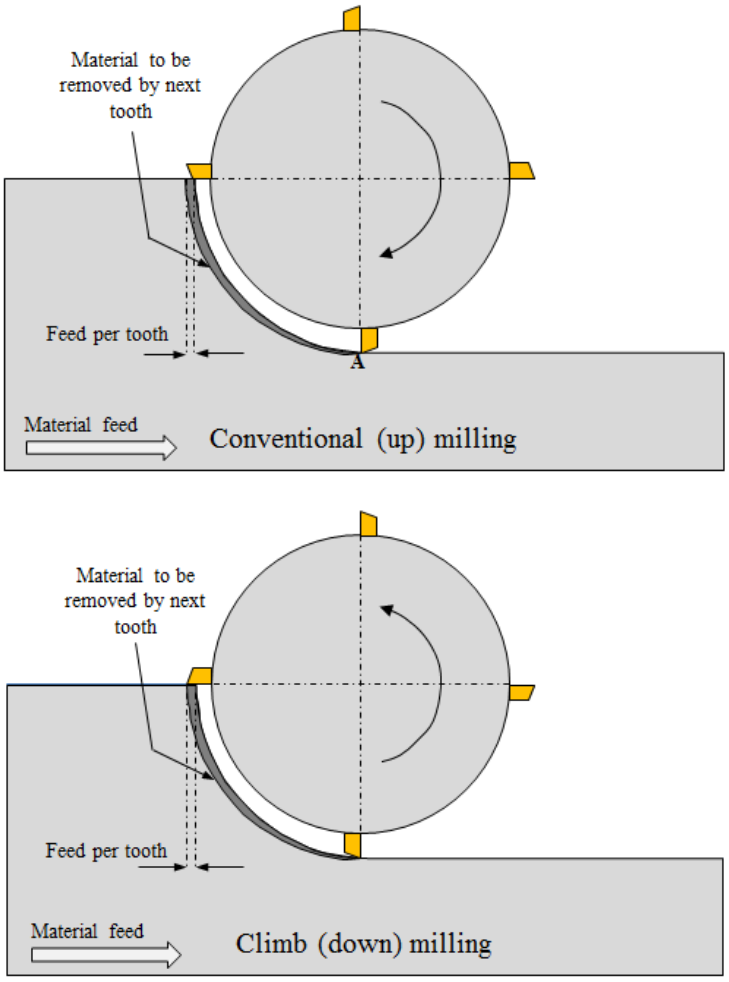

Figure 21: Conventional milling vs. climb milling (Groover, 2007)

In conventional milling (also known as up milling), the direction of motion of the cutter teeth is opposite to the feed direction when the teeth cut into the workpiece, i.e. milling against the feed. The chip thickness starts at zero and gradually increases to the size of feed per tooth of the cut. Initially, the cutter teeth do not cut the material but slides on the material until sufficient pressure starts to engage the material. As a result of the pressure, the material is deformed at the point where it comes into contact with the material (point A in Figure 21) work hardening it. The initial sliding cause tool wear and a poor surface finish on the workpiece but the cutting forces are low.

In climb milling (also known as down milling), the direction of motion of the cutter teeth is the same as the direction of the feed, i.e. milling with the feed (Groover, 2007). Here, the tool engages the material at a definite point, starting at the feed depth and ending at a chip thickness of zero. As the tool does not slide, the tool wear is decreased but the cutting forces are higher. This type of milling is not suited for older milling machines.

Climb milling is standard practice when milling titanium and its alloys. Friction and sliding between the insert and workpiece is minimal as the tool enters the material at full feed depth. Heat is reduced by dissipating it partly into the chip and partly into the insert. With less heat entering the workpiece and less pressure between the tool and the workpiece surface, work hardening is reduced.

2.4.8 Chip Formation

During the machining process, excess material is removed from a workpiece to create a part. The excess material that is removed is in the form of chips. These chips provide insight into the machining process and can be used as a diagnostic tool into the cutting temperature, cutting speed, tool geometry, material type, tool wear and overall effectiveness of the process.

In the machining process, the cutter tooth shears the chip from the surface of the workpiece, giving it a certain profile. As illustrated in Figure 22, there are two distinct shear zones during machining, namely the primary and the secondary shear zones. The primary shear zone is the zone where the newly formed chip experiences drastic deformation, from where it is part of the workpiece to where it is in the form of a chip. The secondary shear zone is where the chip passes over the surface of the tool. This shear results from the friction of the chip moving over the surface of the rake face of the tool. The friction between the tool and the chip is responsible for the rake wear on a tool.

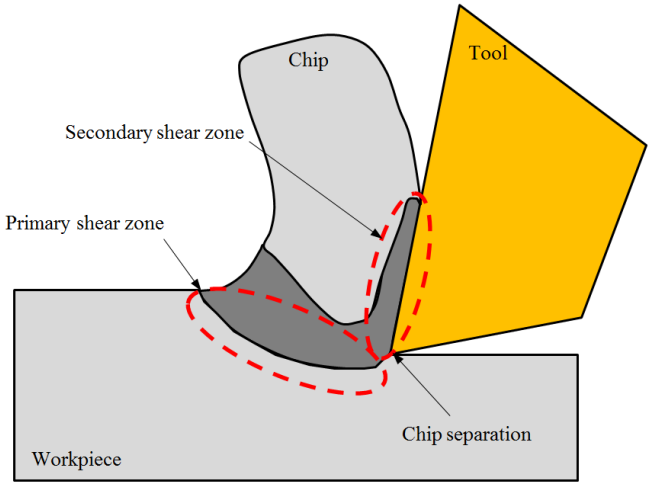

Figure 22: Chip formation shear zones (Bayoumi & Xie, 1995)

Chips can be distinguished into 4 types: discontinuous chips, continuous chips, continuous chip with built-up edge and serrated chips. Of importance to this study are the serrated chips, also called segmented chips, which are produced when machining certain difficult-to-machine materials such as titanium alloys, nickel-based super-alloys, and when a material such as steel is cut at high speed (Sun, et al., 2009). On these chips, each segment has bands of high deformation and little deformation, which are the high shear and low shear zones respectively. These zones are indicated on Figure 23.

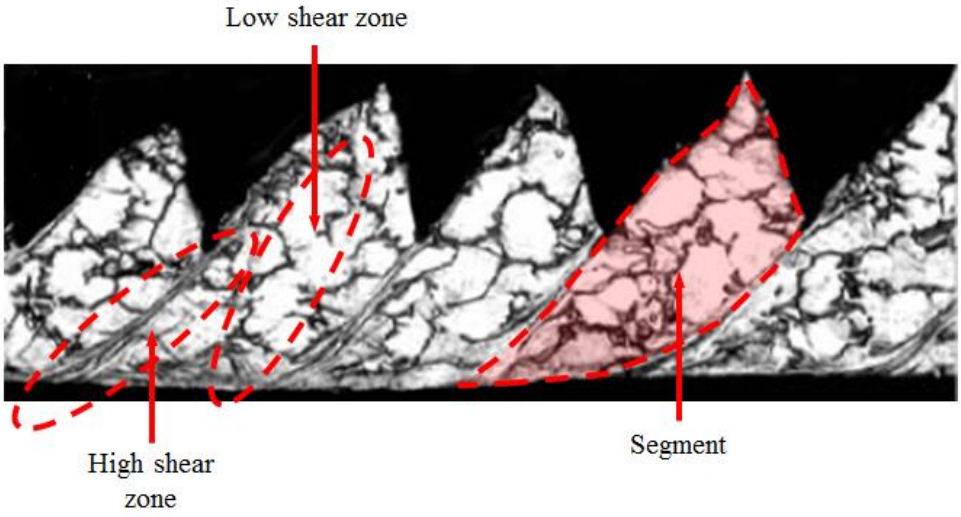

Figure 23: Micrograph of titanium chips showing shear zones (Gente & Hoffmeister, 2001)

Serrated chips create fluctuations in the cutting force as the different strain zones are formed. The fluctuation in cutting force is increased when cutting α-β titanium alloys (Komanduri & Von Turkovich, 1981). This fluctuation of force, together with the high temperature at the tool-workpiece interface, exerts a fatigue loading on the cutting tool, which is believed to be partially responsible for flank wear. The contact length between the chip and the tool is extremely short and implies that the high cutting

temperature and the high cutting forces are concentrated near the cutting edge, which exerts a significantly influence on the tool life.

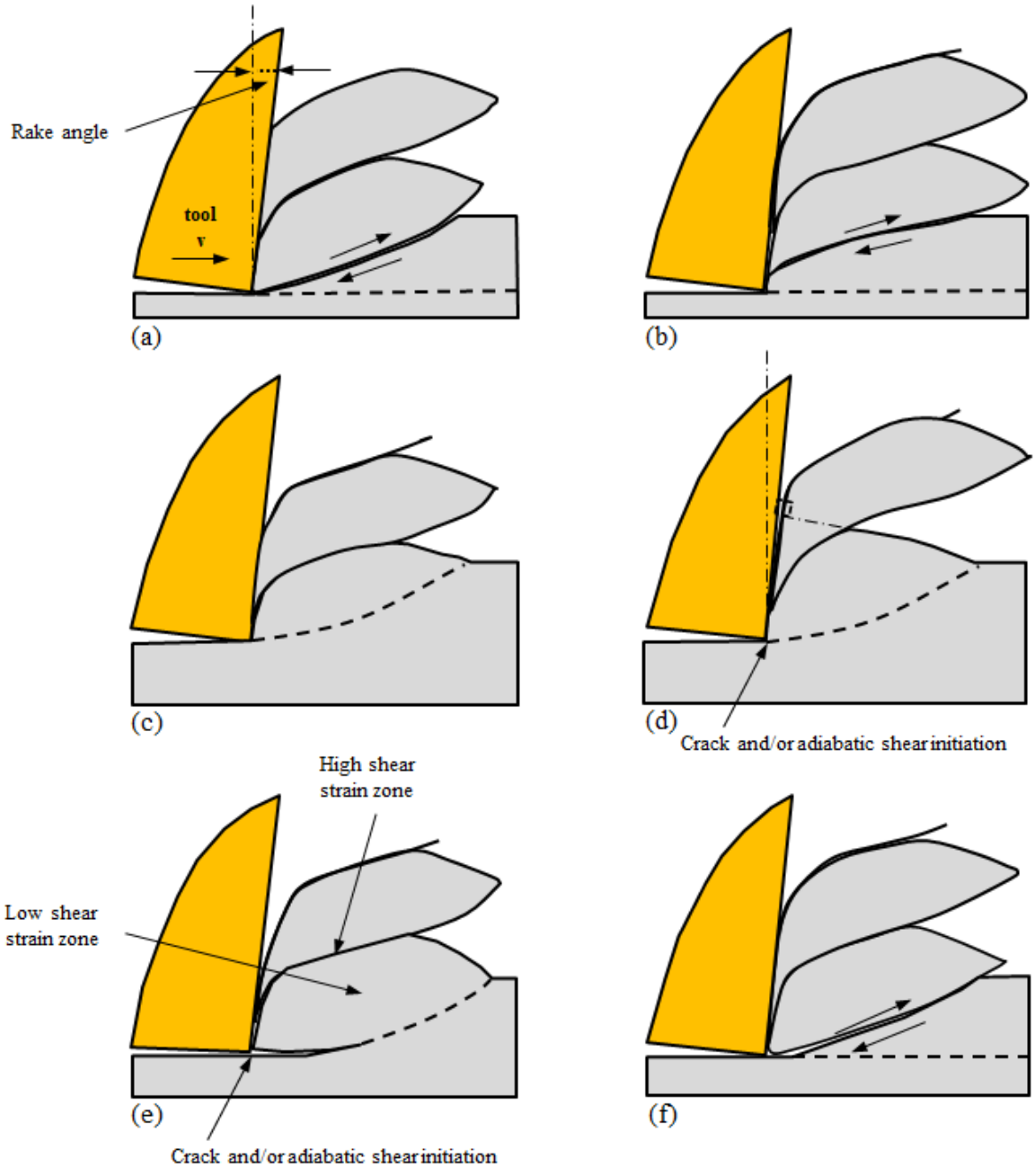

Figure 24: Schematic diagrams of a sequence of events, showing various stages involved in chip formation when machining titanium alloys (Komanduri & Von Turkovich, 1981)

Figure 24 (a – f) illustrates the sequence of events, showing how the serrated chips are formed when machining titanium alloys. The segment starts building up before the tool in a wedge shape and starts to lengthen in the flattening process. There is almost no relative motion between the lower part of the chip segment and the tool until the flattening stage is complete. The contact area between the tool and the chip is small, which forces a rapid transfer of heat to the tool tip. Thus, the heat and contact time on the

small area results in a chemical reaction between the tool and the chip causing accelarated tool wear (Komanduri, 1982).

In the next stage (Figure 24 (c)), the chip starts to bulge and forces the chip segment upwards. The cutting forces are at maximum as the chip is bulging, then quickly decrease as the crack is initiated and starts propagating when shear failure occurs. This process repeats itself as each segment is formed, leading to vibration and fatigue of the tool. Depending on the compliance of the tool-work material-machine tool system, complex vibratory events may also take place during cutting.

2.4.9 Cutting fluids

There are two different types of cutting fluids, namely coolants and lubricants. Each type addresses a different challenge: cooling and lubrication. Cutting fluids address the heat generated at the shear and friction zones at the tool-chip and tool-workpiece interfaces, where these zones are illustrated in Figure 22, section 2.4.8.

Coolants have a limited effect on the cutting process itself but, primarily, they absorb and remove the heat generated (Su, et al., 2006). The most important properties of coolants are their thermal properties (Groover, 2007). As such, water based solutions or water emulsions are ideal due to their favourable thermal properties. Lubricants are oil based fluids that reduce the friction between the tool-chip and tool-workpiece interface. The properties of both types of cutting fluid sometimes overlap when additives are added to protect the newly machined surface against atmospheric corrosion and bacterial growth, especially when reused. Effective use of cutting fluids can have a significant effect on tool life, surface finishing and machining economics as higher cutting speeds can be realised.

Cutting fluids, especially coolants, are used in a method called flooding, where the zone in which heat is generated is simply flooded with a stream of directed coolant. This also serves as a way to flush away machined chips and reduce recutting of chips, which can contribute to tool wear. Lubricants can be added through manual application such as a brush or squirt can, or automatic application using spray nozzle or through-spindle lubrication (Brinksmeier, et al., 1999). The use of through-spindle cooling has steadily seen an increase in use, especially with high speed machining applications (Ezugwu, et al., 2007). This allows the coolant to be delivered at the cutting edge of the tool and the high pressure stream of coolant to act as a barrier between the chip and the cutting edge, reducing recutting of chips and crater wear.

There is a renewed focus on the use of no cutting fluids, called dry machining (Dudzinski, et al., 2004). Dry machining eliminates the environmental issues that result from cutting fluid disposal but can lead to a decrease in tool life, lowered cutting speed and no chip removal benefits. Certain carbide grades have been developed to be used effectively with dry machining.

For the machining of titanium, the use of through-spindle cooling is recommended. However, high-pressure through-spindle cooling is only available on certain machines, and the tool has to be designed to be used for through-spindle cooling. Wet emulsion lubrication is recommended for most tools and machines where through-spindle cooling is not available although dry cutting has also been successfully used. It is therefore recommended that the instructions of the tool supplier companies be followed since each tool is made with a specific cooling method in mind (Iscar, 2012) (Mitsubishi Materials Corporation, 2013).

2.4.10 Milling machine requirements

The milling machine plays a critical role in the machining process as it delivers all the energy and power to enable the cutting process. The key components of the machine are the work table where the workpiece is clamped, the spindle that holds the tool and provides torque on the tool to allow cutting, and the computer that controls the cutting parameters as well as the relative positions of the tool and work table. The milling machine has a specified amount of axes (typically either 3, 4 or 5 axis) that refers to the way a workpiece can be orientated. Machines with more axes can produce more complex geometries. Figure 25 shows a picture of a Hermle C40U Dynamic milling machine as found at the Advanced CNC Machining Laboratory at Stellenbosch University.

Figure 25: Hermle C40U Dynamic 5-axis machining centre

Each spindle has a characteristic curve that shows the relationship between the maximum power output and spindle speed. As spindle speed increases, the power and subsequently the torque output is decreased, as illustrated in Figure 26. When machining titanium alloys, the power requirements are high as the specific energy of titanium alloys are high. The spindle characteristic curve for the milling machine has to be referenced to ensure the machine can handle the power required at the desired cutting speed (Groover, 2007) (Siemens AG, 2011).

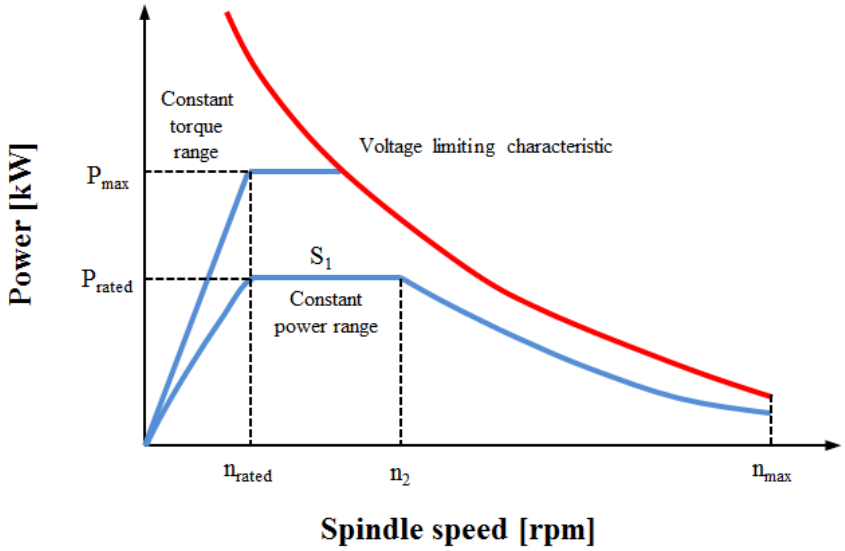

Figure 26: Spindle characteristic curve (Siemens AG, 2011)

The size of the work area is also important as this determines the size of the parts that can be machined. The mounting of the workpiece has to be considered as it reduces the size of the part that can be machined.

When machining titanium, one of the largest challenges encountered is the rigidity of the machine. The rigidity is determined as a combination of the spindle, the tool, the workpiece and the mounting. The system has to be rigid as there is a high fluctuation in cutting forces as was discussed in section 2.4.8. This fluctuation in cutting forces results in a vibration, causing movement of the workpiece on its mount, which reduces dimensional accuracy and increases cutting forces.

The CNC milling centre has a built-in cutting fluid delivery system in place such as flood cooling or through-spindle cooling. Figure 27 shows a tool and machine that has through-spindle cooling capabilities. The machine also has a tool magazine that can hold around 20 different cutting tools, allowing rapid tool changeovers for different geometries and cutting operations.

Figure 27: Spindle, tool holder and cutting tool on milling machine

2.5 Conclusions

All the relevant aspects of the machining of titanium alloys have been investigated and recommendations have been made. Table 5 shows a summary of all the recommendations that have been made, which include the tool insert material, tool coatings, applicable insert angles, expected chips and cutting fluids to be used.

These recommendations would be used further on in the project during experimentation. The recommendations will then be re-evaluated, leading to the use of an improved machining process at the industry partner.

Table 5: Summary of recommended insert geometry for machining titanium

Property	Recommendation
Insert material	Cemented carbide insert (WC-Co)/sintered diamond
Insert coating	Multi-layered PVD coating of TiN/TiCN/TiAlN
Rake angle	5° - 20° in the positive direction
Flank angle	6° to 12°
Side cutting edge angle	Relatively large angle
End cutting edge angle	Relatively small angle
Honing and land	Honing is not recommended, but land could be used
Corner radius	Relatively large radius
Corner angle	Relatively large corner angle
Cutting strategy	Down (climb) milling
Chip formation	Serrated chips
Cutting fluids	Flood or dry cutting (where through spindle cooling is not available)

3. Case study at industrial partner

3.1 Introduction

In the previous chapter, a detailed review of literature relating to the topic under investigation was presented. The current chapter discusses the case study at the industrial partner including case selection, selection of the demonstration part and the analysis of existing processes.

A critical part of the AMTS initiative is the transfer of key knowledge areas to the industry. As part of the study, therefore, collaboration with an industry partner was needed to facilitate experimentation, and to develop as well as transfer key competencies. An industry partner was identified and the machining process of selected parts was studied and improved. The case study served as an exploratory phase of the project to identify where improvements in the machining process could have been realised. The current machining process was documented, pilot experimentation was done and knowledge on the improved process was transferred to the industry partner.

3.2 Selection of industry partner

Working with an industry partner formed a key part of the project. The industry partner was selected on the basis of the following criteria:

The company:

- has to have capabilities to machine materials economically
- should not be established in the titanium manufacturing industry yet
- should be preferably locally based in the surrounding region (Cape Town)
- must have existing and established aerospace contracts
- has the potential to machine titanium

Daliff Precision Engineering (Pty) Ltd was chosen as the industry partner since it conformed to all the criteria specified and it had previous relationships with the university. The company had existing contracts with large aerospace companies and was ISO 9001 certified. They previously had contracts for machining titanium parts, but it was found that they could not machine the material economically. As a result they did not have existing contracts for machining titanium parts at the time.

Daliff has some existing contracts for the machining of parts made from difficult-to-machine metals and super-alloys. A decision was made to study these processes in order to assess their capabilities, determine the feasibility of machining titanium parts and the factors that contribute to not being able to machine titanium economically.

3.3 Selection of demonstration part

The purpose of selecting an existing demonstration part and examining the current processes was to propose improved processes for manufacturing aerospace parts at the industry partner. The starting point for the study was the selection of aerospace parts made from difficult-to-machine material or super-alloys. The process to machine this part was studied to determine whether the parts were effectively machined. As Daliff has standing relationships and contracts with various companies in the aerospace industry, they were asked to recommend candidate aerospace parts according to certain selection criteria.

The parts would be evaluated according to properties and features from section 2.2, as summarised below. The parts:

- have to be aerospace parts, with the applicable geometry and features such as pockets, thin-walled, thin-based, bosses, holes, ribs, radii and undercuts
- are to be machined from a solid metal billet with a high amount of material to be removed
- have to be made in small quantities, but high variety of similar geometries
- have to be cyclic with a constant, low volume demand

Additionally, Daliff had to have existing orders for these parts so that the machining process could be analysed.

The first candidate part that was investigated, from the possible aerospace parts recommended by Daliff, was a machined dome, presented in Figure 28. The part had to be manufactured from titanium and Daliff was in the process of acquiring a contract for production of this part. Various manufacturing techniques were investigated to manufacture this part, including machining on a lathe and milling as well as near-net shaping using abrasive water-jet cutting and rotary forging.

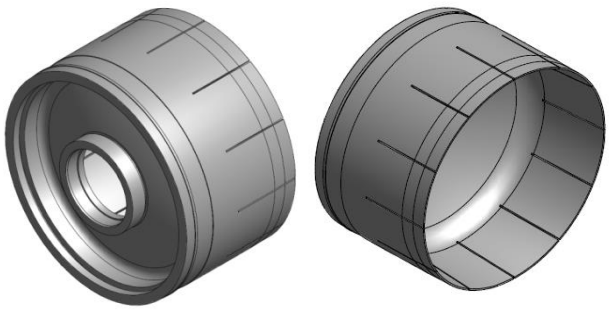

Figure 28: Isometric views of the machined dome.

Rotary forging was identified as a possible manufacturing technique for the machined dome, as a near-net shaping technique. The part would be forged into a near-net shape and machined to final shape using conventional milling. The near-net shaping process would reduce the amount of material to be removed from the billet, thus, effectively reducing machining time. After initial investigation, other candidate

parts were selected because the near-net shape processing did not fit into the project framework and Daliff was not awarded the order for the machined dome.

Daliff was approached for further candidate parts that had standing orders for the near future as well as a profile that aligned with the project roadmap. Two parts were identified that suited the criteria, i.e. the spigot rib and lug rib presented in Figure 29. Both parts have a similar machining strategy, size and use the same billet size.

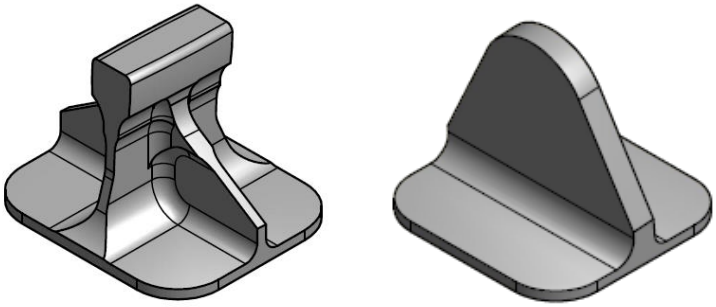

Figure 29: Spigot Rib (left) and Lug Rib (right)

The spigot rib and lug rib are both manufactured for the same customer. Both of these parts are made from 15-5 PH stainless steel that has similar physical properties as Ti-6Al-4V, as described in Table 6. The lug rib had a monthly order of a batch of 8 parts whereas the spigot rib had an order of 4 parts per quarter. Table 6 gives a summary of selected properties of the selected candidate parts. Owing to the scheduling of part production, only the machining process of the lug rib could be analysed. Although the lug rib had a significantly less complex geometry when compared to the spigot ribs, it was deemed suitable for the scope of the project.

Table 6: Selected properties of candidate parts

	Spigot rib	**Lug rib**
Rough dimensions	68 (l) x 58 (w) x 53 (h) [mm]	64 (l) x 62 (w) x 55 (h) [mm]
Billet size	Ø 90 x 90 [mm]	Ø 90 x 90 [mm]
% material machined away from original billet	94.98%	95.035%
Existing machined time	380 min (estimated*)	156 min (measured)
Material	15-5 PH Stainless steel	15-5 PH Stainless steel
Part number	M53811422	M53810337

* No order for spigot ribs had been placed at the time. Time estimated from quotes and historical data.

3.4 Analysis of existing process at industry partner

The analysis at the industry partner consisted of identifying the different machining processes that were required to machine the lug rib. Daliff had a certain protocol that had to be followed when machining each of these parts as these were classified as critical. Part integrity and tolerances were of high priority. Traceability was also important since all properties of the part and material needed to be documented

and traced to source. For the analysis, each of these processes was observed, the cutting parameters documented and the time taken to complete each process measured. This information was used to gain insight into the different machining processes and to determine where machining time and costs could be saved.

The demonstration parts were machined according to Daliff's standard machining strategies using conventional 5-axis CNC milling machines and tools. According to agreements with the customers, no part of the fabrication process could be sub-contracted to ensure part integrity and process control. The entire manufacturing process was consequently dependent on the facilities at Daliff. The standard machining process consisted of the following list of operations:

1. Roughing - where the majority of the material volume is removed using a larger roughing cutter.
2. Rest roughing - where some material is removed to create features using a smaller roughing cutter.
3. Semi-finishing - where some features are defined using smaller tools before using a ball nose cutter
4. Finishing - where the surface is machined with a ball nose cutter to the required surface finish.
5. Drilling - where all the required holes are drilled in the part.
6. Final finishing - that may include various tools to deburr corners, ream holes and give final required surface finish.

To prepare the billet for machining, the billet was attached to a mounting plate connected to a riser, to allow the spindle to reach all the features of the part without having the operator to reposition the workpiece. The riser was connected to the machining bed and the machining process was initiated by the operator. The machining centre was equipped with a tool selection carousel capable of making automatic tool changeovers. The tool changeovers took only a few seconds and did not require any input of the operator.

The process for the machining of the lug rib was recorded and analysed at Daliff. The machining time only included operations done on the machining centre and excluded operations such as setup time, removal of temporary part mounting base and quality control. The results are contained in Table 7 and Figure 30.

Table 7: Lug Rib machining time

Elapsed time [min]	Process	Cutting speed [m/min]	Spindle speed [rpm]	Additional details
113	Roughing	111	1100	Seco High Feed Cutter Ø32, 3 inserts: Seco F40M, Depth of cut: ≈ 0.65mm, Flood Cooling
3	Surface finishing	136	1350	Face mill
4	Drill (Bottom)	65	650	(1) Drill Pilot Holes (2) Drill Mounting Holes
7	Milling (Angle)	136	1350	Angled Plane
3	Milling (Curve)	70	700	Curved Plane
11	Surface finishing	251	2500	Finishing and filleting
4	Drill (Bearing)	126	1250	Drill hole for bearing, Tolerance 10 µm
2	Measure, redrill	126	1250	
8	Deburring	151	1500	Ballnose cutter

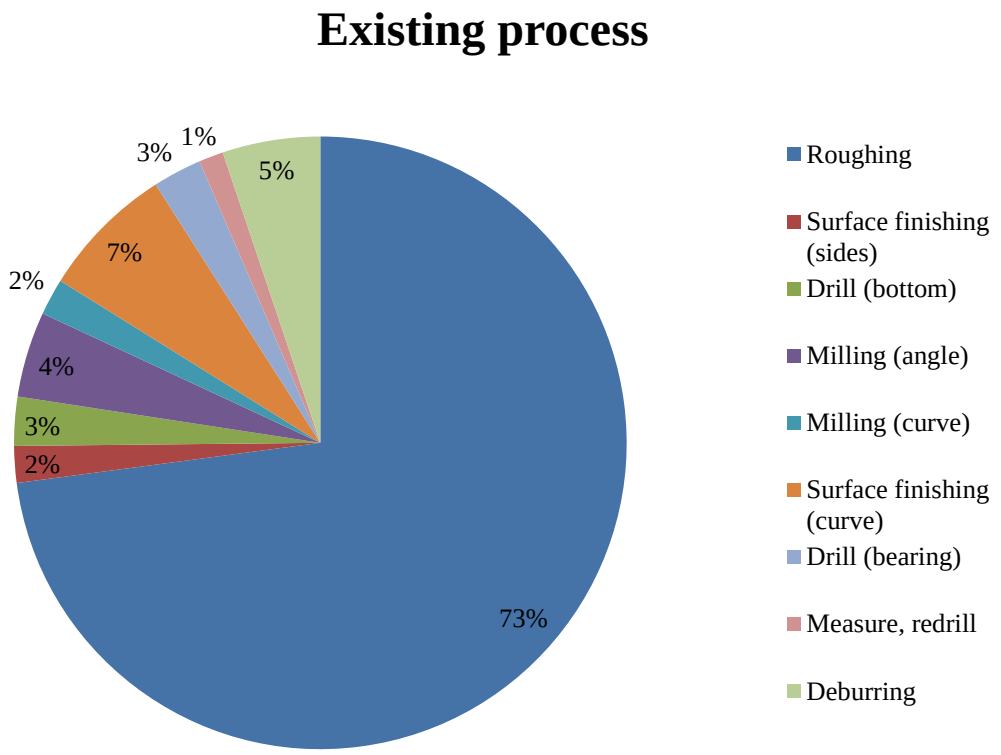

Figure 30: Existing time expenditure on demonstration part

It can be seen from Figure 30 that 73% of the time was spent on the roughing process. This was significantly longer than any other process on the machining centre for the lug rib. Thus, if the roughing process could be improved, significant time saving could be realised.

Table 8: Existing process parameters for roughing

Machine model	Deckel Maho DMU 60 monoblock 5-axis
Operation	Roughing
Spindle speed	1100 [rev/min]
Cutting speed	111 [m/min]
Depth of cut	0.65 [mm]
Cooling	Flood cooling
Tool	Seco high feed cutter Ø 32 [mm] with 3 Seco F40M inserts

3.5 Improved process at industry partner

The improved process at Daliff was done in conjunction with a partner project done by another Masters student, Cilliers Prins, and resulted from the findings from the process parameters. In this partner project, Prins built a numerical model to predict the cutting forces for the roughing process and to minimise the processing time through optimisation of cutting parameters. Prins used a high-feed cutter from Iscar and a split tool with through-spindle cooling acquired from Kennametal. The split tool process is however, outside the scope of this project.

The Iscar tool was selected using the knowledge gained from the literature review, the machine-tool supplier technical manuals and through in-house expertise from Daliff. Through the numerical model of Prins, an optimised set of parameters was selected for experimentation. Thus, a 3 or 4 axis machine would be used for the experimentation and validation of the improved roughing process as only the roughing process was run and evaluated. Figure 31 shows the billet on its mounting bracket (left) and the part with the roughing process completed.

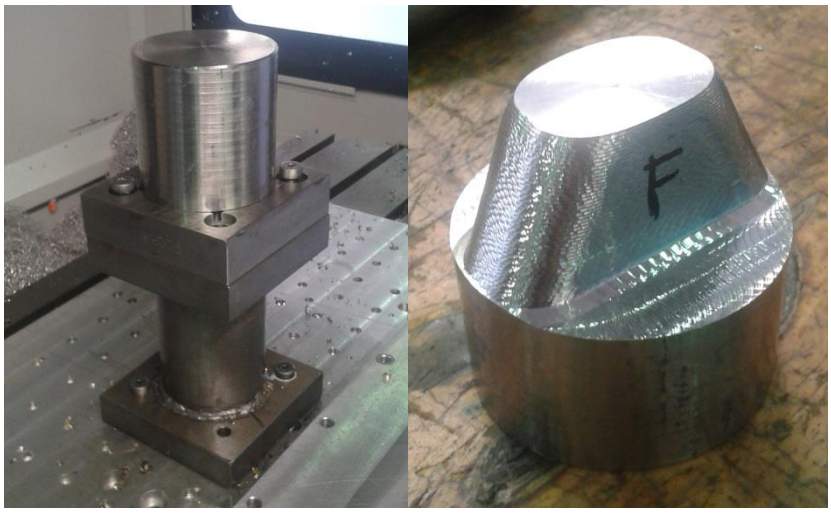

Figure 31: Billet mounted in machine (left) and lug rib with roughing process finished (right)

The experiment was run on the lug rib and the time of the run was 4min 38sec. This showed a significant improvement of 95.90% in production time for the roughing process and a reduction of 69.92% on the overall machining time of the lug rib, where the machining time was reduced from 155 minutes to 46 min 38seconds. Table 9 is a summary for the recommended cutting parameters for the roughing process of the lug rib.

Table 9: Recommended process parameters for roughing

Machine model	Leadwell V40 4-axis [2008]
Operation	Roughing
Spindle speed	892 [rev/min]
Cutting speed	90 [mm/min]
Depth of cut	0.85 [mm]
Cooling	Flood cooling
Tool	Iscar high feed cutter Ø32 [mm] with 4 H600 WXCU 05T312T inserts

Figure 32 shows the existing time expenditure for the machining process with the improved roughing process. As such, the roughing process only took 10% of the overall machining time. The process that consumed the most time now was surface finishing, but owing to the scope of the project, only the roughing process was investigated. In the existing processes, the roughing process took up the bulk of the process time.

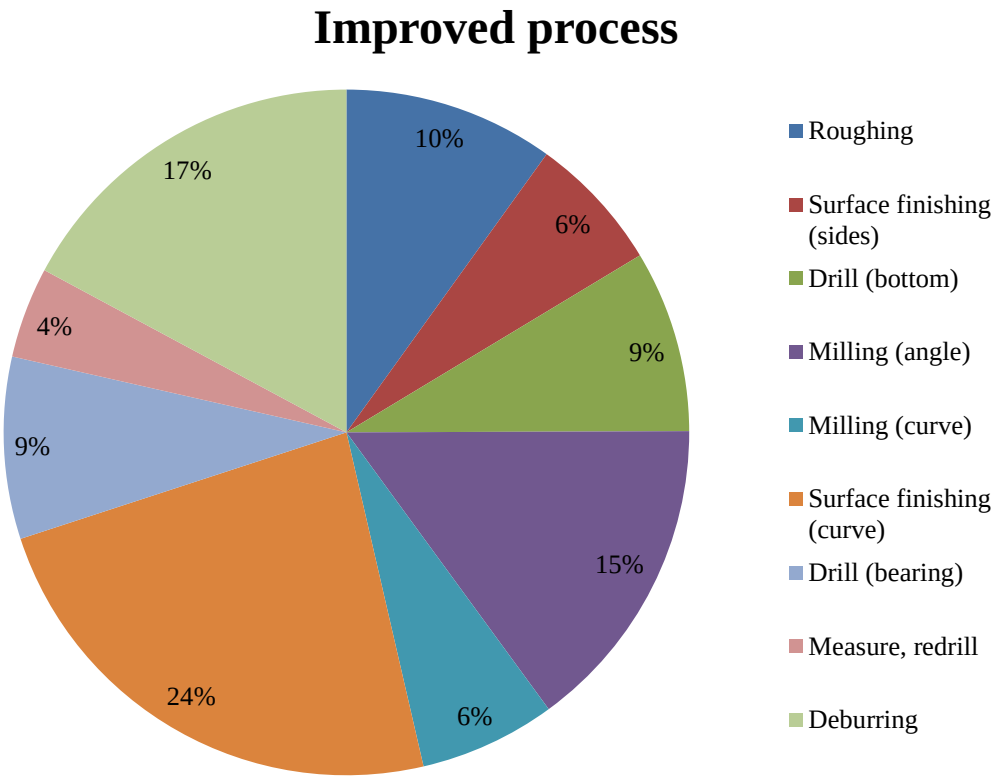

Figure 32: Relative time expenditure on the improved roughing process

4. Experimental design and setup

4.1 Introduction

Chapter 3 presented the case study at the industrial partner including case selection, selection of the demonstration part and the analysis of existing processes. The focus of this chapter is the experimental setup as well as the different conditions that may affect the outcome of the experiments, such as workpiece properties, cutting strategy, cutting tool properties, selection of cutting parameters, machine properties and measurement of wear. The tool wear was measured and used as a basis for a statistical analysis that will be presented in the next chapter.

The goal of the experimentation was to validate the conclusions drawn from literature, gain insight into the machining of titanium alloys and prove the capability of machining titanium alloys at the industry partner. The experimentation would be used to study the effects of different process parameters on the machining process and produce an optimised set of parameters for the roughing process when machining the demonstrator part, based on the selected tool and material. A full three-factor two-level experimental design was conducted to study the effect of different process parameters on the tool wear experienced with each cutting edge, which further provides insight into the mechanisms that cause uniform and non-uniform wear.

4.2 Workpiece

The scope of the study covers the machining of titanium aerospace parts; therefore, Ti-6Al-4V (grade 5) was used for experimentation. A titanium workpiece of an unknown composition and favourable size was acquired and analysed using SEM (Scanning Electron Microscope) to determine the chemical composition of the material. A sample of the material was removed from the original workpiece, mounted in resin and the surface treated with Kroll etch to enable the SEM spectrum analysis to be done. The results of the analysis are summarised in Table 10 and the micrograph of the SEM can be seen in Figure 33. Table 10 and Figure 33 are to be used together to determine the composition of the material, as each grain and area has a different chemical composition. Hardness tests were done of the sample material, resulting in readings of 30.9 to 34.4 on the Rockwell HRC scale. From the SEM analysis of the sample material and assigning weighting according to relative area of each grain type, it can be concluded that the titanium workpiece of unknown composition is Ti-6Al-4V (grade 5) and was suitable for use in experimentation.

Table 10: Workpiece chemical composition

Spectrum	Weight% Al	Weight% Ti	Weight% V	Weight% Fe	Weight% Total
Lighter area β	2.881591	76.43056	18.7791	1.908749	100
Large dark grains α	7.20181	90.93492	1.86327	0	100
Small dark grains α + β	7.265938	90.75805	1.976014	0	100

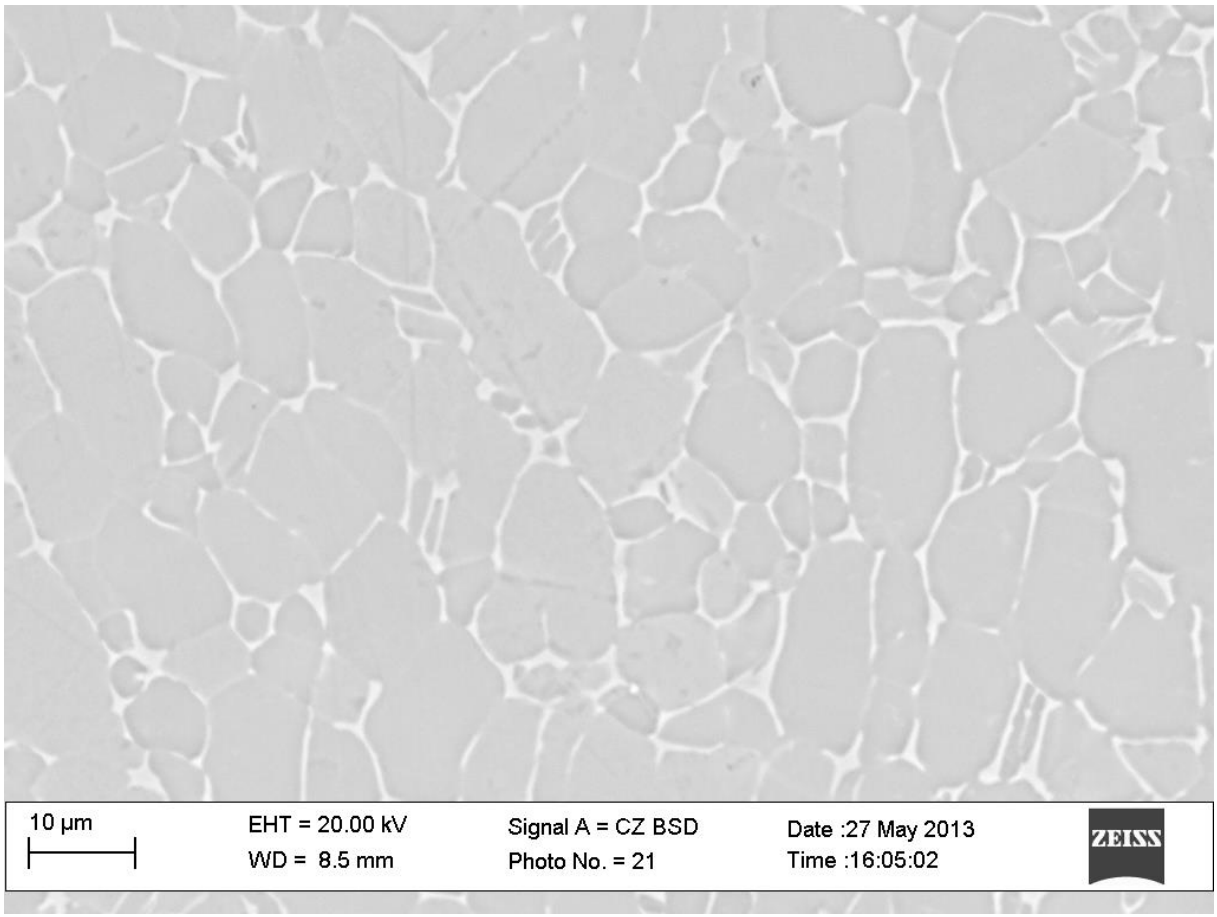

Figure 33: SEM micrograph

A limited amount of material was available for experimentation. The dimensions of the workpiece are shown in Figure 34, has a volume of 6847.86 cm^3. The experiments are structured to ensure an effective use of the available material, without compromising on the statistical and scientific integrity of the data. This allows a thorough investigation into the most economic machining parameters, while using less than or equal to the amount of material available.

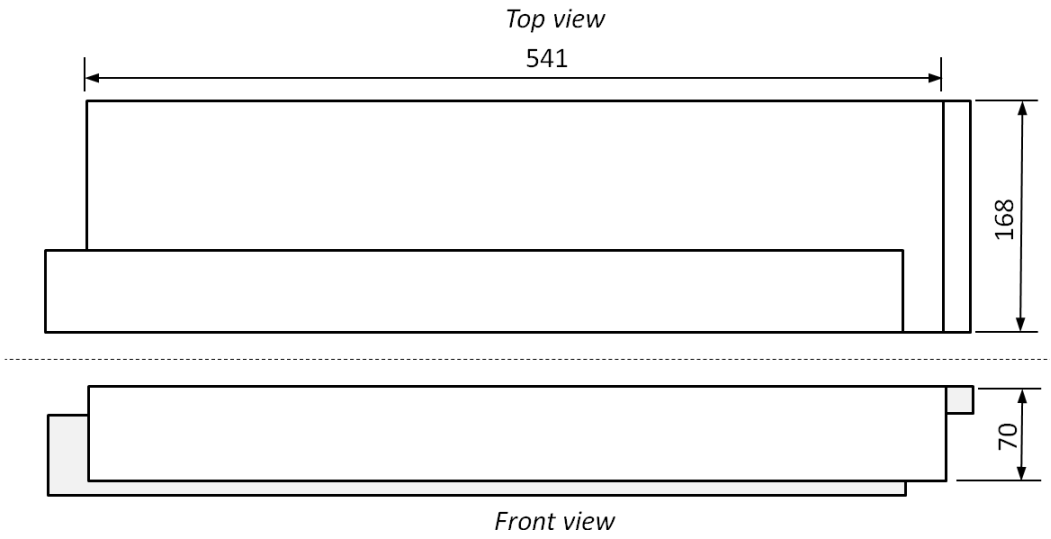

Figure 34: Workpiece available for experimentation

The lug rib (Figure 35) whose machining process was studied at the industry partner, was selected as basis for the experimental design. The part, with rough dimensions of 64 x 62 x 55 mm, was machined from an Ø90 x 90 mm billet. 95.04% of the material was removed from the billet to form the final part. The base of billet was bolted to a pedestal, as seen in Figure 31 above. After the machining process, the base of the billet was removed by means of wire-cutting.

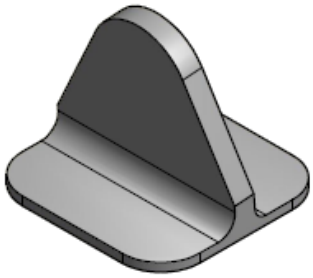

Figure 35: Lug demonstrator part

From the case study at the industry partner, it was ascertained that the roughing process took approximately 73% of machining time, which amounted to 113 minutes for a single operation. During the roughing process, 42% (237.99cm^3) of the volume of the billet (572.56cm^3) was removed. For the experimentation, each experiment would remove the same volume of material as the roughing process, which means that the volume of material available would allow for 28 roughing experiments to be conducted.

The 8-to-1 rule for machining ribs and thin walls was used for machining the thin wall for the lug rib. As already discussed, the high cutting forces when machining difficult-to-cut material may deform the thin-walled features. Thus, a machining strategy was followed where material was left in place to support the thin walled feature, which was then machined away afterwards. The material was removed in the order as illustrated in Figure 36 in a step-wise manner (Boeing Phantom Works, 2008). The cutter only had an effective cutting diameter of 22 mm and would require two passes to form the thin-walled

feature. When the 8-to-1- rule was followed, two passes of 17.5 mm had to be used to remove the required material. As a result, the width of cut that was required for these experiments was 17.5mm and required two passes.

To simulate the roughing process for this part, straight-line cuts were considered to be adequate and would not reserve material due to the part geometry and resulted in efficient use of the available material. The workpiece was 70 mm wide and the width of each straight line cut was 17.5 mm. As a result, 4 straight line cuts could be made for each vertical increment of the experimental runs.

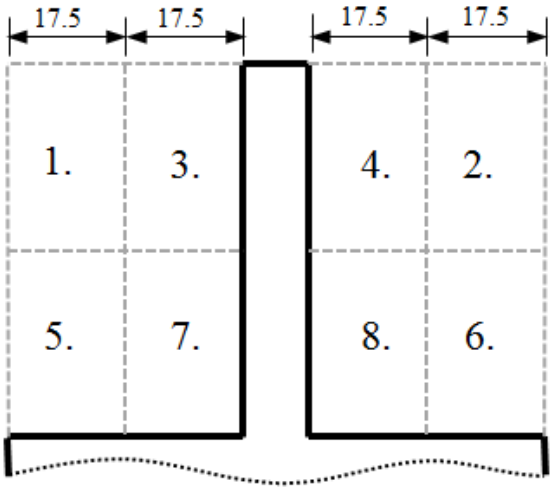

Figure 36: 8-to-1 rule for machining ribs and thin walls in titanium

4.3 Tool: cutter

The cutter that was used for experimentation was the same as the one used for the improved process at the industry partner, as it had the same features recommended from the literature review in chapter 2. Figure 37 illustrates the measurements of the insert geometry while Table 11 provides a summary of the recommended feature list, as well as the compatibility of each feature with the Iscar insert.

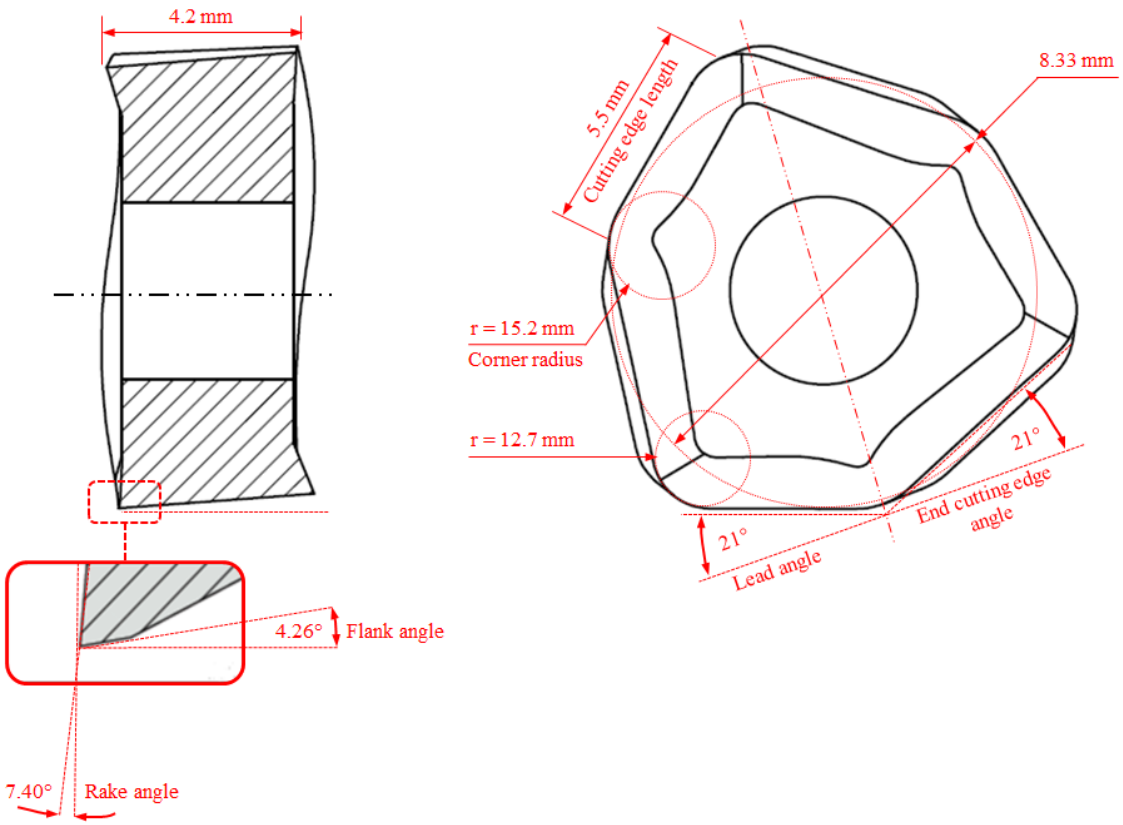

Figure 37: Insert geometry measurements (Iscar high feed cutter H600 WXCU 05T312HP)

Table 11: Iscar H600 WXCU 05T312HP recommended feature checklist

Property	Recommendation	Compatibility
Insert material	Coated carbide insert (WC-Co)	Yes
Insert coating	Multi-layered PVD coating of TiN/TiCN/TiAlN	Yes, multi-layered PVD TiN and PVD TiAlN used
Rake angle	5° - 20° in the positive direction	Yes
Flank angle	6° to 12°	Acceptable
Side cutting edge angle	Relatively large angle	Yes
End cutting edge angle	Relatively small angle	Acceptable
Honing and land	Honing is not recommended, but land could be used	Yes, land used
Corner radius	Relatively large angle	Yes
Corner angle	Relatively large corner angle	Yes
Cutting strategy	Down (climb) milling	Yes
Cutting fluids	Flood or dry cutting (through spindle is available)	Flood cooling available

The insert that was used for the improved process at the industry partner has the “T” profile, illustrated in Figure 38. The “T” profile is recommended for alloy steel and cast iron, where the “HP” profile is

recommended for stainless steel and high temperature alloys. The "T" profile was used for the improved process, as it was not known at the time there were two profiles available. The "HP" profile would have been better suited for the 15-5PH stainless steel material. For the experiments on Ti-6Al-4V, the "HP" profile was acquired. From Figure 38, it can be seen that both profiles have the same effective rake and flank angles, but the land have been used differently for the two inserts. The sharper cutting edge corner is more suited for the machining of titanium because the contact time for the flank of the tool is shorter. This reduces the heat generated and flank wear as well as the toughness of the tool.

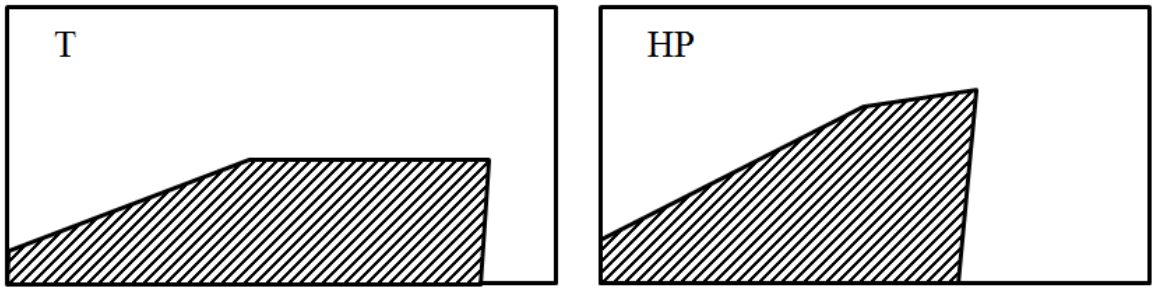

Figure 38: Iscar H600 WXCU 05T312 T (left) and HP (right) profiles

Table 12 and Figure 39 provide the tool holder measurements. The same tool holder was used for the improved process at the industry partner as for the experimentation. The diameter of the tool is 32 mm and an end cutting edge angle of 17° was used. Detailed documentation on the insert and cutting tool can be found in Appendix C, as supplied by Iscar.

Table 12: Tool holder measurements

Designation	D_1	D	Z	L_1	H	L	$A_{p\ max}$	d	Shank	$R_{d°}$	kg
FF EWX D32-4-060-W32-05	32.0	22.00	4	-	63.00	125.00	1.00	32.00	W	4.0	0.64

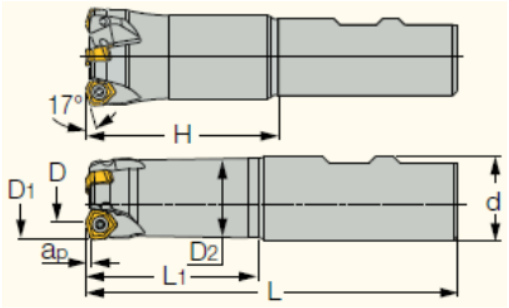

Figure 39: Tool holder measurements

4.4 Cutting parameters

Iscar had specified the range depth of cut (a_p) and feed per tooth (f_z) that the specified insert could be used at as well as recommended cutting speeds for the indexable milling cutters and insert grade to be used on α-β alloys of titanium. These values are supplied in Appendix D that was taken from the Iscar Milling Tools Catalogue (2012), in which the H600 WXCU 05T312HP insert and FF EWX D32-4-060-

W32-05 tool holder could be found. These values were used to setup a 3-factor 2-level factorial experimental design (Gitlow, et al., 2005). These parameters are summarised in Table 13.

Table 13: Recommended cutting parameters

Unit	a_p [mm]	f_z [mm/tooth]	v_c [m/min]
Minimum value	0.8	0.3	30
Maximum value	1.0	0.8	70

4.5 Tool deterioration and tool-life criteria

For the experimental design, a response variable needed to be chosen. The cutting parameters were changed in various combinations and the response variable was measured. The influence each cutting parameter had on the response variable was evaluated as were the interactions that the cutting parameters had on the response variable. The response variable chosen was tool wear since it could easily be measured and was heavily dependent on the cutting parameters. Measurement and study of the wear, wear types and failure also provided insight into the machining process.

In order to determine the useful life of a tool, it was necessary to define the life of the tool in terms of wear. There are two types of wear, i.e. flank wear and face wear. There are other forms of tool deterioration that also can affect tool life such as chipping, cracks, flanking, plastic deformation and catastrophic failure.

According to ISO 8688:1, which deals with tool life testing in face milling, there are different criteria for each type of wear and tool deterioration phenomena. The tool life criteria according to different tool deterioration phenomena are provided in Table 14. These criteria are the ISO standard for tool life in face milling tools, since the maximum tool wear is not supplied by the tool supplier. The S/N/L classification (small/normal/large) refers to the testing time, where at the large testing time classification, the tool is still useful but close to the end of its useful life. Further cutting with the edge will result in an increase in cutting forces, deterioration of the workpiece surface and an increase in vibration.

Table 14: Tool life criteria

Tool deterioration phenomena		**Criteria [mm]**		
		S	**N**	**L**
Flank wear	*Uniform*	0.2	0.35	0.5
	Non-uniform	0.9	1.2	1.5
	Localised	0.8	1	1.2
Rake wear	*Crater wear*	0.05	0.1	0.15
	Stair-forms	0.25	0.3	0.35

4.6 Equipment

4.6.1 Machine

The machine used for experimentation was a Leadwell V40M CNC Machining Centre. It was installed at the industry partner and had a work area that could accommodate the workpiece. The machine properties are given in Table 15. This is a model that is quite common in the South African machining industry because it is rather inexpensive and easily maintained. The machine is, however, not as rigid as some of the more costly machines and may cause some vibration during machining.

Table 15: CNC machine properties

Machine model	Leadwell V40M 1 off
Year	2008
# of axis	4
Work area	1000(x)×500(y)×500(z) [mm]
Tool magazine	20 tools
Spindle	Siemens Sinamics 1PH8133-1DF02-0LA1 drive
Spindle speed	15000 rpm
Feed	20 m/min

4.6.2 Other equipment

Further equipment that was used was an Olympus Microscope to measure the tool wear, where the inserts were mounted and placed on the microscope and analysed using a ×50 magnification. The microscope was connected to a computer, where Olympus Stream Essentials software was used to take micrographs and graphically measure various features. The microscope was located at the Department of Mechanical Engineering at Stellenbosch University.

4.7 Procedure

The experiments were done on a CNC milling machine at Daliff Engineering. The tool inserts were ordered by Daliff Engineering from Iscar and the same tool holder was used as in the improved process in the case study. The experiments were set up as a screening test as there is a low level of knowledge about the cutting factors that are critical to optimising the tool wear for these cutting conditions. Due to the amount of factors that had to be tested, the experiments had to be set up as a 2-level 3-factor factorial design with 3 centerpoints. This resulted in a total of 11 experimental runs that had to be conducted. The workpiece allowed for up to 28 experimental runs, which meant there would be a surplus in material, indicating an efficient use of the available material. The material utilisation is illustrated in Figure 40.

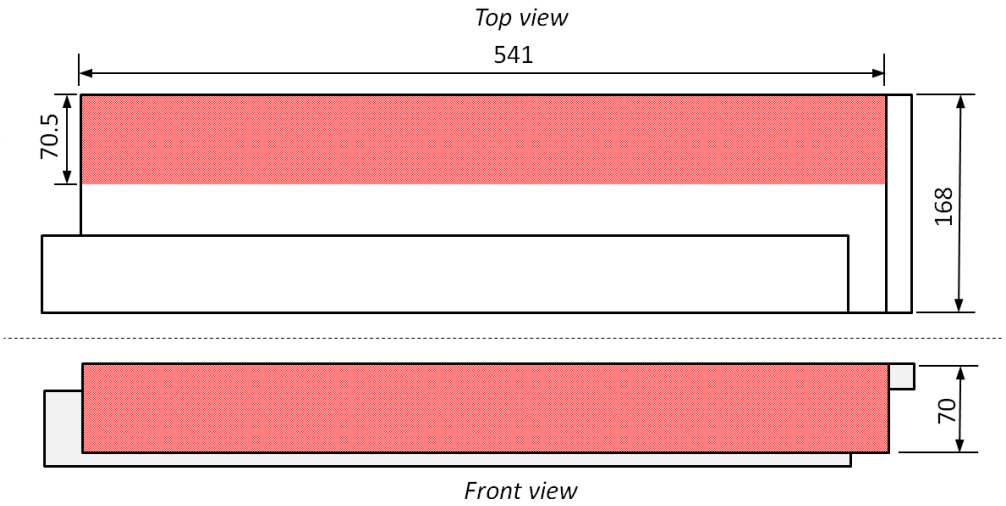

Figure 40: Workpiece (shaded area to be machined away)

The factors of interest during experimentation were depth of cut (a_p), cutting speed (v_c), and feed per tooth (f_z) as well as the primary response variable is tool wear. The upper and lower levels for each variable were the recommended cutting parameters from the tool supplier listed in Table 13. The tool wear was measured and used as primary response. During each experiment, a set amount of material was removed, which was the same amount of material removed during the roughing process of the lug rib. As the machining time was dependent on the cutting factors, it varied during each experiment where these values were adjusted.

The cutting factors were adjusted during each experimental run so that both levels of each cutting factor could be evaluated against both levels of each of the other cutting factors. There were also 3 replications for the centerpoints to determine the variation and reproducibility of the experimental data (Sahin & Motorcu, 2004). The centerpoints were distributed evenly throughout the experimental runs: at the first, middle and last runs. The rest of the runs were placed randomly in the different runs. The experiments were run and the measurements and analyses are presented in the next chapter. The experimental run order, primary cutting parameters and derived cutting parameters are given in Table 16 and the experimental design region is displayed in Figure 41.

Table 16: Experimental parameters

		Primary cutting parameters			Derived parameters			
Exp nr	**Run nr**	**a_p** Depth of cut [mm]	**v_c** Cutting speed [m/min]	**f_z** Feed per tooth [mm/tooth]	**N** Spindle speed [rev/min]	**v_f** Table speed [mm/min]	**f_N** Feed per revolution [mm/rev]	**Q** Metal removal rate [cm^3/min]
9	1	0.8	30	0.3	434	521	1.2	7.29
3	2	1	30	0.3	434	521	1.2	9.12
4	3	0.8	70	0.3	1013	1215	1.2	17.02
2	4	1	70	0.3	1013	1215	1.2	21.27
7	5	0.8	30	0.8	434	1389	3.2	19.45
10	6	1	30	0.8	434	1389	3.2	24.31
8	7	0.8	70	0.8	1013	3241	3.2	45.37
1	8	1	70	0.8	1013	3241	3.2	56.72
6	9	0.9	50	0.55	723	1592	2.2	25.07
5	10	0.9	50	0.55	723	1592	2.2	25.07
11	11	0.9	50	0.55	723	1592	2.2	25.07

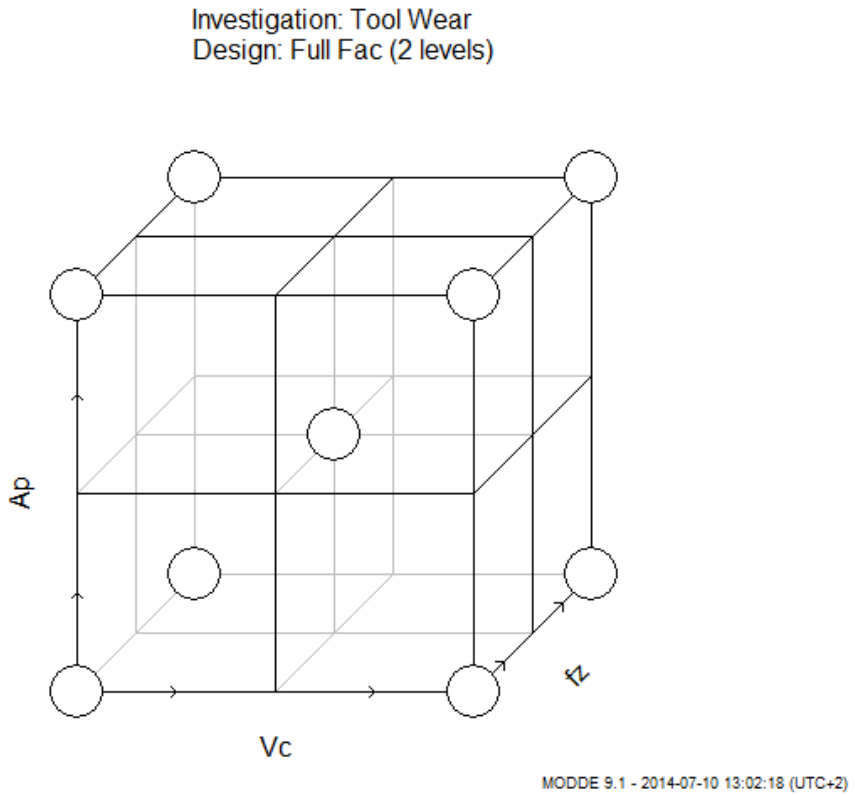

Figure 41: Experimental design region

4.8 Preliminary observations

Preliminary observations were made during the measurement on the microscope. It was seen that the frequency of tool chipping increased as feed per tooth were increased. Another observation was made on some of the inserts with significantly less wear than the other inserts on the same test run. This can

be attributed to the operator incorrectly installing the insert on the tool holder due to the small size of the inserts.

Figure 42 shows the stair formation on the rake face of the tool as well as the fracturing of the flank face when machining at a high feed. The micrographs on the left and right were from the same experimental run and show similar chipping and fracturing (machined at a_p = 0.8 mm, v_c = 70 m/min, f_z = 0.8 mm).

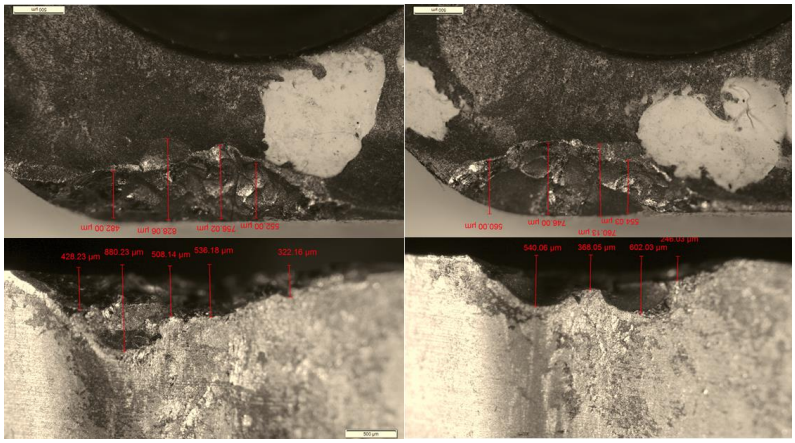

Figure 42: Stair formation on flank face (top) and corresponding non-uniform flank wear (bottom) (32x magnification)

Figure 43 depicts uniform rake wear with some non-uniform rake wear features in the characteristic stair form. These micrographs represent a tool with wear that is just above the target value. The micrographs were from the same experimental run with a medium feed per tooth rate, where some chipping has occurred on the rake face (machined at a_p = 0.9 mm, v_c = 50 m/min, f_z = 0.55 mm).

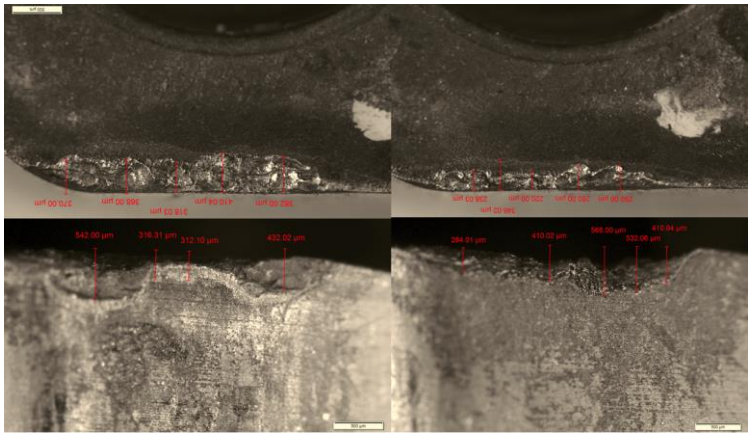

Figure 43: Uniform wear on rake face, with some localised non-uniform wear features (top) and their corresponding non-uniform flank wear (bottom) (32x magnification)

Figure 44 shows a tool with minor uniform rake wear and barely measurable uniform flank wear. Some delamination of the tool coating can be seen on the flank face. The micrographs were from the same experimental run with a low feed rate (machined at a_p = 1.0 mm, v_c = 30m/min, f_z = 0.3 mm). It should be noted that the material removal rate for this experimental run was low and a large amount of tool life was not utilised.

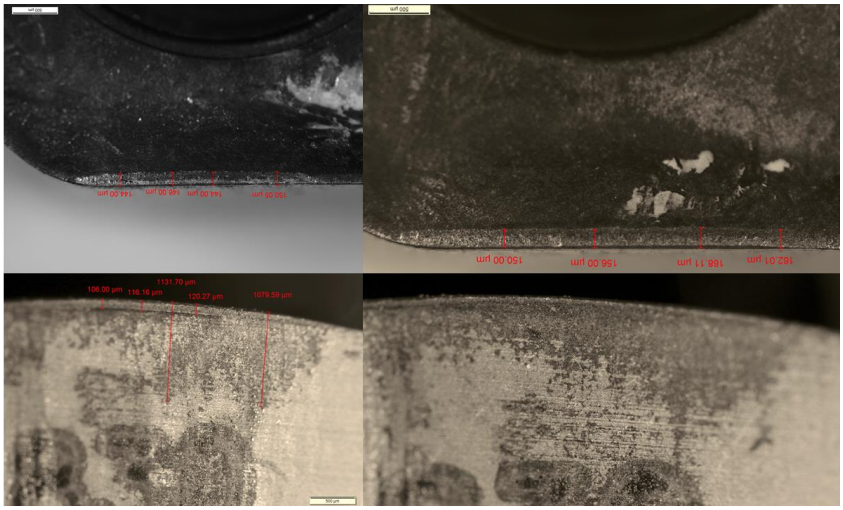

Figure 44: Uniform rake (top) and uniform flank wear (bottom) (32x magnification)

By observing the chips, it could be seen that the cutting parameters had an influence on the geometry and features of a chip. There was a direct relationship between chip width and depth of cut, chip thickness and feed per tooth, and chip length and cutting speed. The depth of cut was equal to the chip width and the feed per tooth could be determined by determining the average thickness of the chip although this was made difficult by the serrated nature of the chip.

Figure 45: (left) A_p = 0.8 mm (middle) A_p = 0.9 mm (right) A_p = 1.0 mm (8x magnification)

Figure 46: (left) f_z = 0.3 mm (middle) f_z = 0.55 mm (right) f_z = 0.8 mm (8x magnification)

Figure 47: (left) v_c = 30 m/min (middle) v_c = 50 m/min mm (right) v_c = 70 m/min (8x magnification)

The cutting speed had an influence on the length of the chip that was formed. The chip length was not equal to the length that each tooth of the tool was engaged in the material, indicating that some recutting of the chips had occurred. The recutting of chips might have had an influence on the tool wear in this situation.

There was no heat discoloration of the chips due to elevated temperatures observed on the chips. It was argued that no elevated temperature was present during machining and the flood cooling was effective in removing the heat from the tool-chip interface.

4.9 Results

The tool wear was measured on the Olympus Microscope according to ISO 8688:1 guidelines (ISO, 1989) that are concerned with tool life testing for face milling applications. The ISO standard states that for flank and face wear, the primary wear phenomena should be identified and used as tool life criteria. For these tests, both uniform and non-uniform stair-form wear were identified on the rake face, but neither was the dominating factor on the full range of tests. For flank wear, there was no significant uniform wear, thus, only non-uniform wear was measured.

Table 17 shows a summary of the average tool wear of the 4 inserts for each test. The tool wear was measured perpendicular to the original cutting edge for the full length of wear, measured in equal increments over the full length of the cutting edge. The wear was then averaged for each insert cutting edge and then averaged for all the insert cutting edges for each respective test run. The resulting measured values were the average of the average wear measurements. These values formed the basis of the statistical analysis in the subsequent chapter.

Table 17: Summary of selected tool wear

Exp #	Run #	A_p [mm]	V_c [m/min]	f_z [mm]	Uniform Wear rake [um]	Non-uniform wear rake [um]	Non-uniform wear flank [um]
1	8	0.8	30	0.3	65.48	82.3	32.1
2	4	1	30	0.3	51.16	172.8	338.01
3	2	0.8	70	0.3	245.34	415.34	48.91
4	3	1	70	0.3	281.28	606.03	221.05
5	10	0.8	30	0.8	175.15	219.51	94.48
6	9	1	30	0.8	203.71	411.8	483.16
7	5	0.8	70	0.8	523.01	692.53	583.81
8	7	1	70	0.8	586.12	714.3	712.03
9	1	0.9	50	0.55	255.67	337.51	324.44
10	6	0.9	50	0.55	197.24	166.53	141.49
11	11	0.9	50	0.55	227.45	226.48	271.56

5. Analysis of experimental results

5.1 Introduction

In chapter 4, the experimental design and set up was discussed. This chapter presents an analysis of the experimental results using various statistical tools and software. The experiments were set up as a 3-factor 2-level factorial experimental screening test. This analysis gives insight into the effect the different cutting parameters have on the tool wear as well as different tool deterioration phenomena. Various tools exist for numerically analysing intricate sets of data and information. In this study, the analysis was done using Modde 9.1 Design of Experiment software by Umetrics and other design of experiment tools such as regression and ANOVA. The analysis of the raw data is evaluated, then the model is diagnosed and interpreted to propose an improved process for machining the selected aerospace part.

5.2 Raw data inspection

5.2.1 Replicate plot

The replicate plot is used to depict the variation present in the results on an overview level. It clearly shows which of the experimental runs are close to the target value and which of the values are above the maximum values. Repeated experiments appear on the same replicate index. Ideally, the variation of repeated experiments should be less than the overall variation of data. Outliers in the data should be inspected and evaluated.

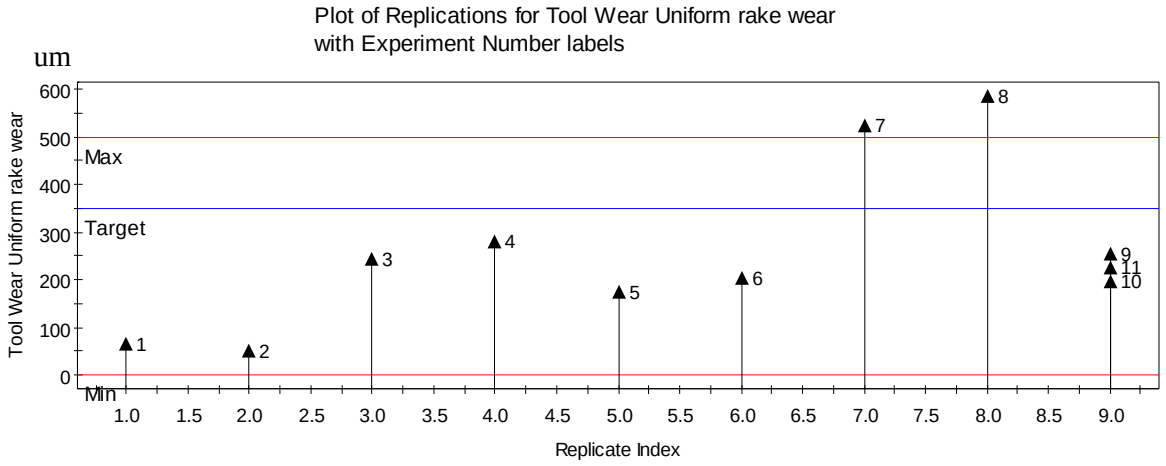

Figure 48: Replicate plot of uniform rake wear

The replicate plot of the uniform rake wear (Figure 48) shows that most of the experimental results are below the maximum and target values. Experiments 9, 10 and 11 show a small variability, which indicates that the process was stable and the repeatability of the experiments was under control. Most of the data points are below the target value, which illustrates that there was still tool life left that was not utilised. Experiments 7 and 8 can clearly be seen as above the maximum wear value. Upon quick

inspection, both experiments 7 and 8 were on the upper level of both cutting speed and feed per tooth, which means that both cutting speed and feed per tooth had a major influence on uniform wear on the rake face.

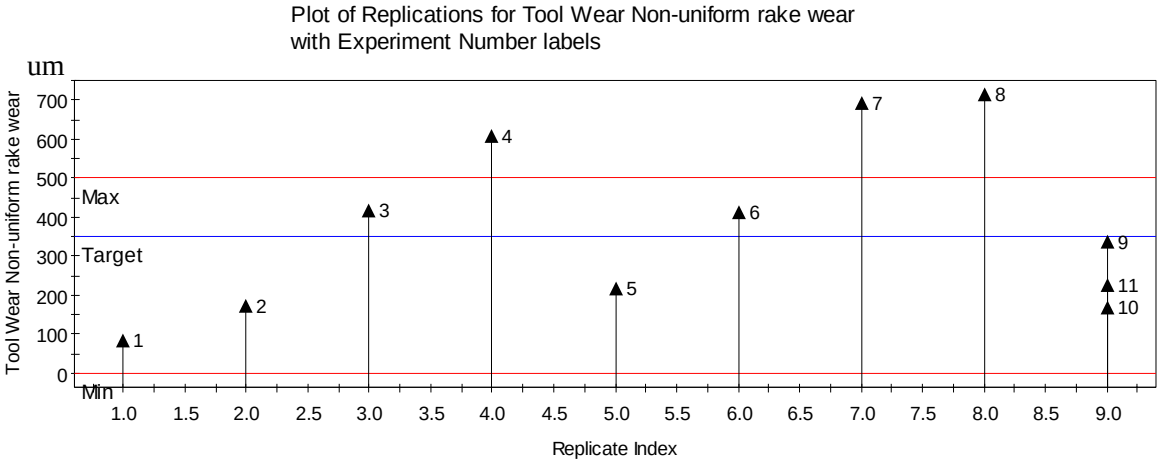

Figure 49: Replicate plot of non-uniform rake wear

The replicate plot of non-uniform wear on the rake face (Figure 49) shows that the variation in experimental results is larger than the uniform rake wear results. The experimental results were closer to the target values but some of the data points still had tool life to be utilised. The variability for experiments 9, 10 and 11 was larger than for uniform rake wear, but corresponds with the non-uniform rake wear having an overall larger variability than the uniform rake wear data. Experiments 4, 7 and 8 were above the maximum values. The same conclusions can be made for experiments 7 and 8 as for uniform rake wear, but for experiment 4, the upper level of depth of cut and cutting speed may have had a significant influence on non-uniform rake wear.

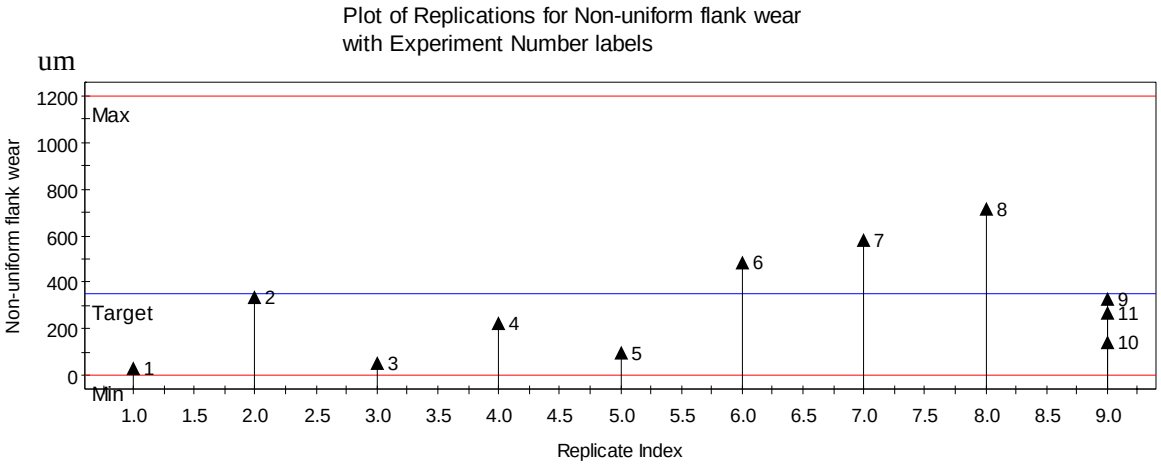

Figure 50: Replicate plot of non-uniform flank wear

The replicate plot for non-uniform wear on the flank face (Figure 50) shows that the data is distributed around the target value. All the data is far below the maximum value for flank wear. The variability for 9, 10 and 11 is small, again supporting the evidence from the uniform and non-uniform rake wear that

the experimental design and execution was successful. Experiments 7 and 8 still had the largest tool wear of all the experimental runs, but the values were still under the maximum tool wear.

5.2.2 Response distribution

A histogram shows the shape of the distribution of the response values. The ideal distribution is a normal distribution that is bell-shaped. To estimate a distribution, at least 11 observations are needed. The experimentation had 11 observations, which is the minimum amount of observations. By selecting an appropriate transformation, a non-normal distribution can be transformed to normal if the data is distributed according to a recognized distribution. Responses that are normally distributed yields better model estimates and statistics.

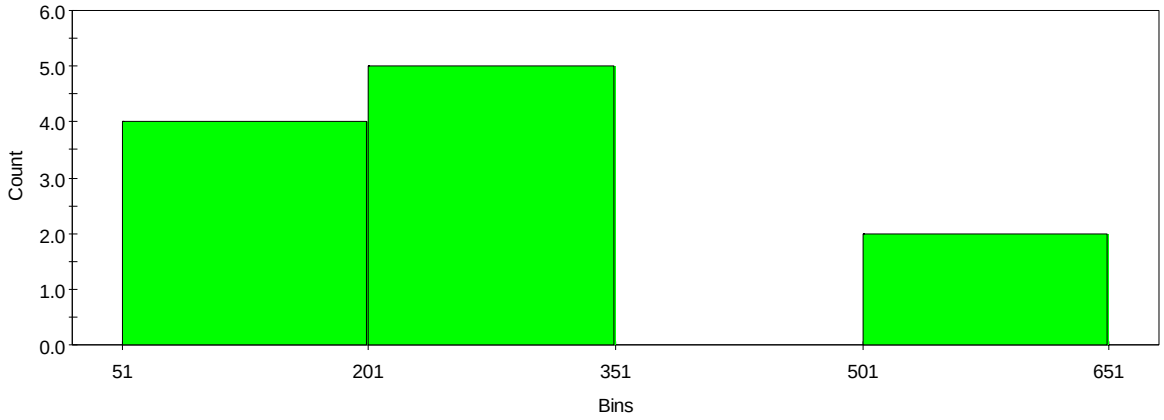

Figure 51: Histogram of the response distribution of uniform rake wear

The histogram of the response distribution of uniform rake wear shows that the data does not follow a known distribution. This could be due to the two observations that fall in the 501-651 bin. With the two outliers removed, as seen in Figure 52, the data follows an apparent normal distribution bell-shape, with the mean situated in the bin below the target value. It should be noted that due to the fact that two observations have been removed, the number of observations is not enough to estimate a distribution.

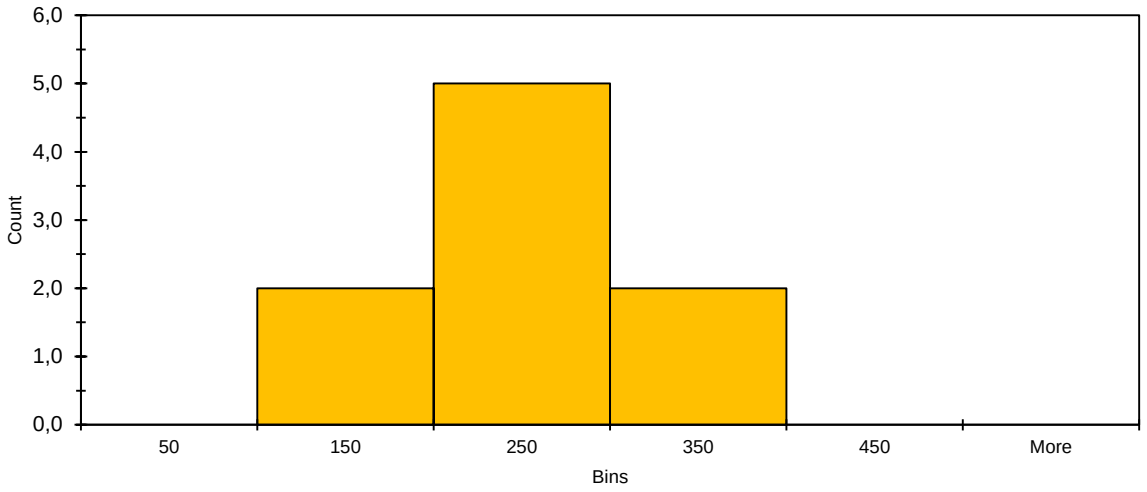

Figure 52: Histogram of the response distribution of uniform rake wear (outliers removed)

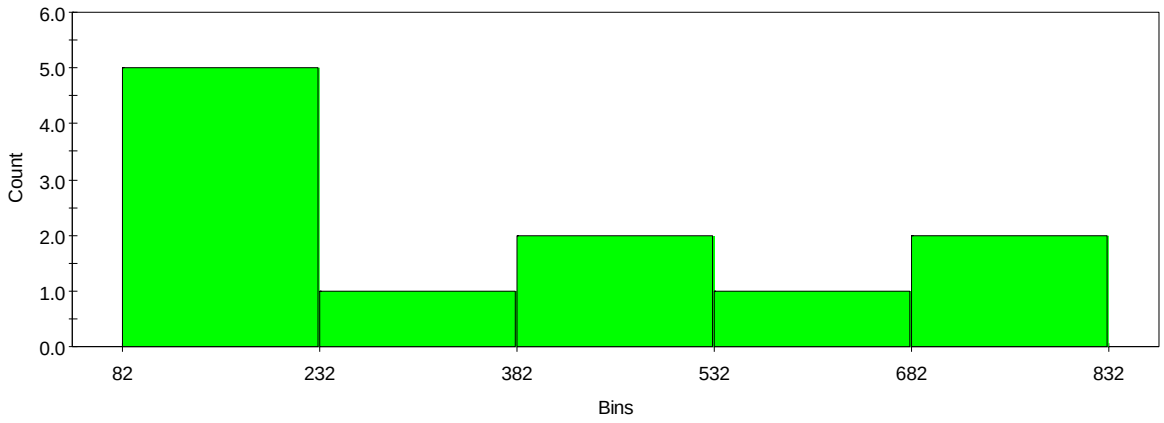

Figure 53: Histogram of the response distribution of non-uniform rake wear

Figure 54 shows that the data for non-uniform rake wear does not follow a known distribution. This could be due to experiment 7 and 8, as seen from the replicate plot for non-uniform flank wear (Figure 49). With the outliers removed (Figure 54), the data seems normally distributed with a mean in the bin just below the target. The observation in bin 650 is the data for experiment 4, which was identified as an outlier from the replicate plot, but was included to increase the number of data points. There are not enough data points to estimate the distribution of data due to the number of observations, but due to the nature of non-uniform wear consisting of a major random or catastrophic failure element, namely tool chipping, the result is considered valid.

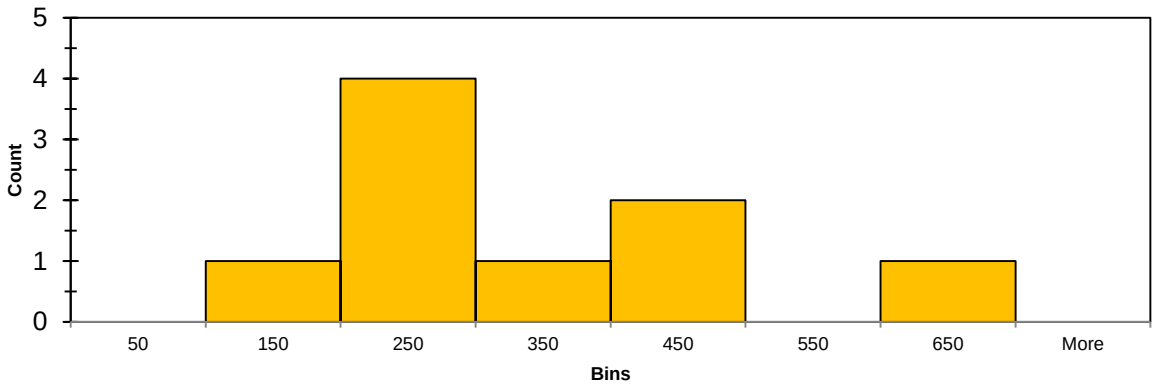

Figure 54: Histogram of the response distribution of non-uniform rake wear (outliers removed)

Figure 55 shows that the response distribution for non-uniform flank wear is apparently not normally distributed but follows a negative linear distribution. Transformation from a linear to normal distribution was unsuccessful and no outliers were identified.

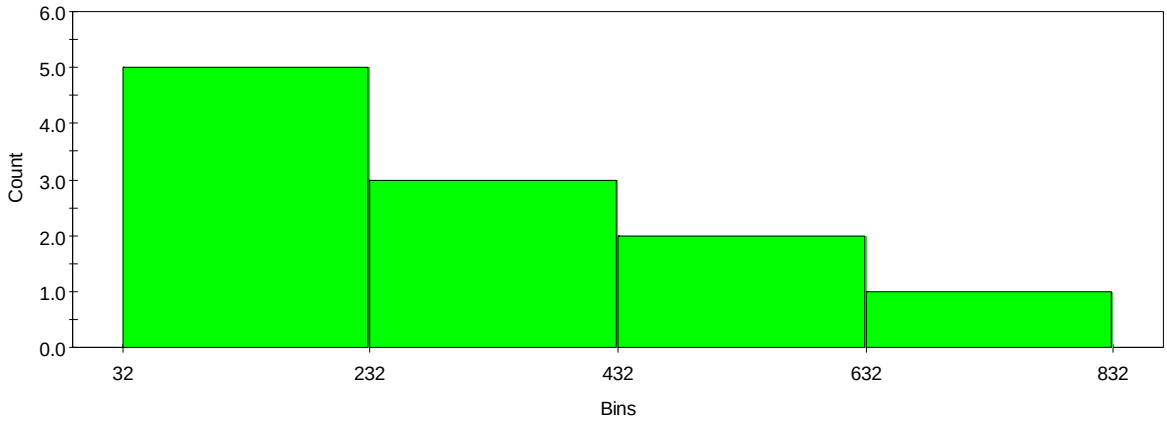

Figure 55: Histogram of the response distribution of non-uniform flank wear

Again, non-uniform flank wear is caused by catastrophic failure of the cutting edge, explaining the absence of a normal distribution. The non-uniform flank wear results show that the predominant result is low flank wear indicating that the machining process was stable with minimal catastrophic failure of the flank edge occurring.

5.3 Model diagnostics

5.3.1 Summary of statistics

The summary of fit statistics is used to determine how the data fits the statistical model. This ensures that the model can be used for analysis and predictions. The fit is evaluated according to four parameters: R^2, Q^2, Model Validity and Reproducibility. Each of these parameters is evaluated between 1 and 0, with 1 being perfect fit.

R^2 value, known as the coefficient of determination, is a parameter that shows basic model fit. It can be loosely defined as the amount of variation in the data that is explained or accounted for by the regression model (Montgomery & Runger, 2007). It is determined by measuring the variability of the data set through different sums of squares such as the total sum of squares, the regression sum of squares and the sum of squares of residuals.

$$R^2 = \frac{SS_{reg}}{SS_{tot}} = 1 - \frac{SS_{res}}{SS_{tot}}$$

With SS_{reg} = *Regression sum of squares*
SS_{res} = *Residual sum of squares*
SS_{tot} = *Total sum of squares*

A large R^2 is a necessary condition for a good model but it is not sufficient to be used on its own to determine if the data is a good fit. A poor model can have a large R^2, especially when the model has a few degrees of freedom for the residuals. The model also has a poor R^2 when the reproducibility or model validity statistics are poor. A model with a R^2 value below 0.5 has a rather low significance, where a model with a value of 1 signifies a perfect fit.

The Q^2 value, known as the predictive squared correlation coefficient, shows an estimate of the future prediction precision (Schuurman, et al., 2008). Q^2 is the percentage of the variation of the response predicted by the model according to cross validation and gives an estimation of how well the model will predict data. A model will have a poor Q^2 if it has poor reproducibility or poor model validity. In case of a model with a good R^2, moderate model validity and a design with many degrees of freedom of the residuals, then a poor Q^2 is usually due to insignificant terms in the model. The Q^2 value of a model should be greater than 0.1 for a significant model and greater than 0.5 for a good model.

Model validity is a test of diverse model problems. It indicates the degree of control the model has over experimental error (Messick, 1990). A model with a model validity of less than 0.25 is indicative of statistically significant model problems such as the presence of outliers, an incorrect model or a transformation problem. When model validity is larger than 0.25, there is no lack of fit of the model and the model error is in the same range as the pure error. When model validity is less than 0.25 a significant lack of fit exists and the model error is significantly larger than the pure error, which can affect reproducibility. A model validity of 1 represents a perfect model.

Reproducibility determines the variation of the replicates compared to overall variability of the data (Lin, 1989). It determines the variation of the response under the same conditions, often at the centerpoints, compared to the total variation of the response. When the reproducibility bar is 1, the pure error is 0, which means that under the same conditions, the values of the response will be identical. When the reproducibility bar is 0, the pure error is equal to the total variation of the response. If the

reproducibility is below 0.5, the pure error is large, thus, there is poor control of the experimental set and the model validity is low. This also results in low R^2 and Q^2 values. Reproducibility requires a value greater than 0.5.

Correct tuning of the model such as removing non-significant model parameters or selecting the appropriate transformations, results in higher summary of fit values. The best and most sensitive statistical indicator is Q^2, but model validity might be low in good models ($Q^2 > 0.9$) due to high sensitivity in the test or extremely good replicates.

Figure 56, Figure 57 and Figure 58 show the summary of fit statistics for uniform rake wear; non-uniform rake wear and non-uniform flank wear respectively, with Table 18 showing a summary of all the fit statistics.

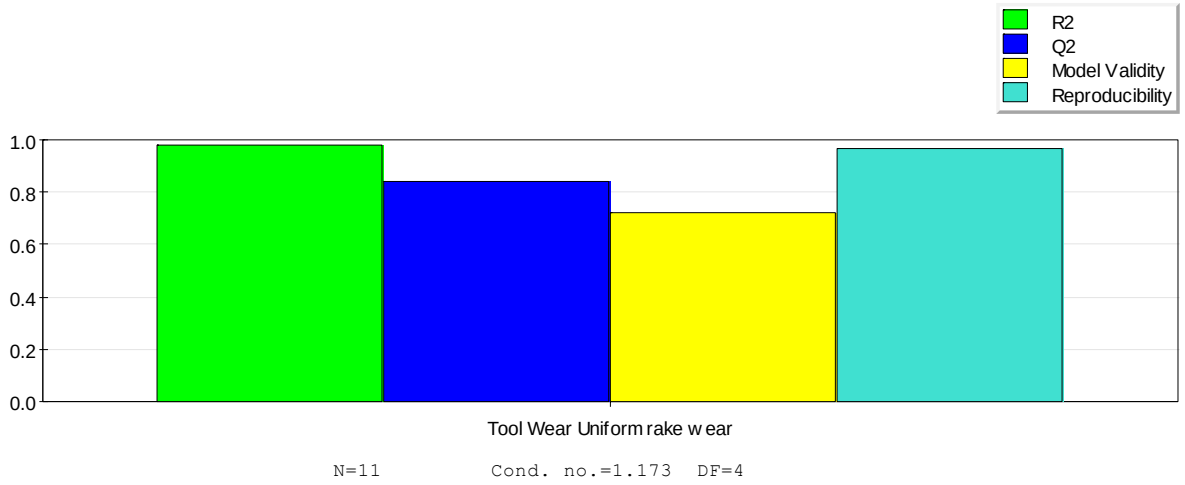

Figure 56: Summary of fit statistics for uniform rake wear

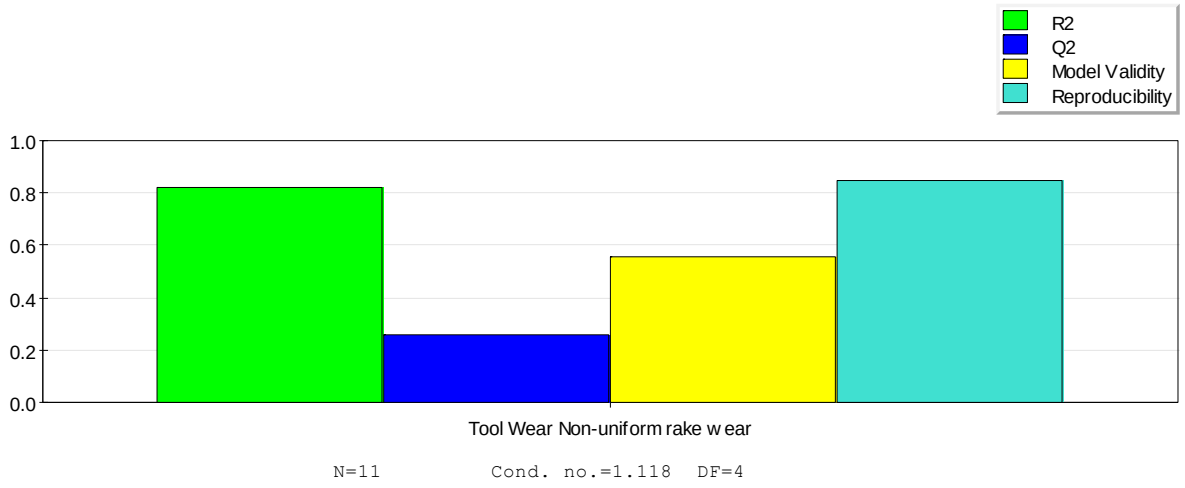

Figure 57: Summary of fit statistics for non-uniform rake wear

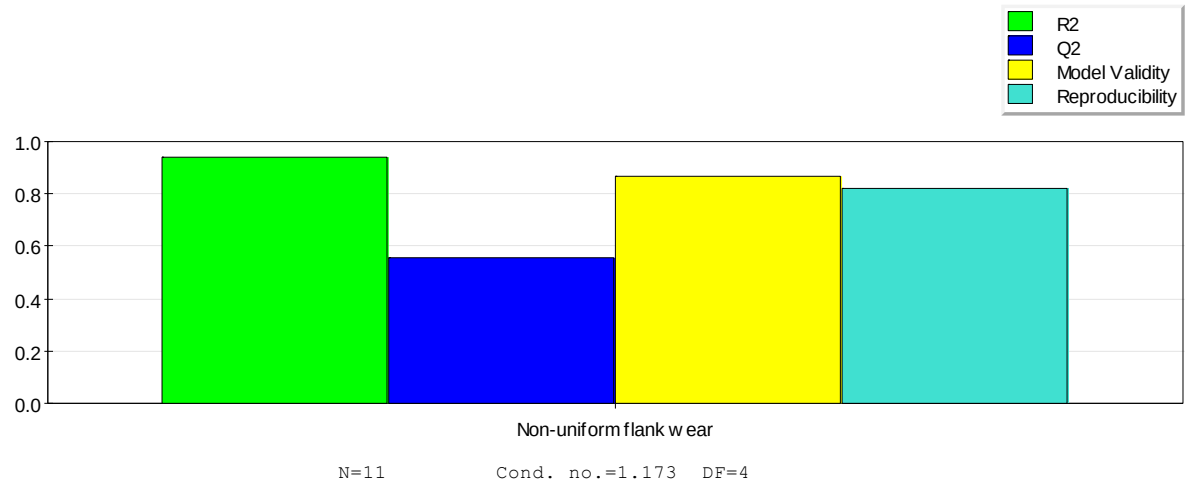

Figure 58: Summary of fit statistics for non-uniform flank wear

Table 18: Summary of fit statistics

	Uniform rake	Non-uniform rake	Non-uniform flank
R^2	0.981074	0.820435	0.939521
Q^2	0.841642	0.256815	0.556342
Model validity	0.722993	0.558263	0.868876
Reproducibility	0.968703	0.846216	0.820893

From Table 18, it can be seen that the data fits the model for uniform rake wear well as the values of all the fit statistics are significant, with the lowest value being model validity, but which still signifies a good fit. The Q^2 value for non-uniform rake wear is low, but all the other fit statistics signify a moderate fit. The low Q^2 value can be attributed to insignificant terms in the model such as the effect of a_p and the interactions of the different cutting parameters addressed in section 5.3.3. For non-uniform flank wear, the fit statistics signify a good fit, with Q^2 having a lower value, but which still signify a moderate fit.

In conclusion, the fit statistics indicate that the data fits the statistical models adequately for prediction as reproducibility is high for all the models. There is some doubt for the fit of non-uniform rake wear, since the Q^2 statistic is low, but still higher than 0.1, indicating that the model is still significant.

In the machining industry, the term catastrophic rake is also used for non-uniform rake wear. Due to the unpredictability of catastrophic wear or chipping, the lower value of the Q^2 statistic is not a disqualification.

5.3.2 Interaction effects

Design of Experiments is a collection of statistical methods for studying the relationships between independent variables and their interactions on a dependent variable. Using these statistical methods,

the cutting parameters that have the biggest effect on tool wear can be identified as well as the effect of the interactions of the cutting parameters on the tool wear.

5.3.2.1 Main effects

The main effects of the cutting parameters are determined by using the average of the response at the lower and upper values and comparing the difference between the values. The line represents the change in the response variable as the cutting parameter is changed from the lower value to the upper value. A steeper slope of the line on the main effect plot signifies that the cutting parameter has a larger effect on the response. In comparing the slopes of the different main effect plots, the parameter that has the largest effect on the response can be identified.

Main effects of uniform rake wear

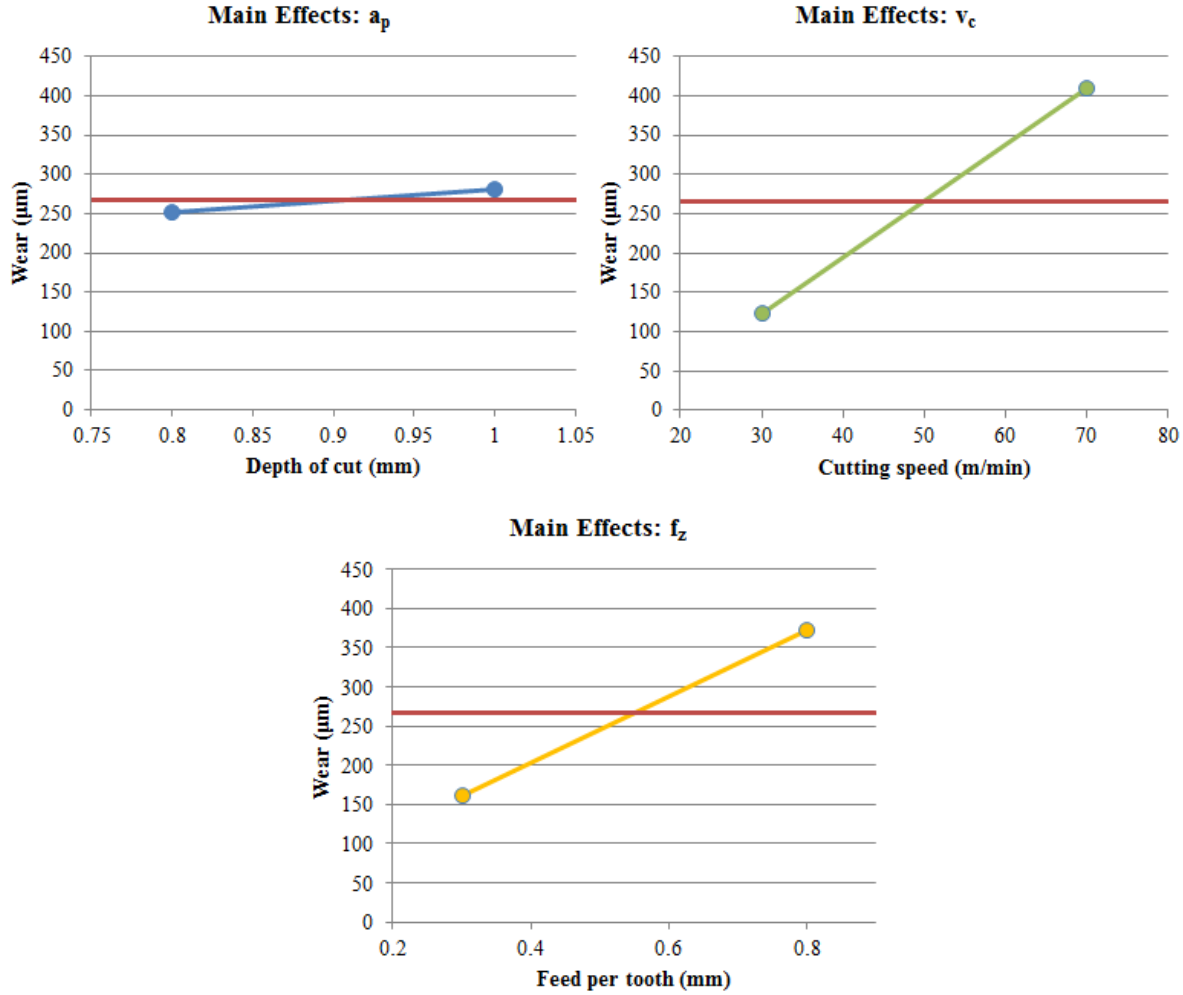

Figure 59: Main effect plots of uniform rake wear

The main effect the different cutting parameters have on uniform rake wear is shown in Figure 59. It can be seen from the slopes of the plots that cutting speed (v_c) has the largest effect on the response (tool wear). This corresponds with ISO 8688, which states that cutting speed is the primary factor determining tool life (ISO, 1989). The influence of feed per tooth is still significant on the tool wear, but depth of cut (a_p) has a minor influence on the response.

Main effects of non-uniform rake wear

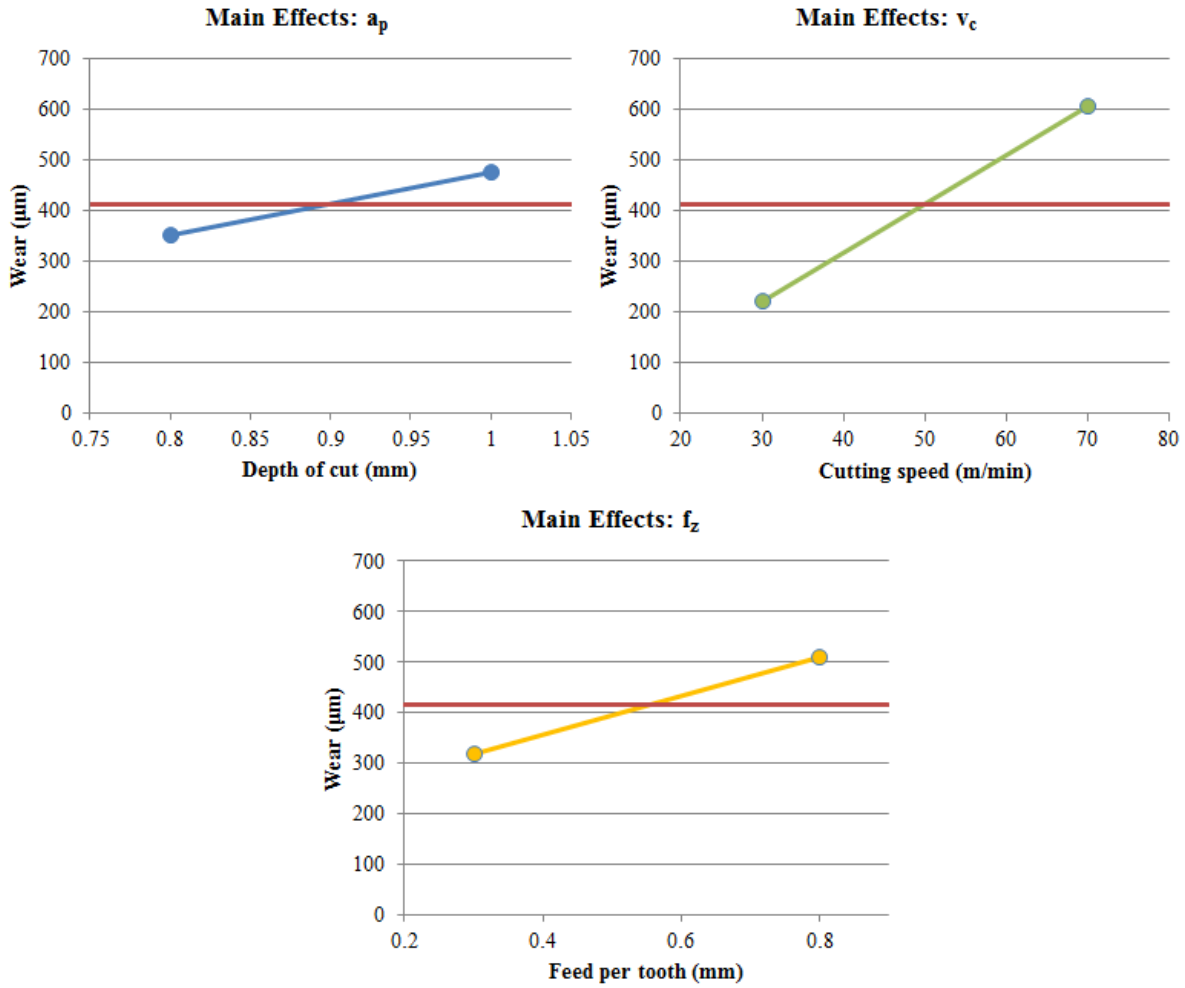

Figure 60: Main effects of non-uniform rake wear

The main effect the different cutting parameters have on non-uniform rake wear is shown in Figure 60. From the slopes of the plots, it can be seen that cutting speed has the largest effect on the response. Depth of cut and feed per tooth has a similar, but smaller influence on the tool wear compared to cutting speed.

Main effects of non-uniform flank wear

The main effect the different cutting parameters have on non-uniform flank wear is shown in Figure 61. From the slopes of the plots, it can be seen that feed per tooth has the largest effect on the response. Depth of cut has a minor effect and cutting speed has a moderate effect on the tool wear.

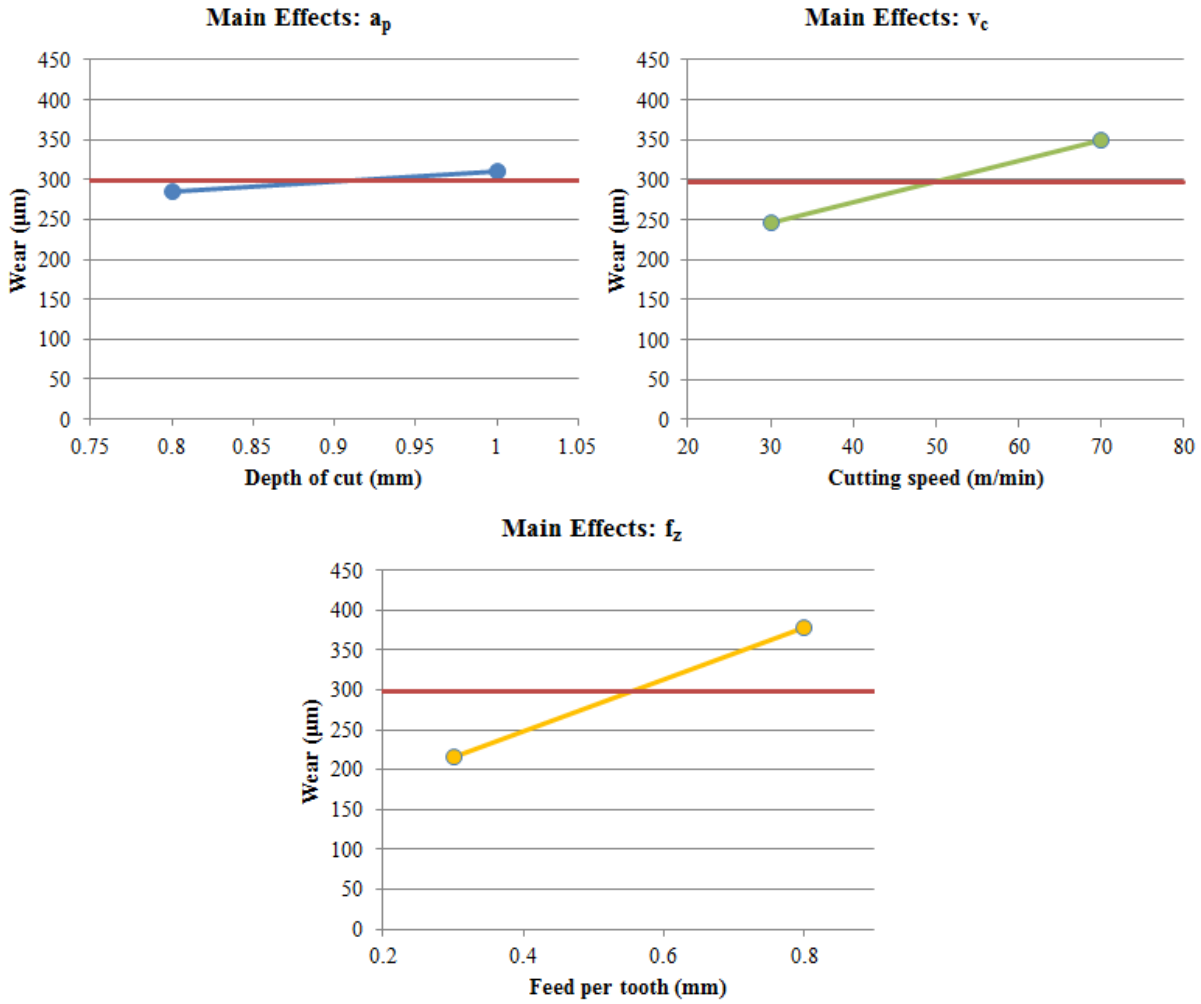

Figure 61: Main effects of non-uniform flank wear

Summary of main effects

When the averages of the main effects of the uniform rake, non-uniform rake and non-uniform flank wear is compared, it can be seen that cutting speed has, on average, the largest effect on tool wear, as shown in Table 19. Cutting speed has a proportional effect of 51.0% on the tool wear, whereas feed per tooth has a proportional effect of 37.2%. This suggests that the majority of tool wear can be attributed to these two factors, where depth of cut has a minor but still significant effect on tool wear.

Table 19: Summary of average effects of cutting parameters

Main effect	a_p	v_c	f_z	Average
Uniform rake wear	28.37	285.06	211.18	174.87
Non-uniform rake wear	123.83	385.45	190.42	233.23
Non-uniform flank wear	26.69	101.79	161.47	96.65
Average	59.63	257.43	187.69	
Proportion	11.8%	51.0%	37.2%	

5.3.2.2 Interaction effects

The interaction the different cutting parameters have on each other is determined by evaluating the average influence one parameter has on another parameter, when that parameter has a low value compared to when it has a high value. When the two lines on the plot are parallel, i.e. it has the same slope, the parameters have no influence on each other. When the two lines are perpendicular to each other, i.e. the values of their slopes are reciprocal, they are totally dependent. The larger the slope of one line is with regard to the other line, the larger the influence the one parameter has on each other.

Interaction effects of uniform rake wear

The interaction of the different parameters on uniform rake wear is shown in

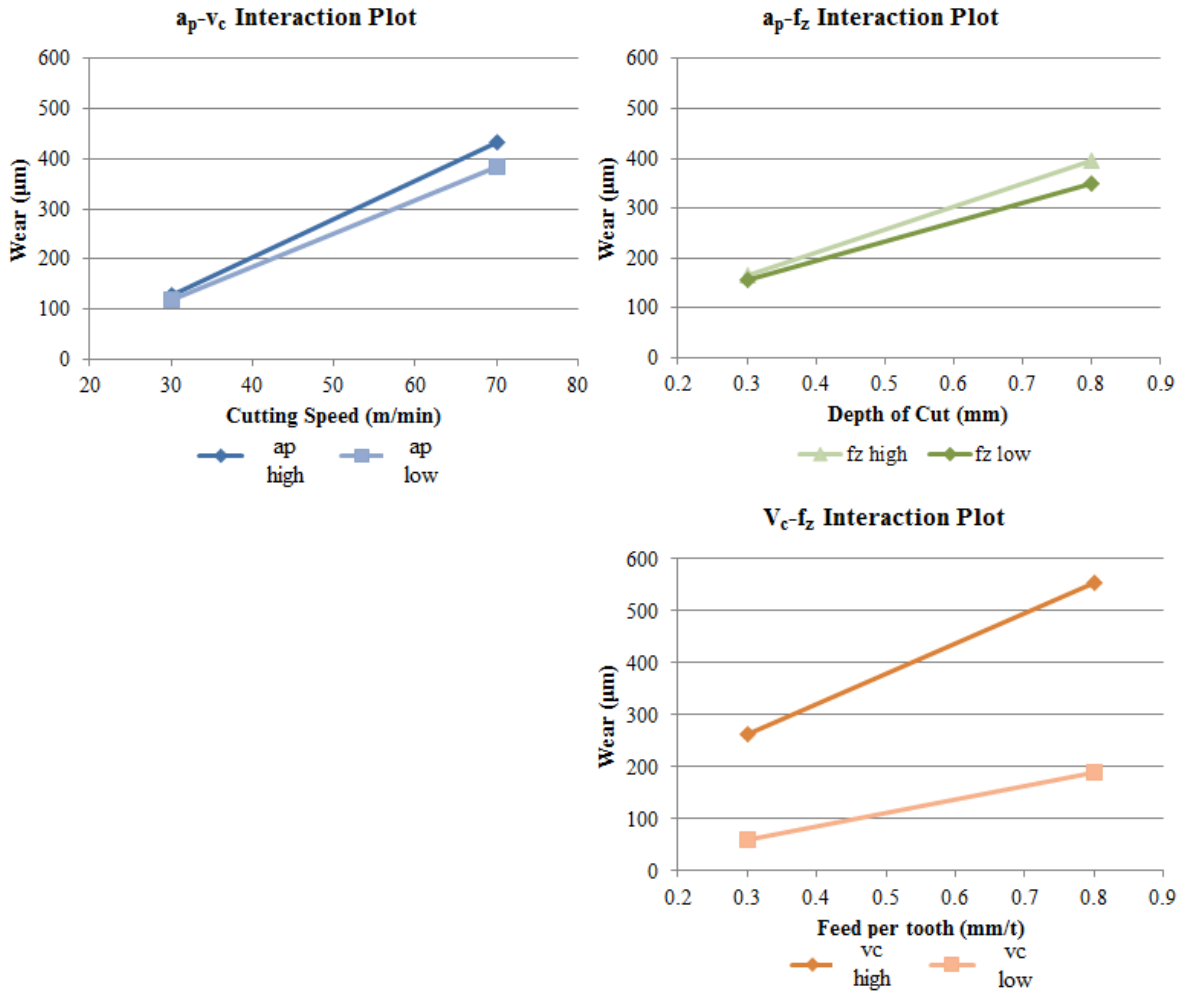

Figure 62. Cutting speed and feed per tooth have the biggest interaction, which corresponds with the significant effects both cutting speed and feed per tooth have on tool wear. Depth of cut and cutting speed, and depth of cut and feed per tooth interaction is minor as depth of cut has a minor effect on tool wear.

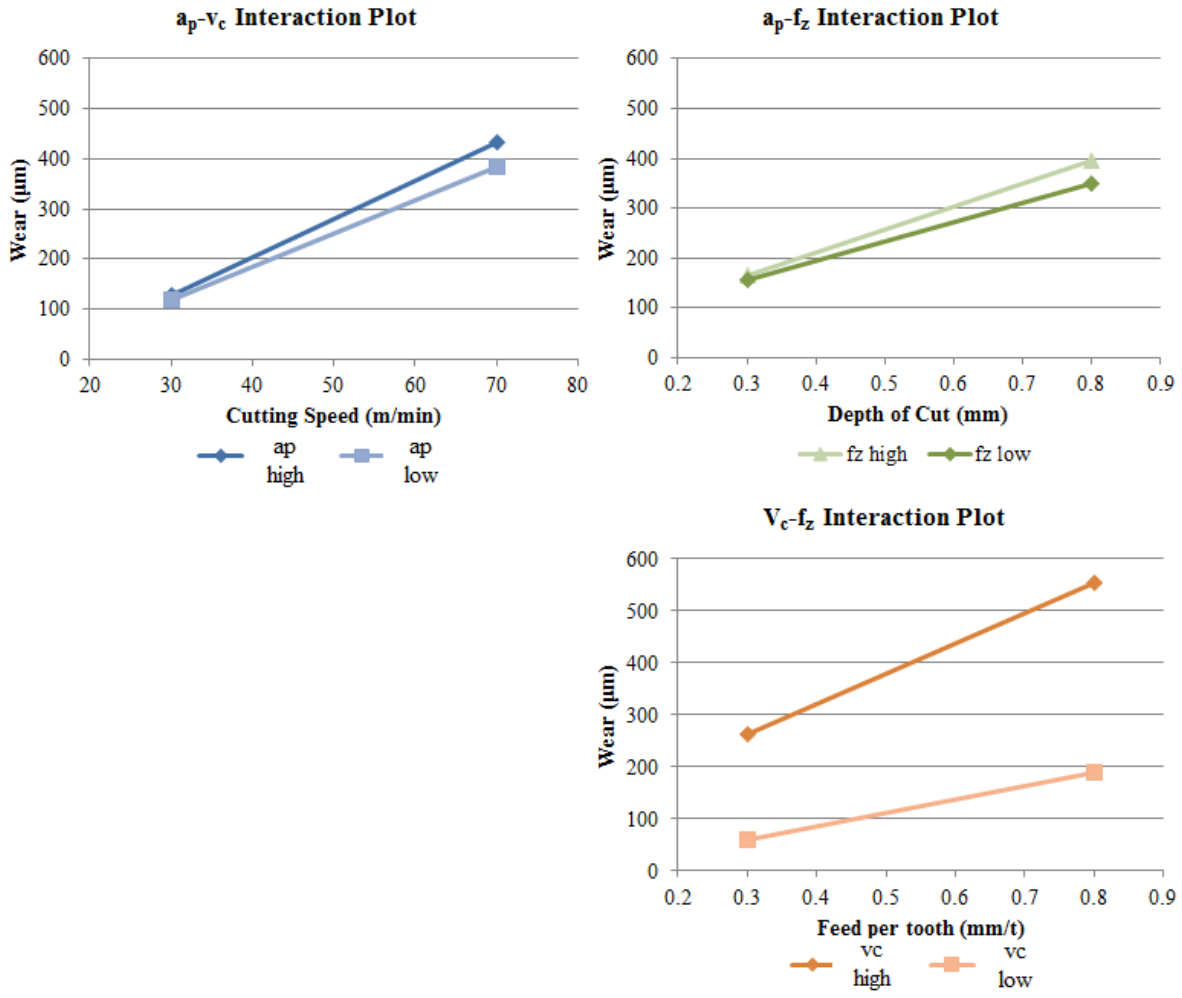

Figure 62: Interaction plot of uniform rake wear

Interaction effects of non-uniform rake wear

The interaction of the different parameters on non-uniform rake wear is shown in Figure 63. The interactions of the different parameters on non-uniform wear are relatively insignificant.

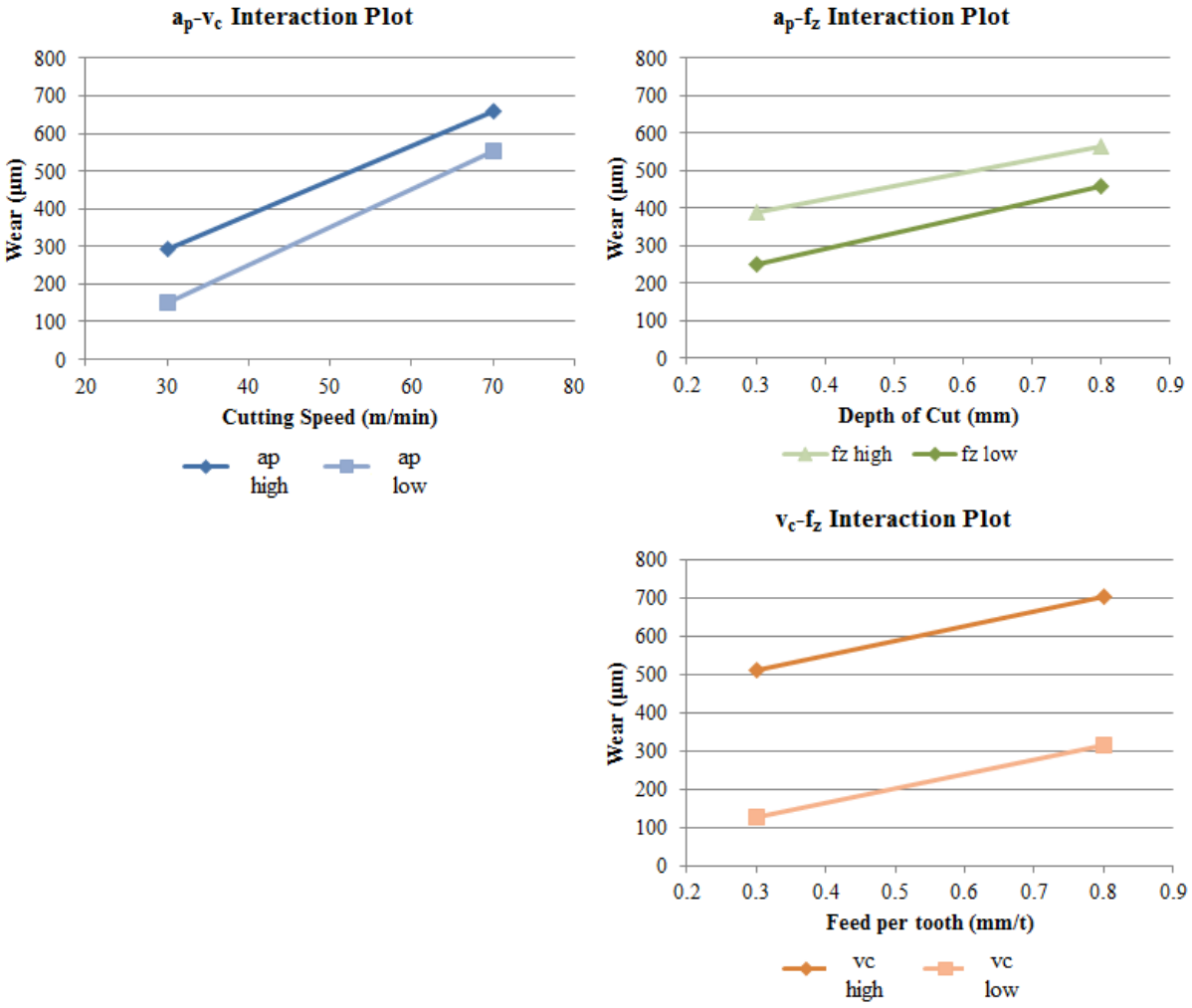

Figure 63: Interaction plot for non-uniform rake wear

Interaction effects of non-uniform flank wear

The interaction of the different parameters on non-uniform flank wear is shown in Figure 64. The interaction of cutting speed and feed per tooth is high, which suggests that the two parameters are nearly fully dependent. The v_c-f_z interaction plot shows that if feed per tooth is lowered and cutting speed is increased, the tool wear will be lower. This suggests that the cutter should be used at a lower feed per tooth and higher cutting speed to reduce non-uniform flank wear.

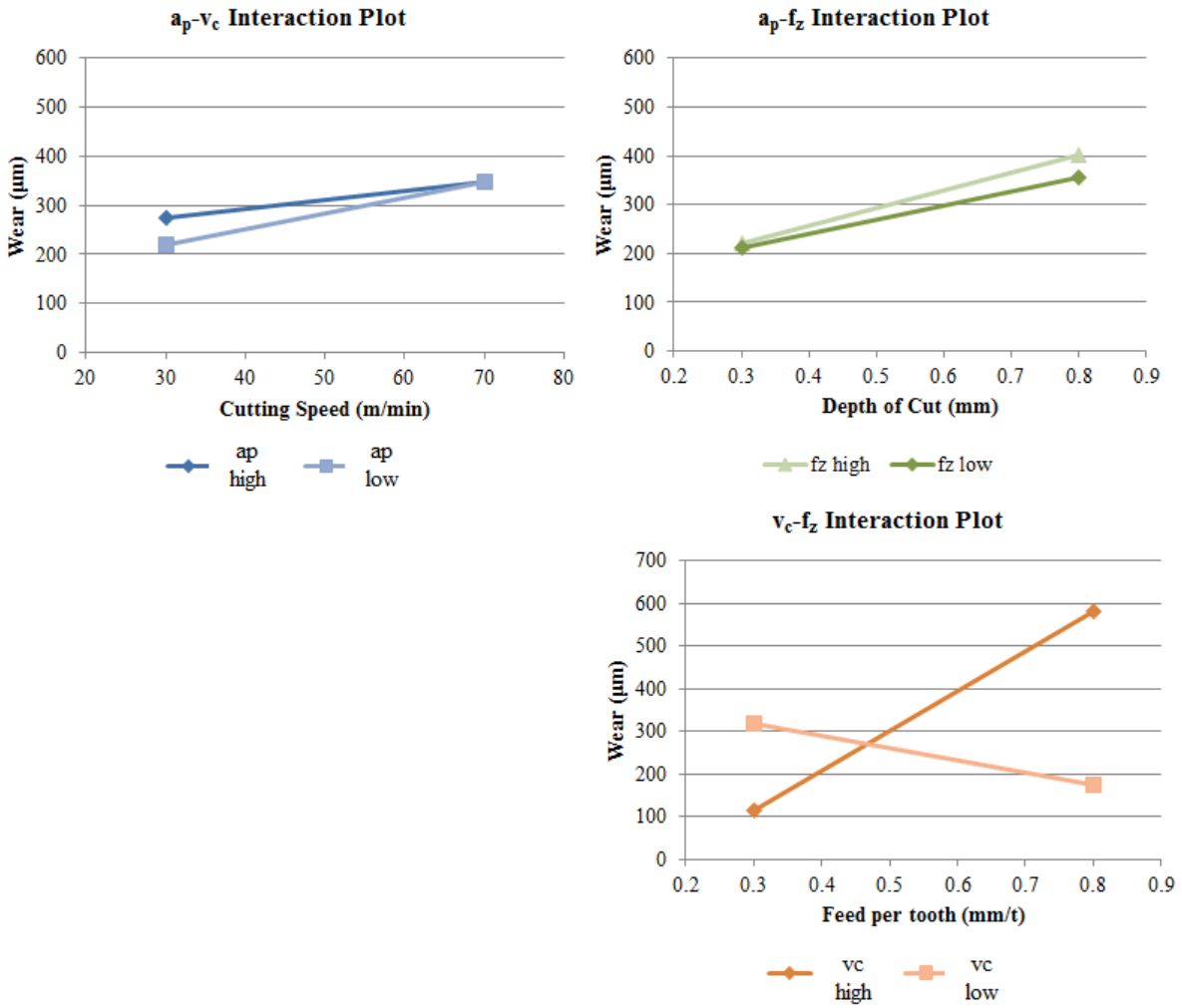

Figure 64: Interaction plot of non-uniform flank wear

Table 20 shows how the non-uniform flank wear is influenced by the feed rate (f_z) and cutting speed (v_c). With low feed rate and low cutting speed, the non-uniform tool wear on the flank is higher than with low feed per tooth and higher cutting speed. To maximise the utilisation of the flank of the tool, the feed rate should be used at its lower value and the cutting speed should be used at its higher value. The result is that the material removal rate is increased while the tool wear is decreased. Note that with a high feed per tooth and cutting speed, the non-uniform flank wear is higher than a high feed per tooth and low cutting speed, which is directly proportionate to the material removal rate (Q). The opposite is true when machining at low feed per tooth. The non-uniform flank wear is higher at a low feed per tooth and low cutting speed than at a low feed per tooth and high cutting speed.

Table 20: Tool wear and material removal rate for non-uniform flank wear

f_z (mm/t)	v_c (m/min)	Q (cm^3/min)	Tool wear (µm)
0.3	30	6.27	317.54
0.3	70	14.62	116.54
0.8	30	16.71	176.21
0.8	70	38.99	580.85

5.3.2.3 Probability plots

The normal probability plot is used to determine which factors and interaction effects are not important. For a factorial design with k factors, the cumulative proportions for an effect are determined using the following equation:

$$p_i = \frac{R_i - 0.5}{2^k - 1}$$

$p_i = cumulative\ proportion\ for\ ordered\ effect\ i$

$R_i = ordered\ rank\ of\ effects$

$k = number\ of\ factors$

(Montgomery & Runger, 2007)

Any factors or interactions whose observed effects are due to chance are expected to be randomly distributed around zero, with some being slightly below and above zero. The effects that may be important have average values different from zero and are located a significant distance away from the hypothetical vertical line that represents no effect.

Probability plot of uniform rake wear

The estimated average effects for the uniform rake wear are calculated and ranked in Table 21. The data is then plotted to form the normal probability plot in Figure 65.

Table 21: Estimated effects, ranks and cumulative proportions for uniform rake wear DoE

Effect	Average Effect	R_i	P_i
a_p-v_c-f_z	-3.9275	1	0.071429
a_p-f_z	17.5125	2	0.214286
a_p-v_c	21.2025	3	0.357143
a_p	28.3225	4	0.5
v_c-f_z	80.0725	5	0.642857
f_z	211.1825	6	0.785714
v_c	285.0625	7	0.928571

From Figure 65, it follows that the factors and effects that are distributed around zero; a_p-v_c-f_z, a_p-f_z, a_p-v_c and a_p have a small effect on the tool wear. Cutting speed (v_c) and feed per tooth (f_z) have a significant effect on the tool wear with the v_c-f_z interaction having a moderate effect on the tool wear.

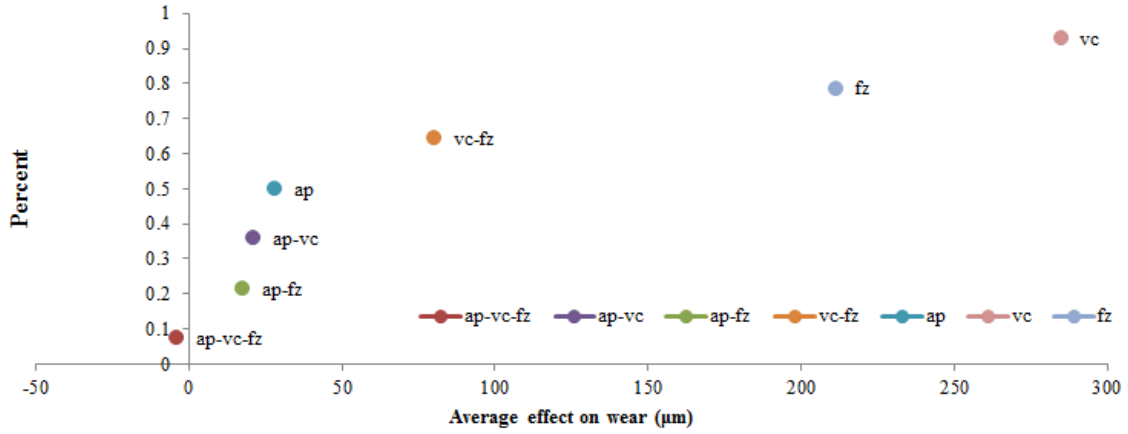

Figure 65: Normal probability plot for uniform rake wear DoE

Probability plot of non-uniform rake wear

The estimated average effects for the uniform rake wear is calculated and ranked in Table 22. The data is the plotted to form the normal probability plot in Figure 66.

Table 22: Estimated effects, ranks and cumulative proportions for non-uniform rake wear DoE

Effect	Average Effect	R_i	P_i
a_p-v_c-f_z	-67.6775	1	0.071429
a_p-v_c	-17.5825	2	0.214286
a_p-f_z	-16.7825	3	0.357143
v_c-f_z	2.3125	4	0.5
a_p	123.8125	5	0.642857
f_z	190.4175	6	0.785714
v_c	385.4475	7	0.928571

From Figure 66, it follows that the factors and effects that are distributed around zero; a_p-v_c-f_z, a_p-f_z, a_p-v_c and v_c-f_z have a small effect on the tool wear. Depth of cut (a_p) and feed per tooth (f_z) both have a moderate effect on the tool wear, where cutting speed (v_c) has a significant effect on tool wear.

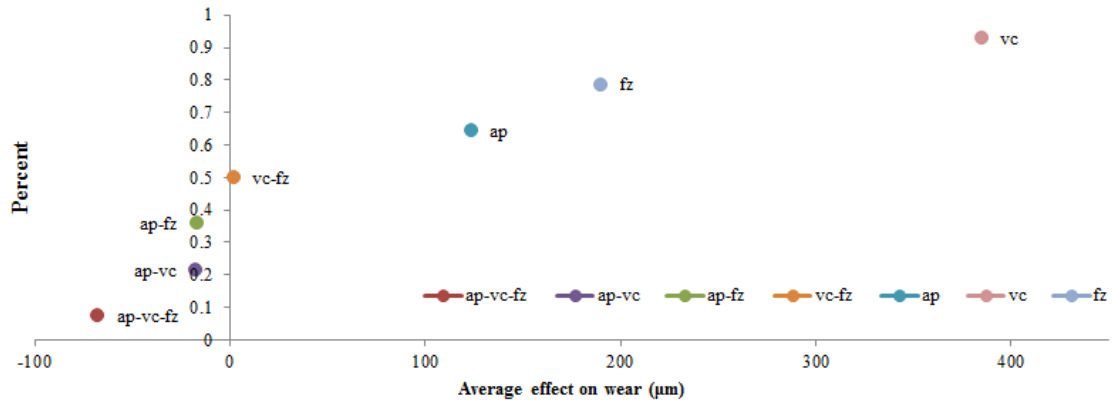

Figure 66: Normal probability plot for non-uniform rake wear DoE

Probability plot of non-uniform flank wear

The estimated average effects for the uniform rake wear is calculated and ranked in Table 23. The data is then plotted to form the normal probability plot in Figure 67.

Table 23: Estimated effects, ranks and cumulative proportions for non-uniform flank wear DoE

Effect	Average Effect	R_i	P_i
a_p-v_c	-27.6775	1	0.357143
a_p-f_z	17.5425	2	0.214286
a_p	26.6925	3	0.5
a_p-v_c-f_z	38.0925	4	0.071429
v_c	101.7975	5	0.928571
f_z	161.4675	6	0.785714
v_c-f_z	302.8375	7	0.642857

From Figure 67, it follows that the factors and effects that are distributed around zero; a_p-v_c-f_z, a_p-f_z, a_p-v_c and a_p have a small effect on the tool wear. Cutting speed (v_c) and feed per tooth (f_z) both have a moderate effect on the tool wear, where the interaction between cutting speed (v_c) and feed per tooth (f_z) has a significant effect on tool wear. The significant effect that the v_c-f_z interaction has on the non-uniform rake wear could be due to the increase in vibration during machining at high feed and high speed causing brittle fracture of the tool cutting edge during interrupted and heavy cutting.

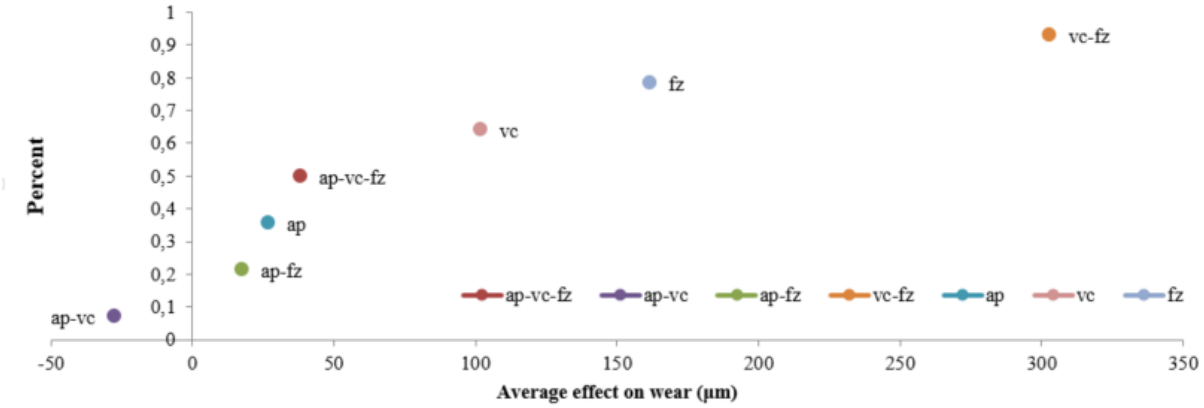

Figure 67: Normal probability plot for non-uniform flank wear DoE

Probability plot of the average effects of all the tool wear types

Figure 67 represents the probability plot of all the average effects, which shows how the average effects are distributed. A small grouping of an average effect shows that a cutting parameter has similar influence on the tool wear across all the different wear types and that the effect can be easily predicted such as feed per tooth (f_z), which has a moderate effect across all wear types.

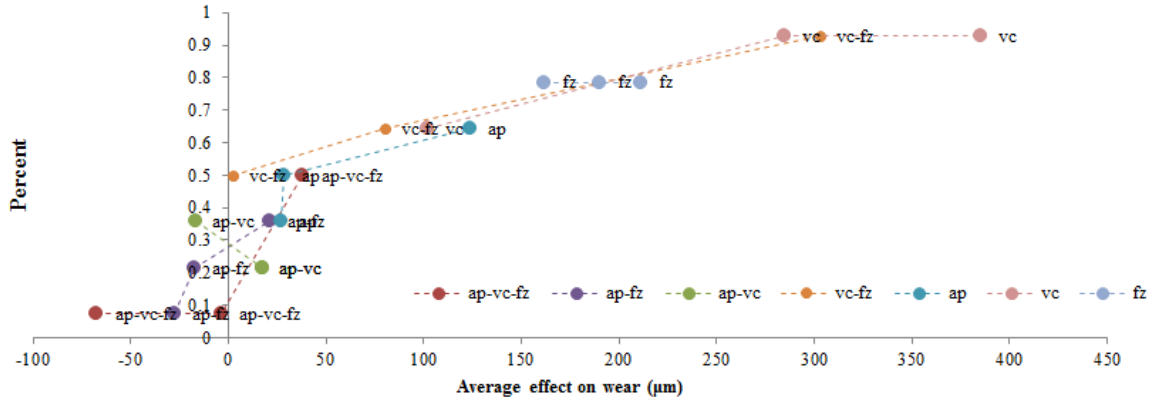

Figure 68: Probability plot of all the average effects

Figure 68 presents the average of the average effects. It shows which effects have on average the largest effect on tool wear. It should be used in conjunction with Figure 67 as it does not show how the data is distributed. It shows how cutting speed (v_c) and feed per tooth (f_z) have on average the largest effect on tool wear, of all the main effects and interactions. The interaction between v_c and f_z is high due to the significant effect v_c and f_z respectively, has on tool wear.

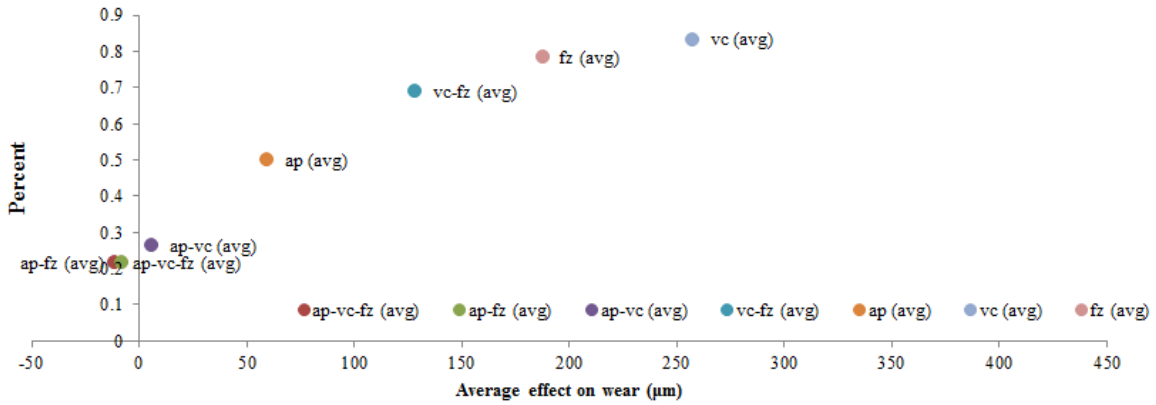

Figure 69: Probability plot of the average of the average effects

5.3.3 Regression coefficients

The coefficient plot displays the regression coefficients with confidence intervals. This plot is used to interpret the regression coefficients. The coefficient plot data is centered and scaled, which makes the coefficients comparable. The size of the coefficient represents the change in the response when a factor is varied from the low to the high level, in coded units, while the other factors are kept at their averages. The coefficient is significant when the confidence interval does not cross zero. With factorial designs, the coefficients are half the size of the effects. The regression coefficients are to be used with the main effects and interaction plots from the previous section.

Regression coefficients for uniform rake wear

The regression coefficients for uniform rake wear are presented in Figure 69. It shows that cutting speed and feed per tooth has the most significant influence on uniform tool wear. The v_c-f_z influence is minor, but still significant. The a_p, a_p-v_c and a_p-f_z is insignificant within a confidence interval of 95%. These findings are supported by the probability plot for uniform rake wear (Figure 65).

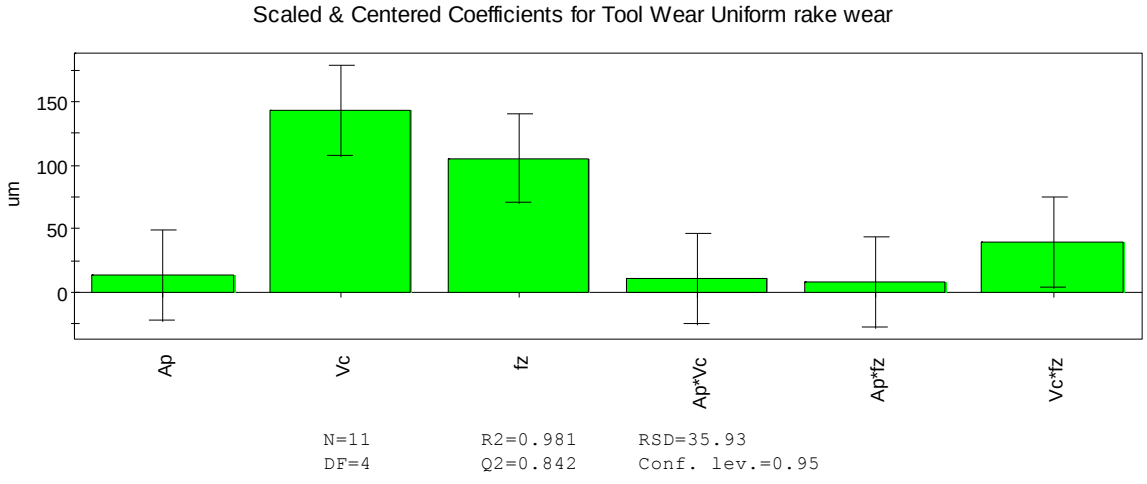

Figure 70: Regression coefficients plot for uniform rake wear

Regression coefficients for non-uniform rake wear

The regression coefficients for uniform rake wear are presented in Figure 70. It shows that cutting speed (v_c) is the only significant coefficient, where all the other effects and influences are insignificant within a confidence interval of 95%. It should be noted that the model for non-uniform wear has a Q^2 value of 0.257, which is sensitive to insignificant terms in the model and the regression coefficient plot shows that all of the terms are insignificant, except v_c.

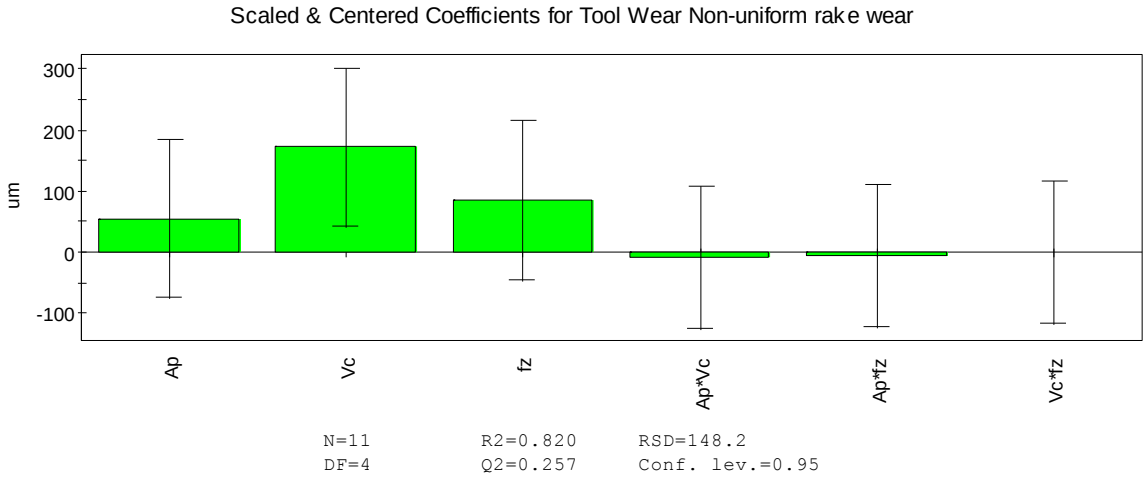

Figure 71: Regression coefficients plot for non-uniform rake wear

Regression coefficients for non-uniform flank wear

The regression coefficients for uniform rake wear are presented in Figure 71. It shows that depth of cut (a_p), feed per tooth (f_z) and the v_c-f_z interaction are significant terms. This corresponds with the normal probability plot for non-uniform flank wear (Figure 67). V_c may also be a borderline significant coefficient since the confidence band barely crosses the zero line.

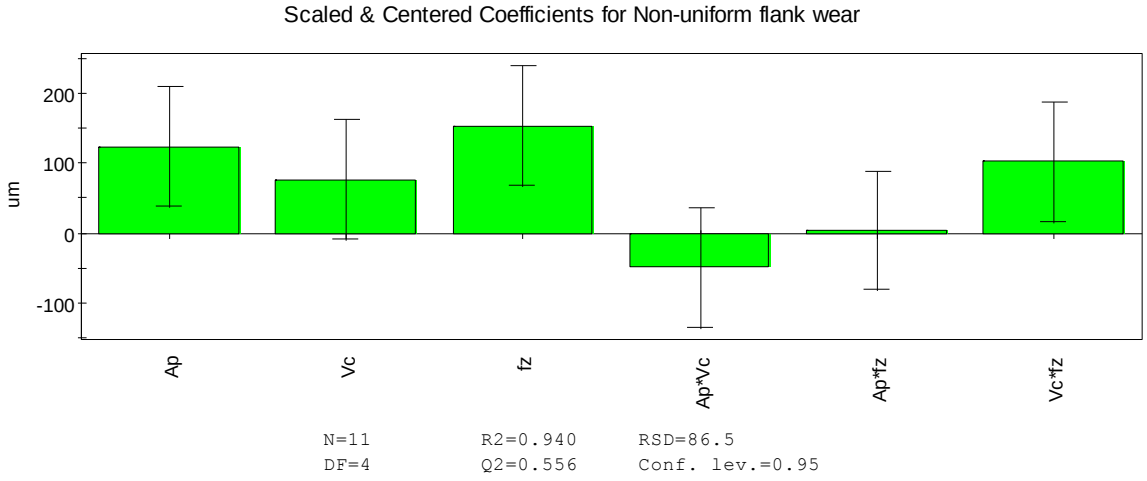

Figure 72: Regression coefficient plots for non-uniform flank wear

5.3.4 Normal probability plots of residuals

Residuals N-plot shows the residuals of a response versus the normal probability of the distribution of data. If all points are on a straight line on the diagonal, the residuals of the response are normally distributed noise, which is the ideal result. Points far from the fitted line indicate outliers that should be evaluated. A curved pattern indicates non-modelled quadratic relations or incorrect transformation of the response. Degrees of freedom less than 5 can result in irregular patterns. This plot identifies outliers and assesses the normality of the residuals.

Normal probability plot for uniform rake wear

Figure 72 represents the normal probability plot for uniform rake wear. The data is fairly distributed around the fitted line with a R^2 of only 0.616. While this is still significant, it suggests that the deviation of the residuals from normal is not due to random generated noise, but by another unidentified factor. Experiments 5, 7 and 9 are the data points that are the furthest from the fitted line. Inspection shows experiments 5 and 7 were machined with a high feed per tooth. The machine experienced vibration at high chip loading due to high feed rates. The deviation in residuals may be due to the factor that caused vibration, but determining the unidentified factor requires further study.

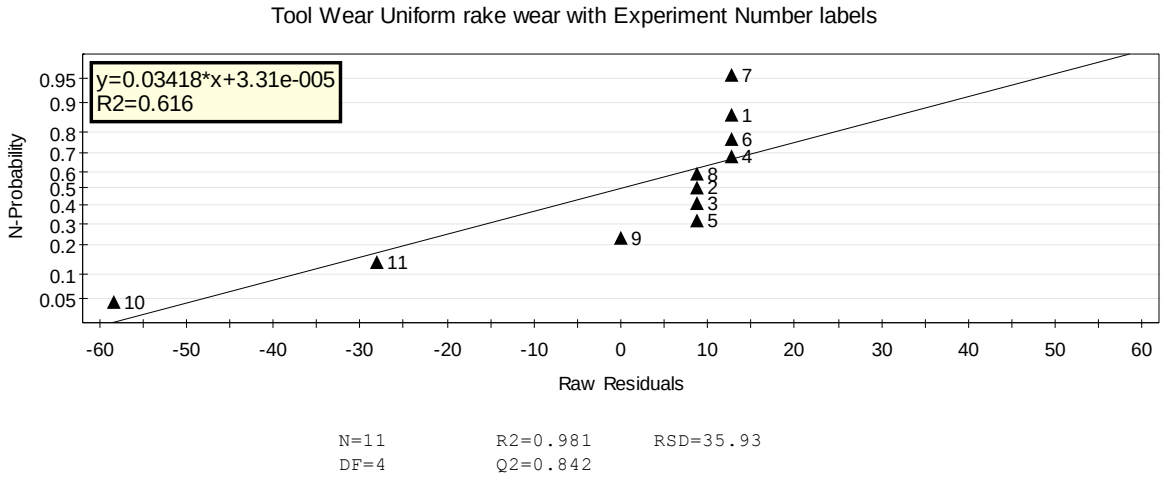

Figure 73: Normal probability plot for uniform rake wear

Normal probability plot for non-uniform rake wear

Figure 73 represents the normal probability plot for non-uniform rake wear. It shows data that is distributed around the fitted line with a R^2 of 0.8083, which signifies a moderate fit. The most apparent outliers are experiments 7, 8 and 9. Experiments 7 and 9 are the same data points identified on the normal probability plot for uniform rake wear. As both of these wear types occur on the same region on the tool, a similar unidentified factor may be responsible for the deviation in residuals.

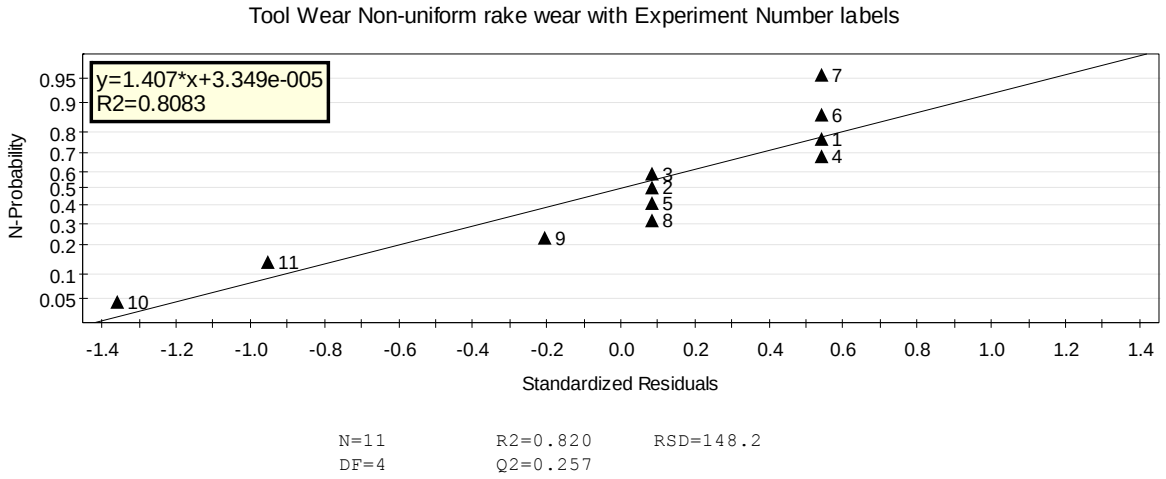

Figure 74: Normal probability plots for non-uniform rake wear

Normal probability plot for non-uniform flank wear

Figure 74 represents the normal probability plot for non-uniform flank wear. The data is distributed around the fitted line with a R^2 of 0.9395, which is a relatively good fit. There is only one apparent outlier, which is experiment 10. There is no apparent factor that could have influenced the residuals of experiment 10.

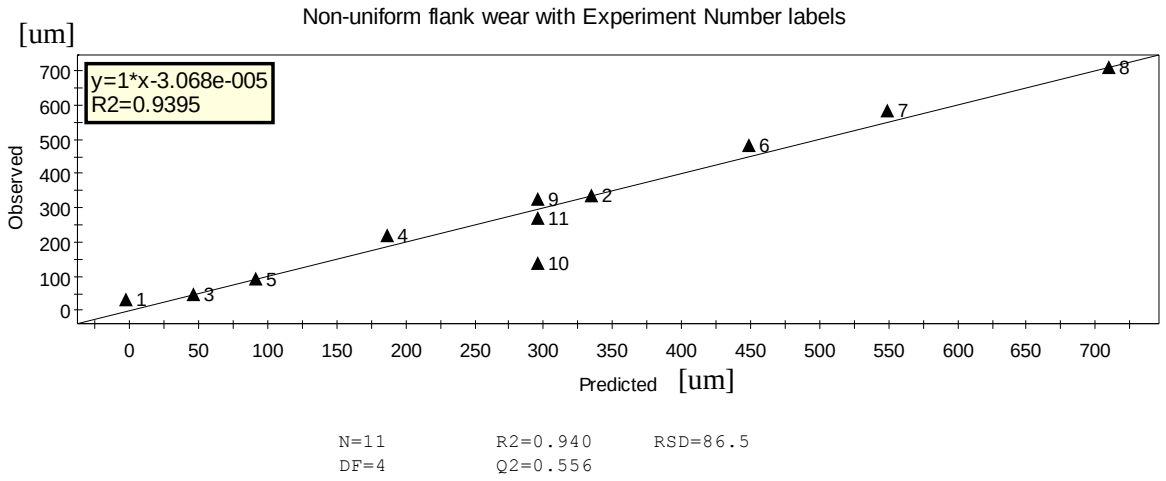

Figure 75: Normal probability plots for non-uniform flank wear

5.3.5 Observed vs predicted data

The plot displays observed values vs. predicted values. The line represents the regression line, where plots with the data points close to a straight line indicate good models. With a good model, all the points will fall on the regression line. Outliers can be identified as the points that are far away from the regression line.

Observed vs predicted data plot for uniform rake wear

Figure 75 shows how good the observed data fits the predicted values with a R^2 value of 0.9811. There are no apparent outliers, with the centerpoints, experiments 9, 10 and 11, being the points the furthest away from the line. This may indicate that the model may be slightly curved due to the variation at the centerpoints.

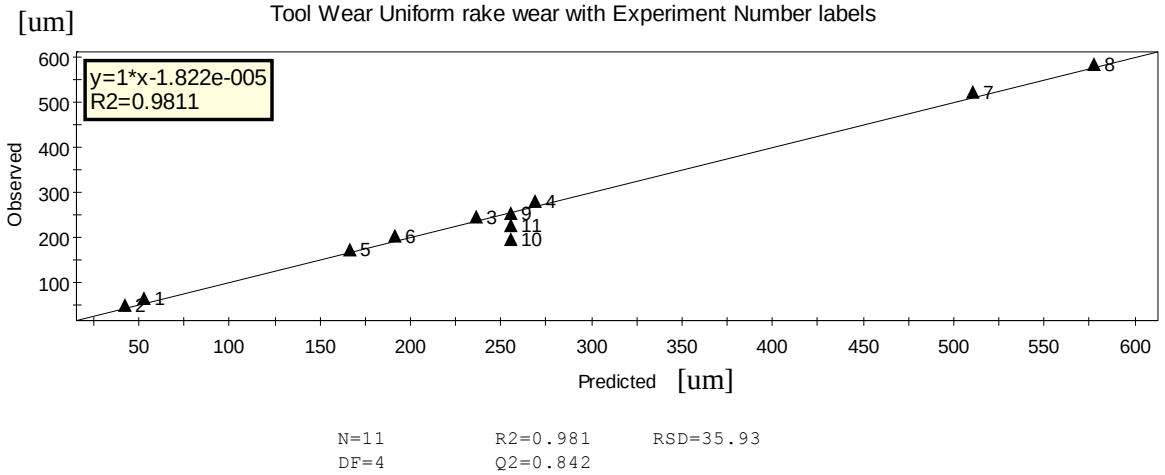

Figure 76: Observed vs predicted data plots for uniform rake wear

Observed vs predicted data plot for non-uniform rake wear

Figure 76 shows that the observed data fits the predicted data relatively well with a R^2 value of 0.8204. The centerpoints are the data points that are situated the furthest from the line. This may coincide with the data plot for uniform rake wear, indicating that the model may have a slight curve.

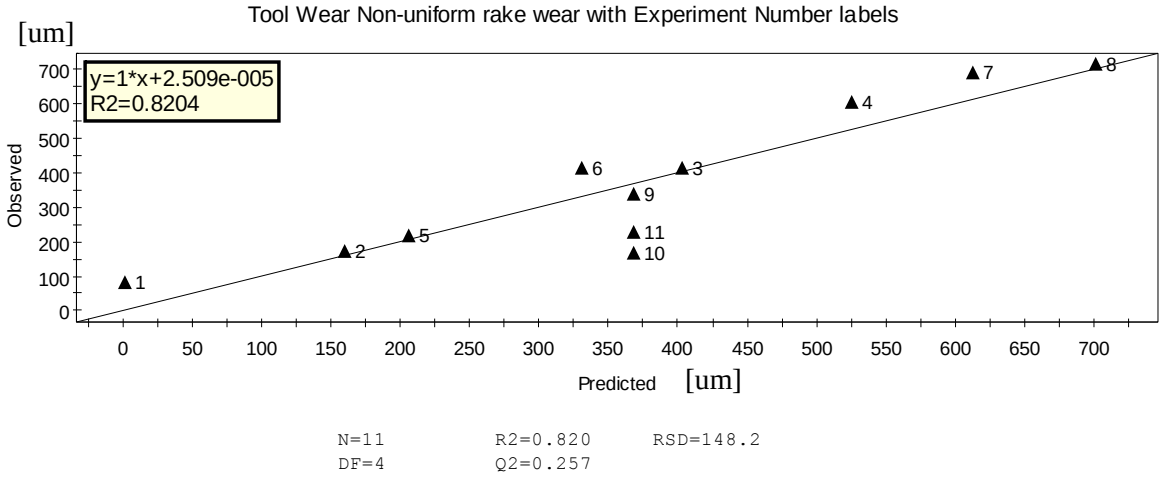

Figure 77: Observed vs predicted data plots for non-uniform rake wear

Observed vs predicted data plot for non-uniform flank wear

Figure 77 shows that the observed data fits the predicted data well with a R^2 value of 0.9395. Again, the centerpoints are situated the furthest away from the line, indicating that the model may not be perfectly linear.

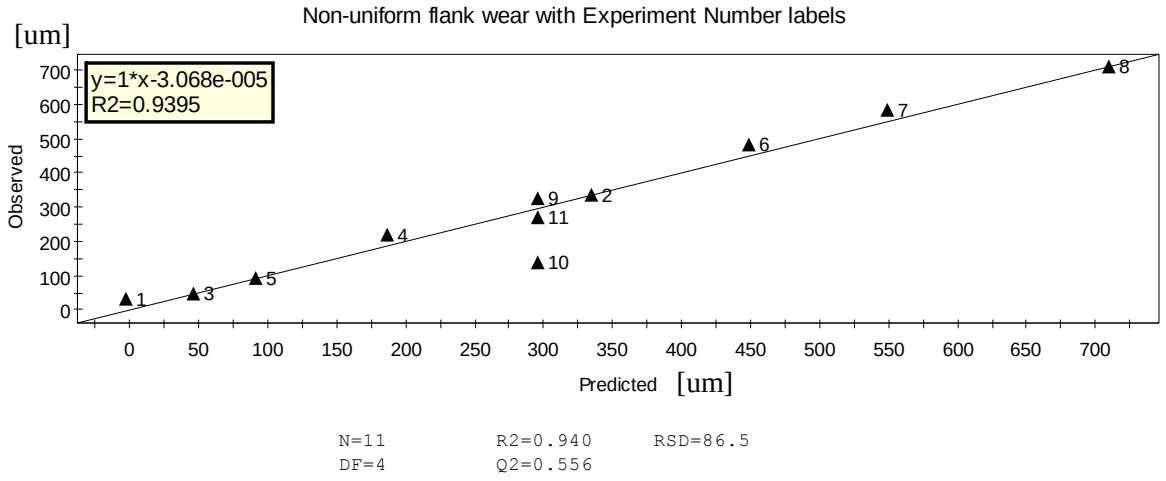

Figure 78: Observed vs predicted data plots for non-uniform flank wear

5.4 Interpretation of the data

Figure 78, Figure 79 and Figure 80 are 4D contour plots representing the tool wear of the different wear types. These plots can be used to predict the different tool wear scenarios when a set of cutting parameters is selected. The target amount of tool wear for each wear type can be selected and a feasible set of solutions can be identified. The areas outlined by the dotted lines represent the feasible set of solutions. The most desirable set of solutions is the set that results in the highest material removal rate. This represents the set of parameters that will rough the part in the shortest amount of time and will result in the predetermined amount of tool wear.

To find the most desirable set of solutions, the feasible areas for all the wear types have to be evaluated and used as constraints to find the area that is common with all the wear types. The area common with all the wear types will be the feasible area that is subject to all the constraints. The set of feasible cutting parameters that yield the highest material removal is the most desirable set of solutions in the design space.

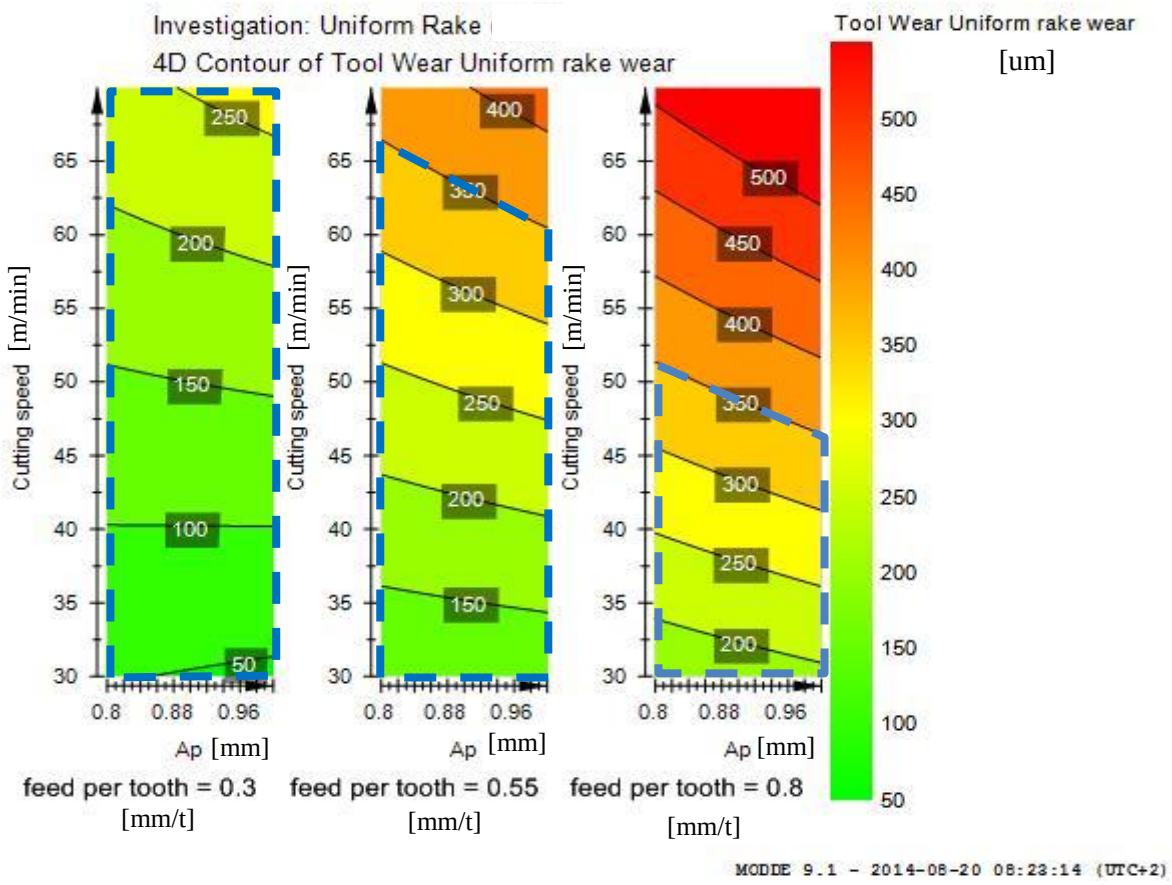

Figure 79: 4D contour plots for uniform rake wear

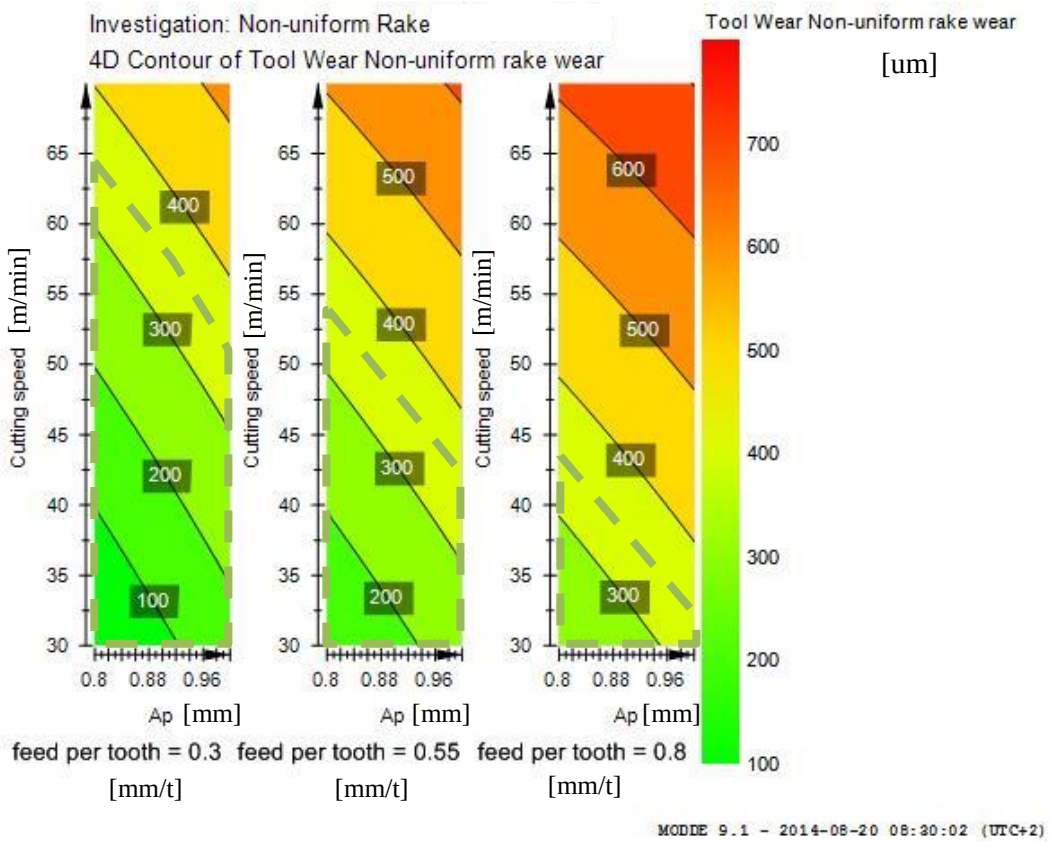

Figure 80: 4D contour plots for non-uniform rake wear

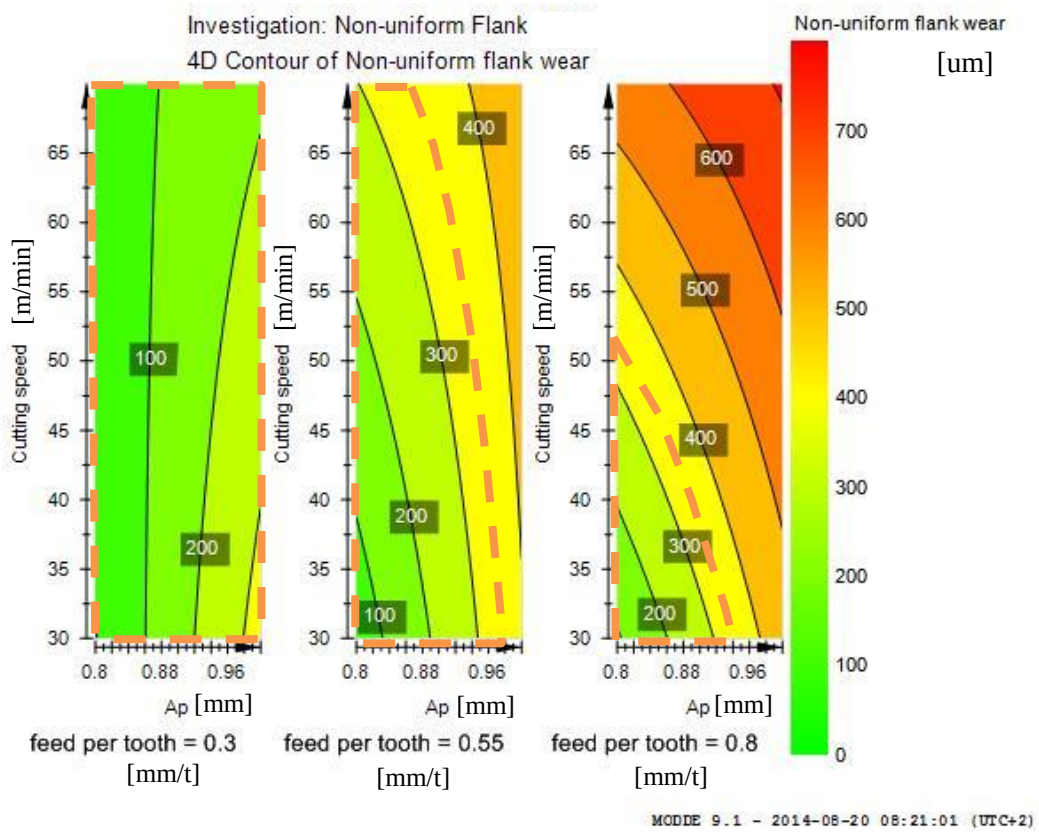

Figure 81: 4D contour plots for non-uniform flank wear

Figure 81 presents the feasible cutting parameters solution space. The objective function of the problem is the function that determines the material removal rate.

$$max\ Q = \frac{a_p \times b \times f_z \times z \times v_c}{\pi \times D}$$

where Q = material removal rate [cm^3/min]

a_p = depth of cut [mm]

b = width of cut [mm]

f_z = feed per tooth [mm/t]

z = number of teeth

v_c = cutting speed [m/min]

D = diameter of the tool [mm]

The value for b is taken as 17.5 mm, z as 4 and D as 32 mm, determined from the experimental design. It is observed that the material removal rate is directly proportional to the cutting parameters, therefore, an increase in one of the parameters results in an increase in the material removal rate. The upper limit of each of the cutting parameters in the feasible solution space would be evaluated to determine the maximum material removal rate. Table 24 shows the material removal rate at each of the possible solutions in Figure 81.

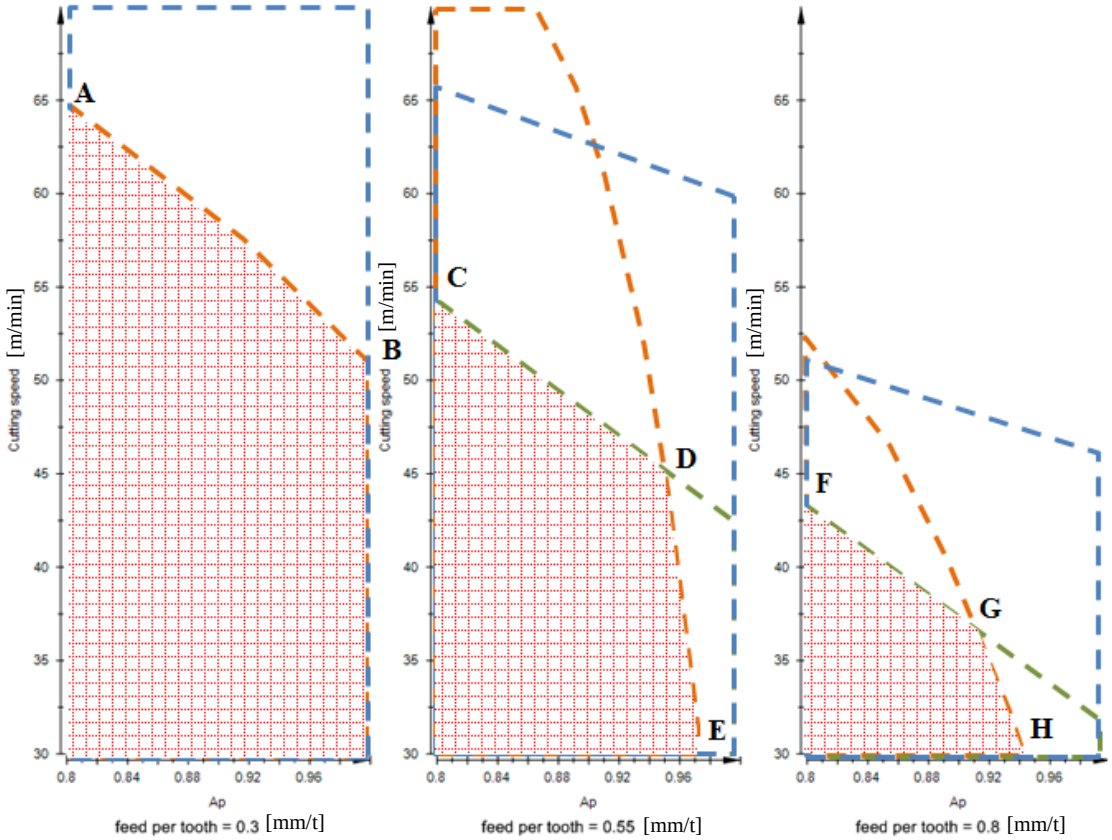

Figure 82: Feasible cutting parameters solution space

Table 24: Feasible solutions

Solution	a_p [mm]	v_c [m/min]	f_z [mm/t]	Q [cm^3/min]	
A	0.8	65	0.3	10.9	
B	1.0	52	0.3	10.9	
C	0.8	54	0.55	16.6	
D	0.95	46	0.55	16.8	
E	0.97	30	0.55	11.2	
F	0.8	43	0.8	19.3	← max
G	0.91	36	0.8	18.3	
H	0.95	30	0.8	16.0	

From Table 24, it is clear that the maximum material removal rate is found at solution F, which has a depth of cut of 0.8 mm, cutting speed of 43 m/min and a feed per tooth of 0.8 mm. This results in a material removal rate of 19.3 cm^3/min and a roughing process of 12.3 minutes. With this solution set, it is expected that the uniform rake wear is 280 µm, the non-uniform rake wear is 250 µm and non-uniform flank wear is 250 µm. Thus, the non-uniform flank wear is the binding constraint. If the target flank wear could be increased, the material removal rate could be increased, resulting in a decreased roughing time.

5.5 Predictions

From a regression analysis, it was seen that there is a linear relationship between average tool wear as well as the material removal rate (MRR), and the average tool wear is dependent on depth of cut, cutting

speed and feed per tooth. The R^2 value of the fitted line is 0.842158, which represents a moderate fit. Figure 82 shows this linear relationship as well as the predicted linear regression relationship and the 95% confidence bands. The regression summary output can be found in Appendix E.

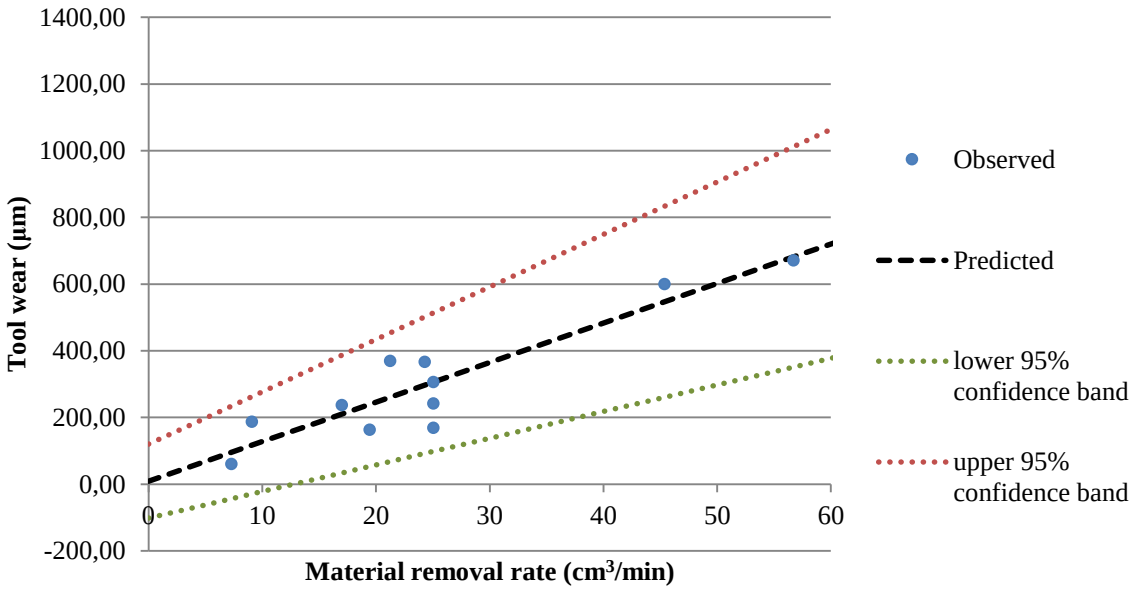

Figure 83: Regression plot for MRR vs uniform rake wear

This relationship can be used to predict tool wear against material removal rate within a confidence level of 95%. It can be seen that as the material removal rate is increased, and subsequently, any combination of the cutting parameters which the material removal rate is dependent on, the tool wear will also increase proportionately.

5.6 Conclusions

A statistical analysis was done from the observations that resulted from the experimentation. The analysis showed that the different cutting parameters have an influence that can be measured across all the wear types. It can be seen from the analysis that cutting speed is the primary cause of tool wear from all the parameters tested. Each of the other parameters also caused different wear types in varying degrees.

The analysis showed that an increase in cutting speed results in an increase in uniform rake, non-uniform rake and non-uniform flank wear. Table 19 shows that, of the main effects, cutting speed is responsible for 51.0% of the wear. This is a well-known phenomenon and it is generally accepted in the machining industry, where the ISO 8688 standard states that tool life should be evaluated against cutting speed. In well-known tool life equations, such as the Tailor Tool Life Equation, tool life is measured against time and cutting speed.

Feed per tooth has the second biggest influence on the tool wear and represents 37.2% of the wear, of the main effects. Feed per tooth had a similar effect on the wear, with a small deviation across the different wear types.

The depth of cut had the smallest influence on the tool wear, of all the main effects, representing only 11.8% of the influence. From the regression coefficients, depth of cut only had a significant influence on non-uniform flank wear. Changing depth of cut does not have a large effect on tool life, but a small depth of cut causes friction when cutting the hardened layer of a workpiece, which shortens the tool life.

6. Conclusions and recommendations

6.1 Overview of project

The aim of this project was to determine if improved machining techniques could be used to contribute to a significantly improved titanium aerospace part manufacturing process in the South African industry. Chapter 1 provided an overview of the importance of establishing a full titanium value chain to manufacture titanium parts in South Africa. The project exists to develop and transfer key competencies in machining titanium to local manufacturing industry. A local industry partner was selected according to specified criteria and work collaboration was established.

Chapter 2 served as the literature review, where aerospace parts, the properties of titanium and its alloys and conventional machining were discussed. A summary of recommended insert properties and selected aspects of machining strategies for use in machining of titanium parts was compiled, which was used as a basis for the experimental design and setup.

Chapter 3 covered the case study at the industrial partner, where a demonstrator part was selected according to criteria specified in Chapter 2. As the industry partner at the time did not have the expertise to machine titanium, a part machined from 15-5PH stainless steel was selected, which was also classified as a difficult-to-machine material. The process to machine this part was investigated and analysed and it was discovered that approximately 70% of the time to machine the part was expended on the single roughing process. The roughing process was re-evaluated and a 70% reduction in machining time was realised.

In Chapter 4, the experimental design and setup was discussed. The goal of the experimentation was to determine if it was possible to effectively machine a titanium part of specified geometry at the industry partner without significant capital expenditure as well as the set of parameters at which this would be possible. The experiments were set up as a 2-level 3-factor full factorial screening test and the tool wear was selected as a response variable at which the effectiveness of the machining test was evaluated.

Chapter 5 captured the analysis of the experimental results. The raw data was inspected and the model diagnosed to see if it was valid to be used for analysis and predictions. The data was interpreted and a feasible set of machining parameters to machine the titanium part was determined. The set of parameters that yielded the highest material removal rate was selected and served as the recommended set of parameters at which the part should be machined.

6.2 Proposed new roughing process

The proposed new cutting process requires a depth of cut of 0.8 mm, a cutting speed of 43 m/min and a feed per tooth of 0.8 mm. The material removal rate that is dependent on these previously stated parameters is 19.3 cm^3/min. This resulted in a roughing time of 12.3 minutes. It should be noted that the cutting parameters are only valid for the specific conditions that the experimentation was conducted under. Any change in mounting, cutting fluid, spindle and machine may cause the set of parameters to be invalid and may influence the expected tool wear.

It is seen that for the proposed new roughing process, the minimum depth of cut and maximum feed per tooth are selected. Due to the high feed per tooth, some chipping and fracturing of the insert may occur. If chipping does occur, Appendix B can be used to diagnose the tool wear type and its causes. It states that the feed per tooth may be too high, the tool rigidity is not high enough, the tool material is too high or lack of tool strength. To reduce chipping and fracturing, the feed per tooth can be reduced to 0.55 mm, with depth of cut increased to 0.95 mm and cutting speed increased to 46 m/min. This solution will result in the required tool wear and an effective material removal rate of 16.8 cm^3/min and a roughing time of 14.2 min. With the reduction in feed per tooth, the roughing time is increased, but the risk of chipping and fracturing is reduced, should a higher process reliability be required.

6.3 Conclusions

It was found that the improved process was capable of economically producing titanium parts at the industry partner using their facilities without significant capital expenditure. This answered the research question that improved machining techniques could be used to contribute to a significantly improved titanium aerospace part manufacturing process in the South African industry. It was confirmed that Daliff Precision Engineering could start machining titanium aerospace economically with their available facilities and machinery.

The statistical analysis presented in the document is only valid for the specific part in the specific cutting conditions, tool, spindle, cutting fluid and machine and may differ when any of the parameters are changed. The statistical analysis confirmed the result from literature that cutting speed has the biggest effect on tool wear.

It was seen that the coatings on the tools performed well as the tool showed a small amount of wear, until the tool coating wore off, where after there would be accelerated non-uniform wear. It is suggested that the tool coating served as a chemical barrier, preventing adhesion, diffusion and chemical wear, as stated by Jawaid (Jawaid, et al., 2000). The process parameters should be adjusted to ensure that the tool coating would not delaminate.

It was found that high feed per tooth caused fluctuations in cutting speed. For heavy interrupted cuts, a tougher tool is needed. If a tool is too hard, chipping or fracturing may occur, but the hardness is needed for the sharp cutting edge that is preferred when machining titanium.

A linear relationship of average tool wear and material removal rate was found. An increase in any of the cutting parameters on which material removal rate is dependent results in a proportionate increase in tool wear.

6.4 Recommendations

The following recommendations are made for consideration for further research:

- A study into the rate of delamination or wear of the tool coatings as well as the effect the wear mechanisms have on the tool wear before and after delamination. The cause of tool delamination should also be identified and analysed.
- It can also be of value if the recommended cutting parameters are validated at the industry partner. The recommended cutting parameters were not validated in this project because the repeatability of the experiments was deemed high by the statistical analysis and the experimentation was already done at the industry partner.
- A study into the effect the roughing process has on the fatigue life of the part.
- A study into the chemistry of the surface of the workpiece and tool tip to identify possible attrition and adhesion.
- A study into the tool life testing at the recommended cutting parameters to get the tool life shape characteristic.
- A study into the improvement of the surface finishing process at the industry partner as it is the process that takes the longest to machine, if the improved roughing cut parameters are used.

7. References

Abdel-Aal, H., Nouari, M. & El Mansori, M., 2009. Influence of thermal conductivity on wear when machining titanium alloys. *Tribology International,* Issue 42, pp. 359-372.

Bayoumi, A. & Xie, J., 1995. Some metallurgical aspects of chip formation in cutting Ti-6wt.%Al-4wt.%V alloy. *Material Science and Engineering,* A(190), pp. 173-180.

Boeing Phantom Works, 2008. *High Performance Ti Machining,* St.Louis: The Boeing Company.

Boeing, 2014. *Boeing 777 Family facts.* [Online] Available at: http://www.boeing.com/boeing/commercial/777family/pf/pf_facts.page [Accessed 12 Aug 2014].

Boothroyd, G., 1989. Machine Tools and Machining Operations. In: 2nd, ed. *Fundamentals of Metal Machining and Machine Tools.* New York: Marcell Dekker Inc., pp. 1-11.

Boyer, R., 1995. Titanium for Aerospace; Rationale and Application. *Advanced Performance Materials,* Volume 2, pp. 349-368.

Boyer, R., 1996. An overview on the use of titanium in the aerospace industry. *Materials Science and Engineering,* A(213), pp. 103 - 114.

Boyer, R., Welsch, G. & Collings, E., 1994. *Materials Properties Handbook: Titanium Alloys.* Ohio: ASM International.

Brewer, W. D., Bird, K. R. & Wallace, T. A., 1998. Titanium alloys and processing for high speed aircraft. *Materials Science and Engineering,* A(243), pp. 299-304.

Brinksmeier, E., Walter, A., Janssen, R. & Diersen, P., 1999. Aspects of cooling lubrication reduction in machining advanced materials. *Institution of Mechanical Engineers: Journal of Engineering Manufacture,* Issue 213, pp. 769 - 777.

Chunxiang, C., Baomin, H., Lichen, Z. & Shuangjin, L., 2011. Titanium alloy production technology, market prospects and industry development. *Materials and Design,* Volume 32, pp. 1684 - 1691.

Defence Metals Information Center, 1965. *Machining of titanium.* Columbus: Battelle Memorial Institute.

Dudzinski, D. et al., 2004. A review of developments towards dry and high speed machining. *International Journal of Machine Tools & Manufacture,* Volume 44, pp. 239-456.

Endres, W. J. & Kountanya, R. K., 2002. The Effects of Corner Radius and Edge Radius on Tool Flank Wear. *Journal of Manufacturing Processes,* 4(2), pp. 89 - 96.

Ezugwu, E., 2005. Key improvements in the machining of difficult-to-cut aerospace superalloys. *International Journal of Machine Tools & Manufacture,* Issue 45, pp. 1353-1367.

Ezugwu, E., Bonney, J., Da Silva, R. & Cakir, O., 2007. Surface integrity of finished turned Ti–6Al–4V alloy with PCD tools using conventional and high pressure coolant supplies. *International Journal of Machine Tools & Manufacture,* Issue 47, pp. 884-891.

Ezugwu, E., Bonney, J. & Yamane, Y., 2003. An overview of the machinability of aeroengine alloys. *Journal of Materials Processing Technology,* Issue 134, pp. 233-253.

Ezugwu, E. & Wang, Z., 1997. Titanium alloys and their machinability - a review. *Journal of Materials Processing Technology,* Issue 68, pp. 262-274.

Froes, F., Yau, T. & Weidinger, H., 1996. Chapter 8: Titanium, Zirconium and Hafnium. In: *Structure and Properties of Nonferrous Alloys.* s.l.:VCH Verlagsgesellschaft mbH and VCH Publishers Incorporated, pp. 399 - 468.

Gente, A. & Hoffmeister, H., 2001. Chip Formation in Machining Ti6Al4V at Extremely High Cutting Speeds. *CIRP Annals Manufacturing Technology,* 50(1), pp. 49-52.

Ghani, J., Choudhury, I. & Hassan, H., 2004. Application of Taguchi method in the optimization of end milling parameters. *Journal of Materials Processing Technology,* Issue 145, pp. 84 - 92.

Gitlow, H. S., Oppenheim, A. J., Oppenheim, R. & Levine, D. M., 2005. *Quality Management.* 3rd ed. New York: McGraw Hill.

Groover, M. P., 2007. *Fundamentals of Modern Manufacturing: Materials, Processes, and Systems.* 3rd ed. Hoboken: John Wiley & Sons.

Guilin, Y., Nan, L., Yousheng, L. & Yining, W., 2007. The effects of different types of investments on the alpha-case layer of titanium castings. *The Journal of Prosthetic Dentistry,* 97(3), pp. 157-164.

Huang, N., Qingzhen, B., Wang, Y. & Sun, C., 2014. 5-Axis adaptive flank milling of flexible thin-walled parts based on the on-machine measurement. *International Journal of Machine Tools and Manufacture,* Volume 84, pp. 1-8.

Iscar, 2012. *ISCAR Milling Tools (Metric Version) Catalogue.* Jerusalem: Iscar.

ISO, 1989. *ISO 8688-1:1989.* Geneve: International Organisation for Standardisation.

Jawaid, A., Sharif, S. & Koksal, S., 2000. Evaluation of wear mechanisms of coated carbide tools when face milling titanium alloys. *Journal of Materials Processing Technology,* Volume 99, pp. 266-274.

Kitagawa, T., Kubo, A. & Maekawa, K., 1997. Temperature and wear of cutting tools in high-speed machining of Inconel 718 and Ti-6Al-6V-2Sn. *Wear,* Issue 202, pp. 142-148.

Komanduri, R., 1982. Some clarifications on the mechanics of chip formation when machining titanium alloys. *Wear,* Issue 76, pp. 15-34.

Komanduri, R. & Von Turkovich, B., 1981. New observations on the mechanism of chip formation when machining titanium alloys. *Wear,* pp. 179 - 188.

Kopac, J., Sokvic, M. & Dolinsek, S., 2001. Tribology of coated tools in conventional and HSC machining. *Journal of Materials Processing Technology,* Issue 118, pp. 377-384.

Kramer, T. R., 1992. Pocket Milling with Tool Engagement Detection. *Journal of Manufacturing Systems,* 11(2), pp. 114 - 123.

Leyens, C. & Peters, M., 2003. *Titanium and Titanium Alloys: Fundamentals and Applications.* 1st ed. Weinheim: Wiley-VCH.

Lin, L., 1989. A Concordance Correlation Coefficient to Evaluate Reproducibility. *Biometrics,* Issue 45, pp. 255-268.

Lin, T.-R., 2002. Experimental design and performance alnalysis of TiN-coated carbide tool in face milling stainless steel. *Journal of Materials Processing Technology,* Issue 127, pp. 1-7.

Loria, E. A., 2000. Gamma titanium aluminides as prospective structural materials. *Intermetallics,* Issue 8, pp. 1339-1345.

McEvily, A., 2004. Failures in inspection procedures: case studies. *Engineering Failure Analysis,* Issue 11, pp. 167-176.

Messick, S., 1990. *Validity of Test Interpretation and Use,* New Jersey: Princeton.

Minevich, A., 1992. Wear of cemented carbide cutting inserts with multilayer Ti-based PVD coatings. *Surface and Coatings Technology,* Issue 53, pp. 161-170.

Mitsubishi Materials Corporation, 2013. *Cutting Tools: Technical Data,* s.l.: Mitsubishi Tools.

Montgomery, D. & Runger, G., 2007. *Applied Statistics and Probability for Engineers.* 4th ed. Hoboken: John Wiley and Sons.

Nabhani, F., 2001. Machining of aerospace titanium alloys. *Robotics and Computer Integrated Manufacturing,* Issue 17, pp. 99-106.

Nagesh, C. & Ramachandran, C., 2007. Electrochemical process of titanium extraction. *Transactions of Nonferrous Metals Society of China,* Issue 17, pp. 429-433.

Netzsch Thermal Analysis, 2014. *Netzsch Thermal Analysis.* [Online] Available at: http://www.netzsch-thermal-analysis.com/us/landing-pages/thermal-conductivity-diffusivity/definition-thermal-diffusivity.html
[Accessed 18 August 2014].

Nouari, M. & Ginting, A., 2006. Wear characteristics and performance of multi-layer CVD-coated alloyed carbide tool in dry end milling of titanium alloy. *Surface & Coating Technology,* Issue 20, pp. 5663-5676.

Ogot, M. & Kremer, G., 2006. *Engineering Design: A Practical Guide.* 1st ed. s.l.:Trafford Publishing.

Patankar, S., Kwang, Y. T. & Jen, T. M., 2001. Alpha casing and superplastic behaviour of Ti-6Al-4V. *Journal of Material Processing Technology,* Volume 112, pp. 24-28.

Rao, B., Dandekar, C. R. & Shin, Y. C., 2011. An experimental and numerical study on the face milling of Ti–6Al–4V alloy: Tool performance and surface integrity. *Journal of Materials Processing Technology,* Volume 211, pp. 294-304.

Ribeiro, M., Moreira, M. & Ferreira, J., 2003. Optimization of titanium alloy (6Al–4V) machining. *Journal of Materials Processing Technology,* Issue 143-144, pp. 458-463.

Sahin, Y. & Motorcu, R., 2004. Surface Roughness Prediction Model in Machining of Carbon Steel by PCD Coated Cutting Tools. *American Journal of Applied Sciences,* 1(1), pp. 12-17.

Schuurman, G. et al., 2008. External Validation and Prediction Employing the Predictive Squared Correlation Coefficient - Test Set Activity Mean vs Training Set Activity Mean. *Journal of Chemical Information and Modeling,* Issue 48, pp. 2140-2145.

Shaw, M. C., 2005. *Metal Cutting Principles.* 2nd ed. New York: Oxford University Press.

Siemens AG, 2011. *Main motors for Sinamics S110 - 1PH8 asynchronous (induction) motors.* [Online] Available at: https://mall.industry.siemens.com/mall/en/za/Catalog/Products/10122158
[Accessed 10 August 2014].

Sun, S., Brandt, M. & Dargusch, M., 2009. Characteristics of cutting forces and chip formation in machining of titanium alloys. *International Journal of Machine Tools & Manufacture,* Issue 49, pp. 561-568.

Su, T., He, N., Li, L. & Li, X., 2006. An experimental investigation of effects of cooling/lubrication conditionson tool wear in high-speed end milling of Ti-6Al-4V. *Wear,* Issue 261, pp. 760-766.

van Vuuren, D., 2009. *Titanium—an opportunity and challenge for South Africa.* s.l., s.n.

Williams, J. C. & Starke, E. A. J., 2003. Progress in structural materials for aerospace systems. *Acta Materialia,* Issue 51, pp. 5775-5799.

Yang, X. & Liu, R., 1999. Machining titanium and its alloys. *Machining Science and Technology: An International Journal,* 3(1), pp. 107 - 139.

Zhang, W., Zhu, Z. & Cheng, C. Y., 2011. A literature review of titanium metallurgical processes. *Hydrometallurgy,* Volume 108, pp. 177-188.

Appendix A: Titanium properties

Physical and Mechanical Properties of Elemental Titanium (Froes, et al., 1996)

Atomic number	22
Atomic weight	47.90
Atomic volume	10.6 weight/density
Covalent radius	0.132 nm
First ionization energy	661.5 MJ/(kj.mol)
Thermal neutron absorption cross section	560 fm^2/atom
Crystal structure	α: close-packed, hexagonal ≤ 1156 K
	β: body-centered, cubic ≥ 1156 K
Colour	Dark gray
Density	4510 kg/m^3
Melting point	1941 ± 285 K
Solidus/liquidus	1998 K
Melting point	3533 K
Specific heat (at 298K)	0.518 J/(kg.K)
Thermal conductivity	21 W/(m.K)
Heat of fusion	440kJ/kg
Heat of vaporization	9.83 MJ/kg
Specific gravity	4.5
Hardness	HRB 70 to 74
Tensile strength	241 GPa
Modulus of elasticity	102.7 GPa
Young's modulus of elasticity	102.7 GPa
Poisson's ratio	0.41
Coefficient of friction	0.8 at 40 m/min
	0.68 at 300 m/min
Specific resistance	0.554 μΩ.m
Coefficient of thermal expansion	8.64×10^{-6} K^{-1}
Electrical conductivity	3% IACS (copper 100%)
Electrical resistivity	0.478 μΩ.m
Electronegativity	1.5 Pauling's
Temperature coefficient of electrical resistance	0.0026 K^{-1}
Magnetic susceptibility	1.25×10^{-6} emu/g
Machinability rating	40 (equivalent to ¾ hardness stainless steel)

Appendix B: Tool wear types and causes

Tool Damage Form	Causes	Countermeasures
Flank wear 	• Tool grade is too soft • v_c is too high • Flank angle is too small • f_z is extremely low	• Tool grade with high wear resistance • Lower v_c • Increase flank angle • Increase f_z
Crater wear 	• Tool grade is too soft • v_c is too high • f_z is too high	• Tool grade with high wear resistance • Lower v_c • Lower f_z
Chipping 	• Tool grade is too hard • f_z is too high • Lack of cutting edge strength • Lack of shank or tool holder rigidity	• Tool grade with high toughness • Lower f_z • Increase honing • Use large shank size
Fracturing 	• Tool grade is too hard • f_z is too high • Lack of cutting edge strength • Lack of shank or holder rigidity	• Tool grade with high toughness • Lower f_z • Increase honing • Use large shank size
Plastic deformation 	• Tool grade is too soft • v_c is too high • f_z and a_e are too large	• Lower v_c • Decrease a_e and f_z • Tool grade with high thermal conductivity
Adhesion 	• v_c is too low • Poor sharpness	• Increase v_c • Increase rake angle • Tool grade with low affinity
Thermal cracks 	• Expansion or shrinkage due to cutting heat • Tool grade is too hard	• Dry cutting (For wet cutting, flood work piece with cutting fluid or for through spindle cooling, increase coolant pressure and flow) • Tool grade with high toughness
Notching 	• Hard surfaces such as uncut surface, chilled parts and machining hardened layer • Friction caused by jagged shape chips (caused by small vibrations)	• Tool grade with high wear resistance • Increase rake angle to improve sharpness • Increase a_e and f_z

(Mitsubishi Materials Corporation, 2013)

Appendix C: Insert Catalogue

Excerpts from ISCAR Milling Tools (Metric Version) Catalogue 2012

Insert dimensions and geometry

HELIDO
600 UPFEED LINE

H600 WXCU 05

Double-Sided Inserts with 6 Cutting Edges, for Fast Feed Machining

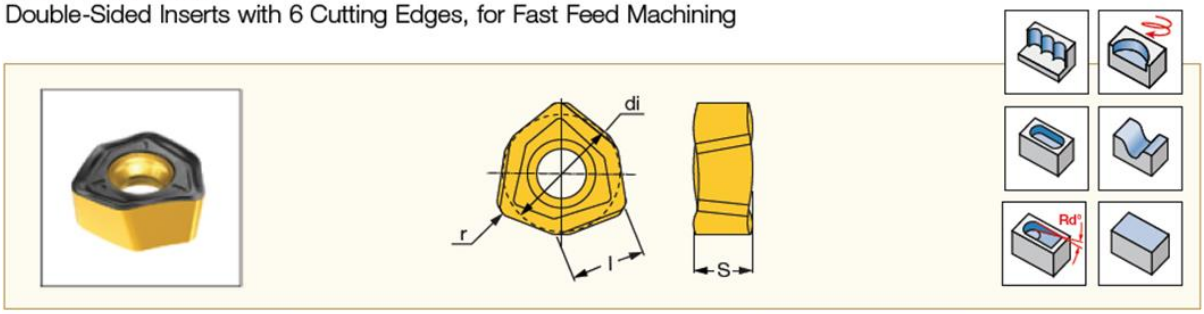

Designation	Dimensions di	l	S	r(3)	Tough ⟷ Hard C330	C830	C810	C808	Recommended Machining Data ap (mm)	fz (mm/t)
H600 WXCU 05T312HP (1)	8.33	5.50	4.20	1.20	●	●			0.80-1.00	0.30-0.80
H600 WXCU 05T312T (2)	8.33	5.50	4.20	1.20		●	●	●	0.80-1.00	0.70-1.20

• Recommended machining data on MF tools: For H600 WXCU 05T312HP ap=0.8-2.0 mm, fz=0.2-0.6 mm/t, For H600 WXCU 05T312T ap=0.8-2.0 mm, fz=0.5-1.0 mm/t. • For cutting speed recommendations, see pages L2-8, L16-19.

(1) For stainless steel and high temperature alloys. (2) For alloy steel and cast iron. (3) Insert radius for programming: r=2.3 mm on FF tools, r=3.1 mm on MF tools.

For tools, see: FF EWX-05 (E32) • FF EWX-M-05 (E33) • FF FWX-05 (E37) • MF FWX-05 (E37).

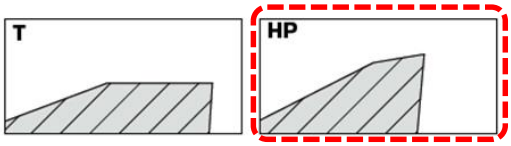

Tool holder

FF EWX-05

Fast Feed Endmills, Carrying Double-Sided Inserts with 6 Cutting Edges

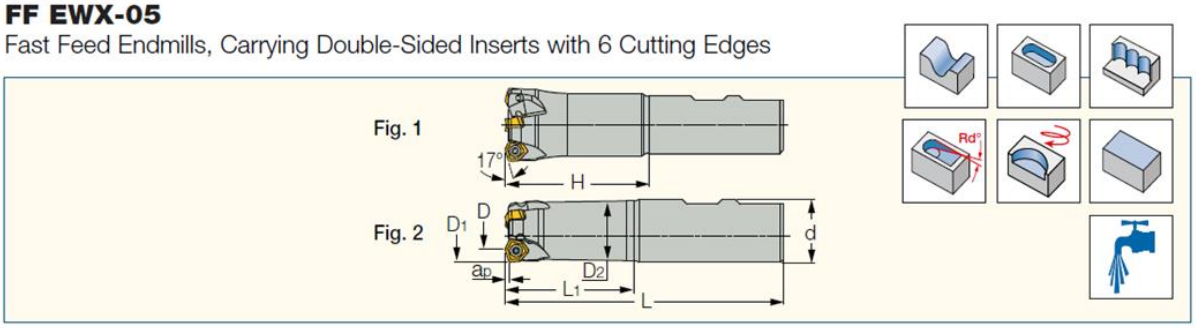

Designation	D1	D	Z	L1	H	L	ap max	d	Shank(1)	Rd°	Fig	Kg
FF EWX D32-4-060-W25-05	32.0	22.00	4	60.0	63.00	120.00	1.00	25.00	W	4.0	1	0.44

• apmax=1 mm; fzmax=1 mm/t; r=2.3 mm for programming • For user guide see pages E57-58

(1) C-Cylindrical, W-Weldon

Cutting speed recommendations for indexable milling cutters

ISO	Material		Condition	Tensile Strength [N/mm²]	Hardness	Coated IC928/830	Coolant
S	High temp. alloys	Fe based	Annealed		200	30 - 50	Wet (emulsion)
			Cured		280	30 - 40	
		Ni or Co based	Annealed		250	20 - 30	
			Cured		350	20 - 30	
			Cast		320	50 - 70	
	Titanium and Ti alloys		Alpha+beta alloys cured	RM 400 RM 1050		30 - 70 30 - 70	

Grade selection for applications and materials

Material Groups / Main Applications	ISO P 1-11 Steel	ISO H 38-41 Hard Steel and Cast Iron	ISO M 12-14 Stainless Steel	ISO S 31-37 High Temp.	ISO K 15-20 Cast Iron	ISO N 21-28 Nonferrous
INDEXABLE MILLING CUTTERS	Harder IC908 (808) IC30N IC830 (928) IC330 (328) Tougher	Harder IB55 IB85 IC808 (908) Tougher	Harder IC908 (808) IC30N IC4050 IC928 (830) IC28 IC330 (328) Tougher (1)	Harder IC08 IC808 (908) IC928 (830) IC328 (330) IC28 Tougher	Harder IS8 IC4100 (5100) DT7150 IC810 (910) Tougher	Harder ID5 ID8 IC07 IC08 IC28 Tougher

First choice

(1) Only for austenitic stainless steel

Iscar Milling grades chart

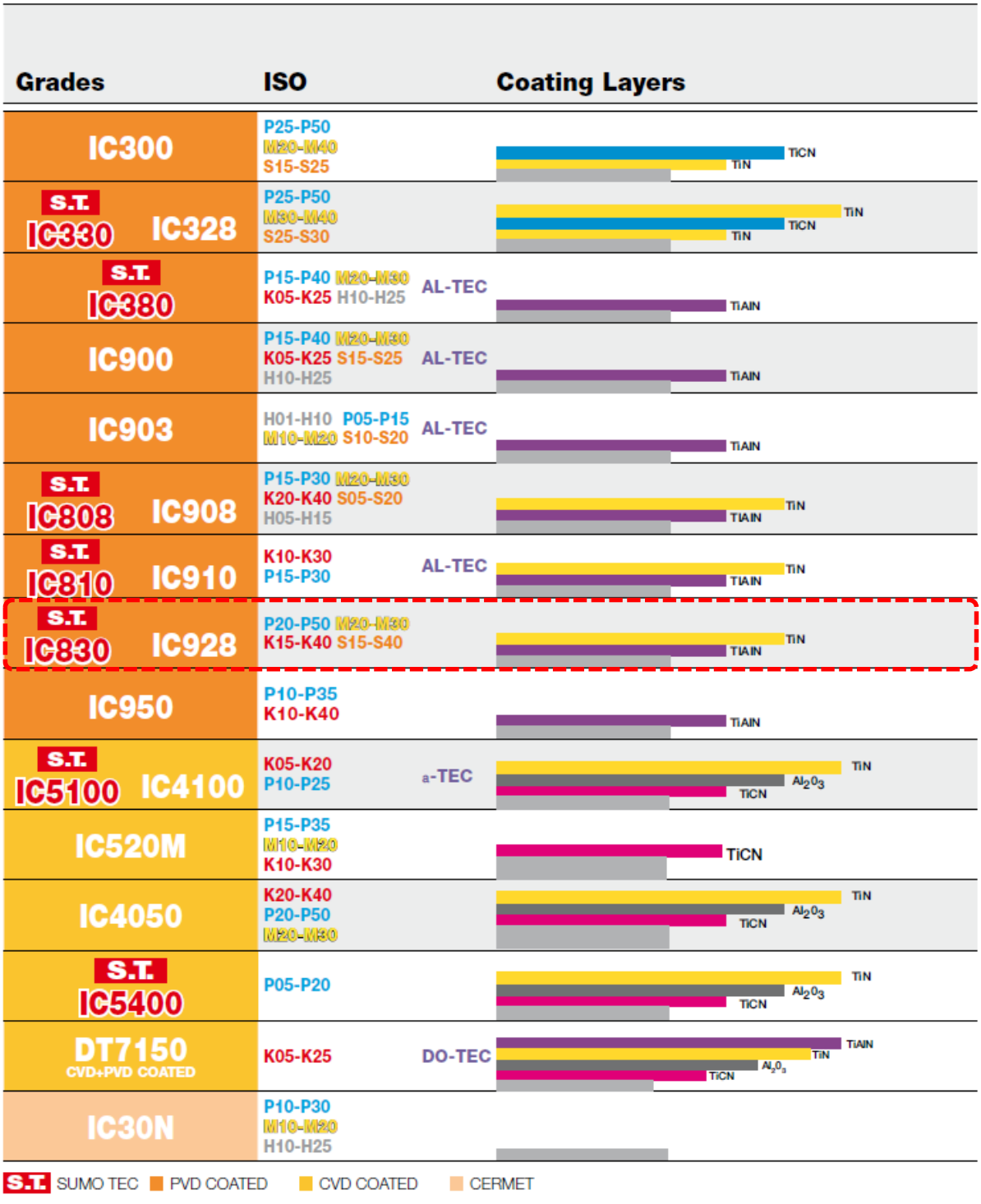

IC830/928

A PVD TiAlN coated tough grade. Suitable for milling stainless steel, high temperature alloys and other alloy steels. Recommended for interrupted cut and heavy operations.

Milling calculations

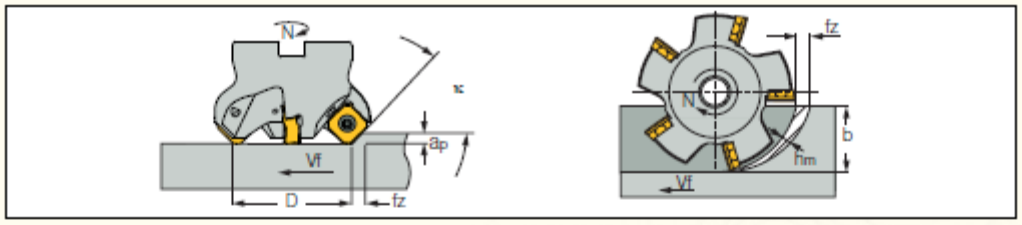

Calculations

Cutting speed	$Vc = \frac{\pi \cdot D \cdot N}{1000 min}$ [m/min]
Spindle speed	$N = \frac{Vc \cdot 1000}{\pi \cdot D}$ [rev/min]
Table speed	$V_f = f_z \cdot Z \cdot N$ [mm/min]
Feed per tooth	$f_z = \frac{V_f}{N \cdot Z}$ [mm/tooth]
Feed per revolution	$f_N = fz \cdot Z$ [mm/rev]
Metal removal rate	$Q = \frac{a_p \cdot b \cdot V_f}{1000}$ [cm³/min]
Machining time	$Th = \frac{L_w}{V_f}$ [min]
Specific cutting force	$K_c = K_{c1} \cdot h_m^{-mc}$
Average chip thickness in shoulder milling for b/D≤0.1	$h_m = f_z \cdot \sqrt{\frac{b}{D}}$ [mm]
Average chip thickness in shoulder milling for b/D>0.1	$hm = \frac{(\sin\kappa \cdot 180 \cdot b \cdot f_z)}{\pi \cdot D \cdot \arcsin(b/D)}$ [mm]
Machining power	$P = \frac{(a_p \cdot b \cdot V_f \cdot k_c)}{6 \cdot 10^7 \cdot h}$ [kW]

Vc	[m/min]	Cutting speed
D	[mm]	Tool diameter
N	[RPM]	Spindle speed
Vf	[mm/min]	Feed speed
fz	[mm/tooth]	Feed per tooth
Z		Number of teeth
f_N	[mm/rev]	Feed per revolution
Q	[cm³/min]	Metal removal rate
a_p	[mm]	Depth of cut
b	[mm]	Width of cut
Th	[min]	Machining time
Lw	[mm]	Machining length
Kc	[N/mm²]	Specific cutting force
Kc_1(1)	[N/mm²]	Specific cutting force for 1 mm² chip section
hm	[mm]	Average chip thickness
mc(1)		Chip thickness factor
k	[degrees]	Cutting edge angle
P	[kW]	Machining power
h		Machine efficiency

P = Pc + PM

P - Total Machining Power
Pc - Net Power = Cutting Power
PM - Motor Power (while not cutting)

Values for Motor Power Pm

Max. Machine Power (kW)	Motor Power Pm (kW)
5.5	0.4
7.5	0.4-0.6
11.0	1.0
15.0	1.5
18.0	2.2
22.0	2.5

Motor Power Pm has a value of approximately 7 to 12% of Maximum Machine Power

Appendix D: ANOVA tables

Uniform rake wear	**DF**	**SS**	**MS (variance)**	**F**	**p**	**SD**
Total	11	991471	90133.7			
Constant	1	718650	718650			
Total Corrected	10	272821	27282.1			165.173
Regression	6	267657	44609.6	34.5585	0.002	211.21
Residual	4	5163.37	1290.84			35.9283
Lack of Fit (model error)	2	3455.68	1727.84	2.0236	0.331	41.5673
Pure Error (replicate error)	2	1707.69	853.846			29.2206
	N = 11	Q2 =	0.842	Cond. no. =	1.173	
	DF = 4	R2 =	0.981	RSD =	35.93	
		R2 Adj. =	0.953			

Non-uniform rake wear	**DF**	**SS**	**MS (variance)**	**F**	**p**	**SD**
Total	11	1.98E+06	179722			
Constant	1	1.49E+06	1.49E+06			
Total Corrected	10	489385	48938.5			221.221
Regression	6	401509	66918.1	3.04601	0.15	258.685
Residual	4	87876.4	21969.1			148.22
Lack of Fit (model error)	2	72824.5	36412.2	4.83821	0.171	190.82
Pure Error (replicate error)	2	15051.9	7525.97			86.7524
	N = 11	Q2 =	0.257	Cond. no. =	1.118	
	DF = 4	R2 =	0.82	RSD =	148.2	
	Comp. = 1	R2 Adj. =	0.551			

Non-uniform flank wear	**DF**	**SS**	**MS (variance)**	**F**	**p**	**SD**
Total	11	1.46E+06	132341			
Constant	1	960842	960842			
Total Corrected	10	494911	49491.1			222.466
Regression	6	464979	77496.6	10.3565	0.02	278.382
Residual	4	29931.6	7482.91			86.5038
Lack of Fit (model error)	2	12203.2	6101.62	0.688345	0.592	78.1129
Pure Error (replicate error)	2	17728.4	8864.2			94.1499
	N = 11	Q2 =	0.556	Cond. no. =	1.173	
	DF = 4	R2 =	0.94	RSD =	86.5	
		R2 Adj. =	0.849			

Appendix E: Regression analysis output

Summary output of regression analysis

SUMMARY OUTPUT

Regression Statistics	
Multiple R	0.917692
R Square	0.842158
Adjusted R Square	0.82462
Standard Error	78.34496
Observations	11

ANOVA

	df	*SS*	*MS*	*F*	*Significance F*
Regression	1	294738.3	294738.3	48.01915	6.84E-05
Residual	9	55241.39	6137.932		
Total	10	349979.7			

	Coefficients	*Standard Error*	*t Stat*	*P-value*	*Lower 95%*	*Upper 95%*
Intercept	9.043309	48.97019	0.18467	0.857582	-101.735	119.8216
Q	11.85793	1.711203	6.929585	6.84E-05	7.986916	15.72894